1973

Report on theoretical and experimental investigations of terminations and splices in 27.6 kV underground distribution systems.

R. Malewicz
University of Windsor

REPORT ON

"THEORETICAL AND EXPERIMENTAL INVESTIGATIONS OF TERMINATIONS AND SPLICES IN 27.6 kV UNDERGROUND DISTRIBUTION SYSTEMS"

by

R. MALEWICZ

A Thesis

Submitted to the Faculty of Graduate Studies through the Department of Electrical Engineering in Partial Fulfillment of the requirements for the Degree of Master of Applied Science at the University of Windsor.

Windsor, Ontario

1973

ACKNOWLEDGEMENTS

I wish to express my sincere thanks to Professor M. C. Perz for his supervision and constant encouragement throughout these investigations.

I am especially obliged to Mr. M. Kurtz of the Ontario Hydro for his interesting discussions and advise pertaining to this work.

Appreciation is extended to members of the Electrical Engineering Department, especially Dr. Raghuveer and Professor Hazel for their helpful guidance and suggestions.

I am most grateful to the staff of the Windsor Utilities Commission for providing the material for tests and their continuous interest in the investigations.

This project was carried out with financial assistance from the National Research Council of Canada and the Windsor Utilities Commission, for which I am very thankful.

ABSTRACT

An investigation has been made of the performance of terminations and splices in the 27.6 kV underground distribution system. Several phenomena that reduce the expected operating life; such as, corona discharges, treeing and shrinkback are discussed. Computer techniques have been employed to calculate the electric field distributions of several termination and splice models. A study of high voltage gradients and void effects on these field distributions has been useful in predicting performance. Different methods of controlling stresses in practical terminations and their performance when subjected to standard corona and high-voltage tests are described. The results of these tests are presented and the ensuing conclusions leading to recommendations are proposed.

TABLE OF CONTENTS

LIST OF TABLES

LIST OF FIGURES

CHAPTER 1

INTRODUCTION

The advent of urbanization has brought about the increased demand for electric power in residential and industrial areas. In addition, the need has arisen for a reliable and economical power distribution system in these areas. For aesthetic, environmental and safety reasons, underground cables have been employed in power distribution.

The growth of underground residential distribution (U.R.D.) has also stimulated the development of shielded, plastic dielectric cables. These solid dielectric cables have replaced to a large extent the older oil-impregnated paper and oil-filled cables. The new cables are less bulky in size, easy to install and reliable in service.

Cable accessories, such as, terminations and splices (joints) have also utilized lower cost plastic dielectric insulation. At present, thermoset polymers, especially cross-linked polyethylene (XLPE) insulation, are most widely used. The design of new terminations and splices have been adopted from those of well-established existing, oil-impregnated paper. The latter have large safety factors included to compensate for poor workmanship and variety in construction methods. These new termination and splice designs, however, have experienced unexpected failures. Moreover, increased operating voltages in U.R.D., essential for economic power distribution, aggravate this problem. Terminations and splices are vulnerable to mechanical, electrical and chemical deterioration. Phenomena, such as, corona discharges, treeing and shrinkback have severely limited their reliability. The performance of these cable accessories determine to a large extent the life, maintenance and, hence, the ultimate cost of the distribution system. Therefore, an investigation has been made of termination and splice

performance under tests that simulate actual operating conditions.

The preliminary phase of the investigation, which consisted of a literature examination of current research in this area, revealed an intense activity by involved industries. However, most of the research is not published because of the competitive nature of these industries. Visits were arranged to various manufacturers of cables and accessory components to obtain first-hand information that could aid our research. Although a detailed description of the visits is not included in this report, we have found an interest and great co-operation from the companies.

This report consists of six additional chapters and several appendices. Chapters 2 and 3 present the physical and electrical aspects of cable, splice and termination designs. Different electric stress relief methods used by terminations are discussed. A description of the physical, electrical and chemical deterioration that can occur in cables is presented in Chapter 4.

Electric field distributions in practical terminations and splices are analyzed in Chapter 5. This study assisted in locating high electric field intensity regions which may cause dielectric breakdown. Also included is a study of the effect of voids and multi-dielectric regions on the electric gradient distribution.

Chapter 6 contains the results of an experimental study of high-voltage tests and corona measurements. It must be noted that splices were initially investigated but a more immediate priority was attached to a study of terminations. The results of such a study would also apply to the problems encountered in splices. The terminations tested are utilized on the single-phase cables of the 27.6 kV, 3 phase, Y-

connected underground distribution system in Windsor. Test procedures were based on the I.E.E.E. Standard for Potheads.[1] The standard allowed relative performance and acceptability of terminations under operating conditions to be compared.

From the results of the electric field distribution study and experimental investigation, conclusions and tentative recommendations are presented in Chapter 7.

CHAPTER 2

SHIELDED CABLES AND SPLICES

2.1 Introduction

Terminations and splices are an integral part of cables in any underground power distribution network. Short lengths of cable are often joined together by splices in order to extend cable length. Also, to maintain cable continuity, it is necessary to remove defective cable sections by splicing.

Physically, cables and splices are similar in terms of composition. Each has three main components; a current-carrying conductor, insulation surrounding the conductor and an insulation shield. However, splice dimensions are larger owing to the connector or ferrule between the two cable conductor ends.

Electrically, cables and splices are similar in that their respective electric fields are contained within the shielded insulation. The electric field is radially uniform throughout the cable but not in the splice. The distortion in the latter is due to irregularities in the shape of the ferrule.

These physicial and electrical aspects of cables and splices are discussed in this chapter.

2.2 Physical and Electrical Aspects of Cables

2.2.1 Physical Considerations

Consider a single conductor polymeric-insulated 27.6 kV* cable. Several basic materials constitute a single-phase underground cable; a stranded conductor metal core, insulation, a conducting insulation shield

---

*All voltage ratings are phase-to-phase unless otherwise noted.

and often a protective jacket. These components, as illustrated in Figure 1, characterize the most common type of underground cable construction.

The core is either aluminum or copper. Aluminum, though displaying a conductivity approximately 62% of that of electrical grade copper, is used more extensively because of its lighter weight and lower cost. A solid core is impractical at voltages above 15 kV since it does not provide adequate flexibility. Hence, a stranded type core design is utilized. The strand design, however, enhances the formation of interstitial voids near the core surface. This limitation is overcome by using a semi-conducting inner shield.

The semi-conducting inner shield, Figure 1., which is referred to as strand shielding, is extruded directly over the stranded conductor. The extrusion process ensures a smooth transition and tight mechanical bond between the stranded conductor surface and the inner surface of the insulation. Thus, the number of interstitial voids in the insulation proper are considerably reduced.

The most often used polymers for cable insulation are cross-linked polyethylene (XLPE), ethylene propylene rubber (EPR) or butyl rubber. These materials exhibit sufficient dielectric breakdown strength to provide a good barrier between the conductor and surrounding insulation shield. Thermoset XLPE, however, is used more extensively than other polymers. This is attributed to the cross-linking process which increases the insulation melting point, a very desirable property. Therefore, the corresponding increase in the operating temperature of the conductor enables larger current or ampacity rating. The XLPE insulation and the strand shielding are extruded simultaneously, thereby assuring

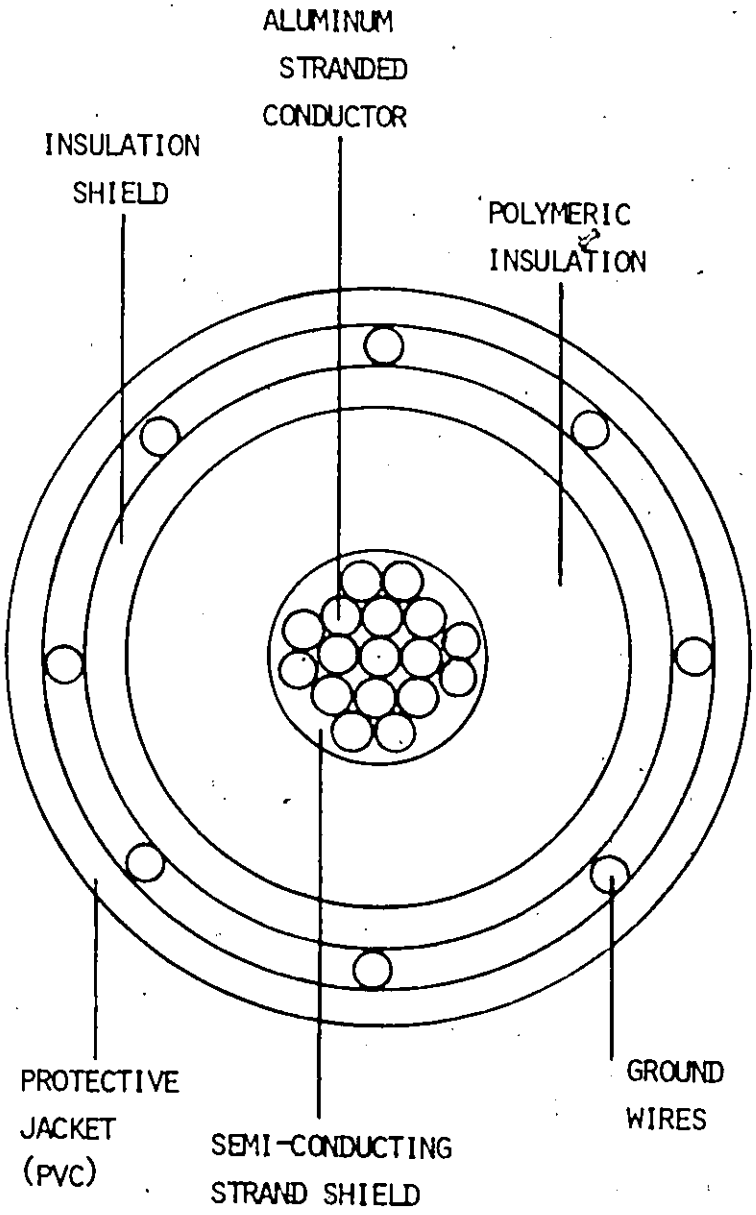

FIGURE 1: - RADIAL CROSS-SECTION OF A SINGLE-CONDUCTOR CABLE (27.6 kV)

a solid, virtually void-free bond to the conductor.

In the single-phase cable, insulation shielding consists of two parts. The first is a semi-conducting layer either taped or extruded over the insulation. The second part consists of helically wound conductors positioned contiguous to the semi-conducting layer. These conductors, either circular tinned copper wires or copper foil strips, act as a low resistance ground return.

An optional jacket is incorporated over the shield if copper foil strips are used. This is generally recommended for areas where severe corrosion conditions exist. Polyvinyl chloride (PVC) insulation is the most common material used for this purpose.

2.2.2 Electric Stresses in a Cable

A continuously shielded high-voltage cable exhibits an electric field distribution similar to that between infinitely long insulated concentric cylinders. The electric field is uniform along the cable axis, varying only in the radial direction. This is illustrated in Figure 2 which shows the field distribution in a radial cross-section of the cable. The field is represented by electric flux and equipotential lines within the cable insulation. Flux lines indicate the direction of the electric field intensity between the conductor and the insulation shield. Equipotential lines represent lines of equal potential magnitude and in this case, they are concentric about the conductor.

As the electric flux lines diverge, Figure 2, and approach the insulation shield, the electric stresses decrease. This is also indicated by the larger spacing of the equipotential lines as the insulation shield is approached. The electric stress at any point within the cable insulation is[2]

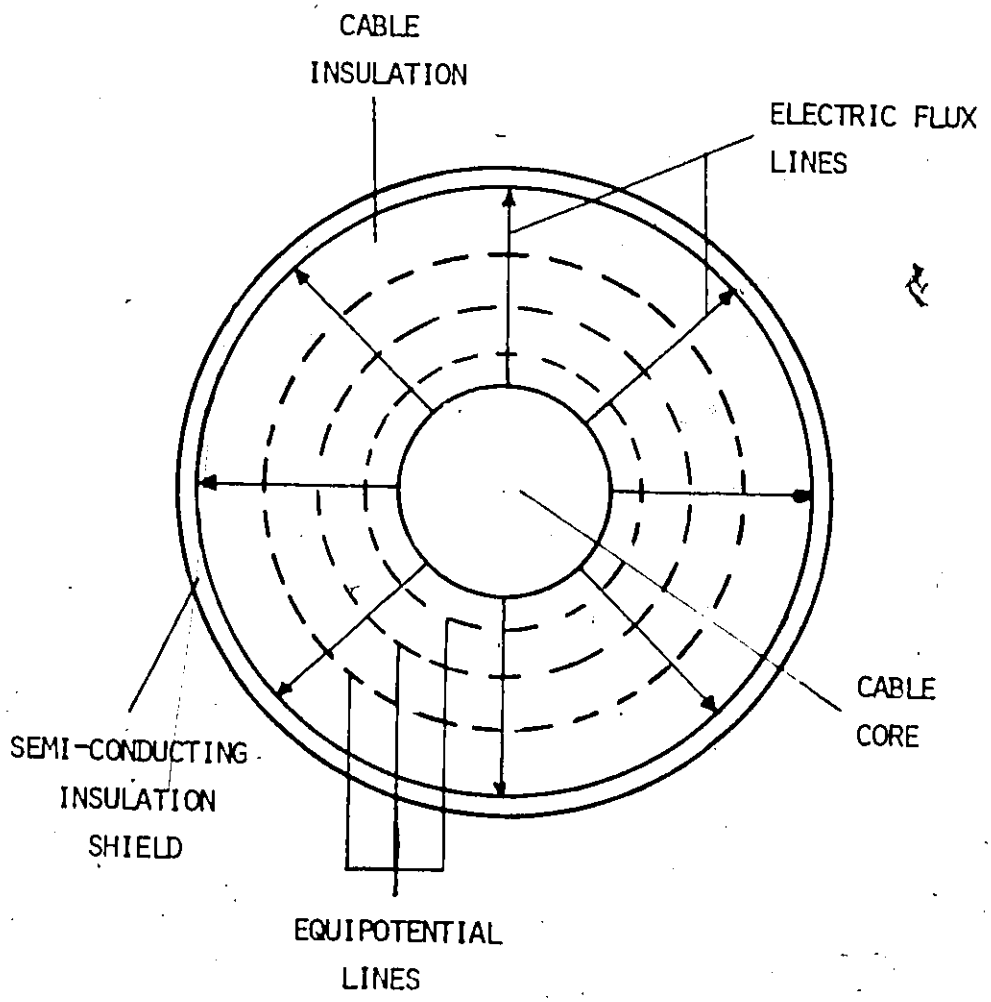

FIGURE 2: - CROSS-SECTIONAL FIELD DISTRIBUTION IN AN UNDERGROUND CABLE

$$E = \frac{V}{x \log_e \left(\frac{R}{r}\right)}, \qquad (1)$$

where E is the electric field intensity (electric stress) in volts/mil at a distance x mils from the axis of the cable,

V is the potential difference in volts,

R is the outer radius of the shield in mils

and r is the inner radius of the insulation in mils.

Equation (1) indicates that the electric field intensity is maximum at the surface of the conductor and minimum at the insulation shield. This electric stress distribution is a direct result of the conductor and insulation shield geometry. The electric stresses at the conductor surface could be minimized by increasing the radius but this would be uneconomical. Points of electric stress concentration would however exist at the outer conductor strands, Figure 2, if not for the presence of strand shielding.

2.3 Physical and Electrical Aspects of Splices

2.3.1 Physical Considerations

The term splicing describes the process of connecting two cable ends so that the continuity of the original cable is retained. The three basic components comprising a splice: a connector or ferrule, insulation and a ground shield, are shown in Figure 3.

The bare conductor ends of the cable are joined together by a connector which may be of the solder or compression type. For XLPE cables, the compression type connectors is usually employed to avoid possible heat damage to the cable insulation. However, crimping (compression connecting) develops indents or surface irregularities on the connector. These are sometimes filled with conducting putty to

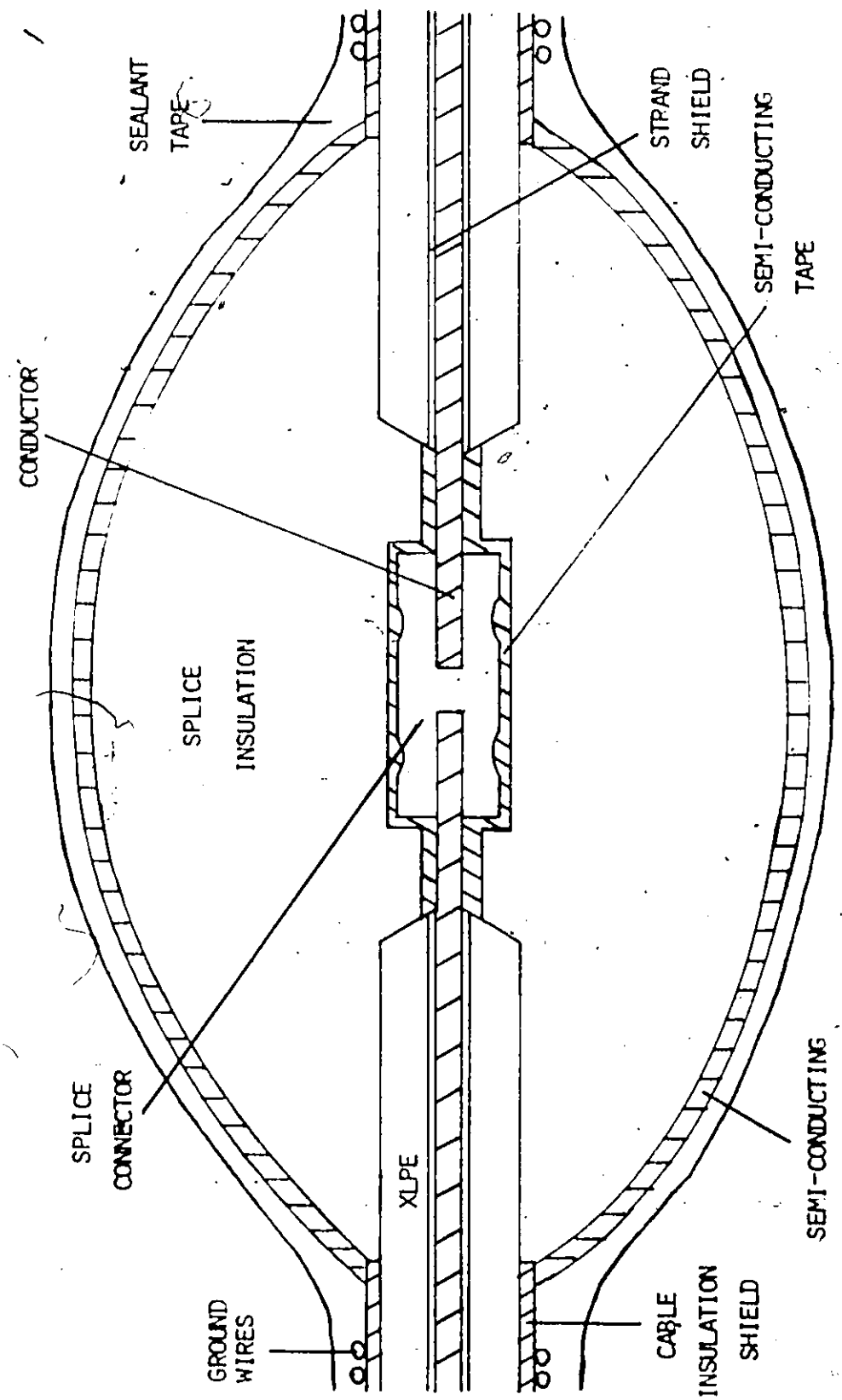

FIGURE 3: - AXIAL CROSS-SECTION OF A 27.6 kV SPLICE

smooth the connector contour. In addition to putty, semi-conducting tape is wrapped over the connector and the conductor (core) to provide a relatively regular surface. This minimizes void formation at the connector-insulation interface.

In a splice, the insulation material surrounding the connector is either hand-applied tape or pre-molded. The selection of insulation material is very important. This material must be electrically, mechanically and chemically compatible with the cable insulation itself. Electrically, the dielectric constant and electric breakdown strength must be of the same order as the cable insulation. Mechanically, the splice insulation must have a similar degree of expansion and contraction. At high operating temperatures, the polymeric insulation must be chemically non-reactive with the cable insulation.

The selection of a suitable insulating material is complicated by the fact that no insulation is yet available which bonds chemically to XLPE (cable insulation). Nevertheless, an amalgamating tape, applied with a high degree of tape elongation may be used. First, however, the cable insulation is pencilled at the end. Pencilling provides a smooth, stepless surface for taping, hence, a tight mechanical bond and a minimum inclusion of voids is achieved.

To maintain continuity of the external shield at the splice, a layer of semi-conducting tape is wrapped over the splice insulation. When the spliced cable is equipped with a concentric neutral shield, then the ground (shield) wires are connected together by a compression connector. On the other hand, if the cable shield consists of helically wound copper foils, a copper mesh is utilized. The mesh is wrapped around the splice and makes contact with the semi-

conducting shield tape. These metallic wires establish a good ground return.

A durable and water-resistant covering over the splice may also be provided. The covering is usually in the form of a PVC jacket and/or a sealant tape.

2.3.2 Electric Stresses in a Splice

The electric field distribution in a splice is somewhat similar to that in a cable. The equipotential and flux lines are all contained within the insulation between the connector and the insulation shield. The geometry of the splice is cylindrically symmetrical, hence, the equipotential lines are concentric about the connector. However, the splice is not axially symmetric as is the cable. The electric field is no longer uniform along the axial length of the connector.

Changes in splice geometry distort the electric field distribution, as illustrated in Figure 4, introducing high local voltage gradients. The irregular shape of the ferrule causes high axial field intensities to occur in the splice insulation off the connector. The pencilled interface between the splice and cable insulations is another source of axial stresses, region A of Figure 4. Radial field intensities are maximum off the connector surface irregularities, region B, and minimum near the insulation shield.

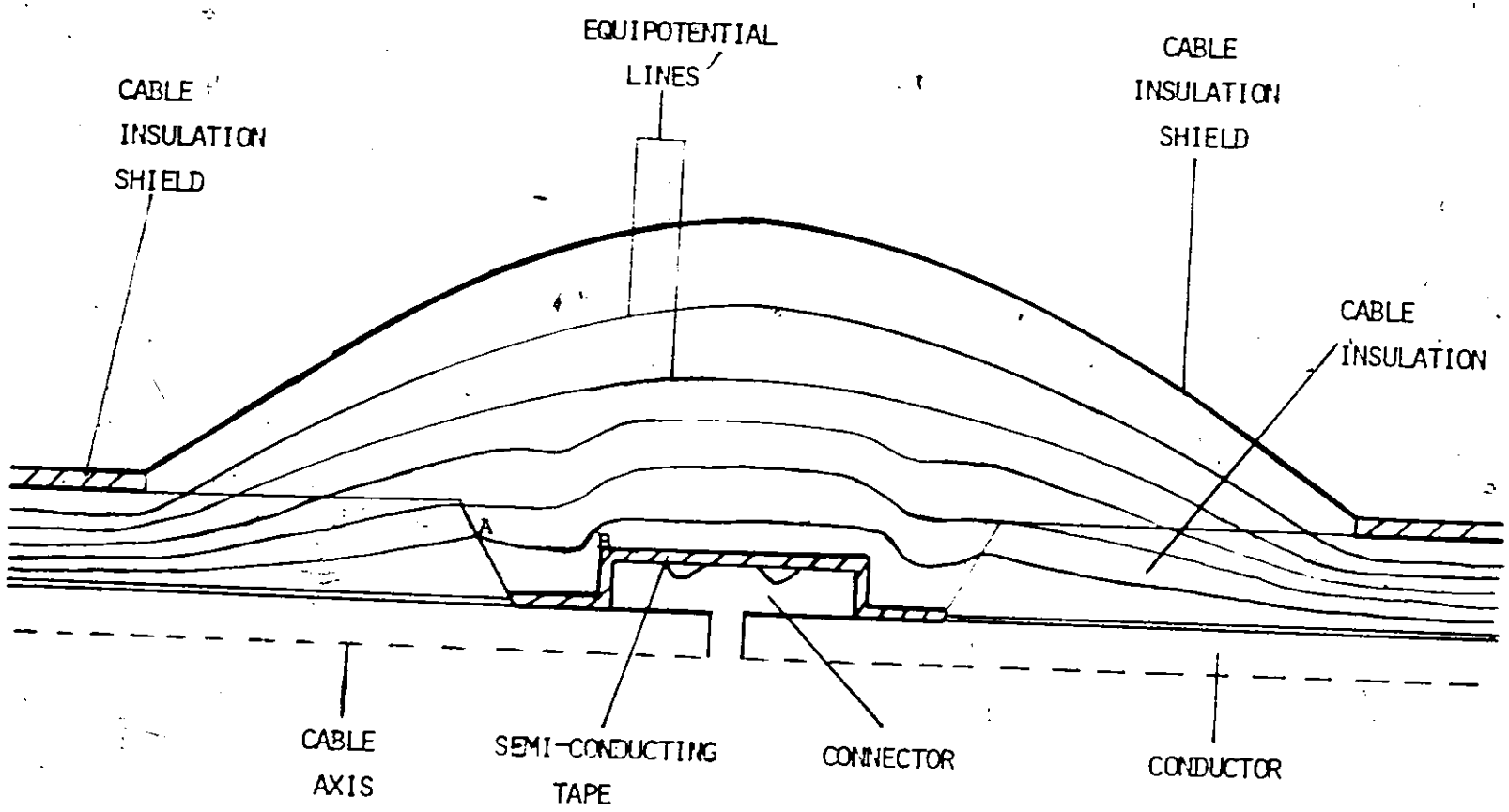

FIGURE 4: - ELECTRIC FIELD DISTRIBUTION IN A SPLICE

CHAPTER 3

CABLE TERMINATION METHODS

3.1 Introduction

When a shielded underground cable is attached to a power source, the end of the shielded cable must be especially prepared before being connected for operation. Certain precautionary measures must be taken as the electric field is not uniform at the cable end. High local electric stress concentrations are established in the cable insulation. The process of relieving or controlling these electric stresses is referred to as termination.

Some of the common methods used in terminations are: capacitive cone, composite-dielectrics and non-linear resistance. Each method reduces the electric stress in the cable insulation to tolerable levels.

3.2 Cable End Prepared for Termination

When a shielded cable end is prepared for termination, a certain length of the shield and ground wires are removed from the cable end, Figure 5. The length of exposed insulation, A B, called the leakage distance, is determined by the operating voltage, thickness of the cable insulation and the electrical characteristics of the insulation. The bare length of insulation, however, does not prevent an increase of the local electric field intensity to exist at the edge of the grounded shield, point A.

Examination of Figure 6 illustrates the electric field distribution at the end of the cable shield. The electric field is no longer axially uniform. Axial stress or field gradient components are particularly severe at the edge of the shield along the surface of the insulation. The electric stress concentration is of much greater magnitude than those occurring in a continuous cable. The high stress concentration at

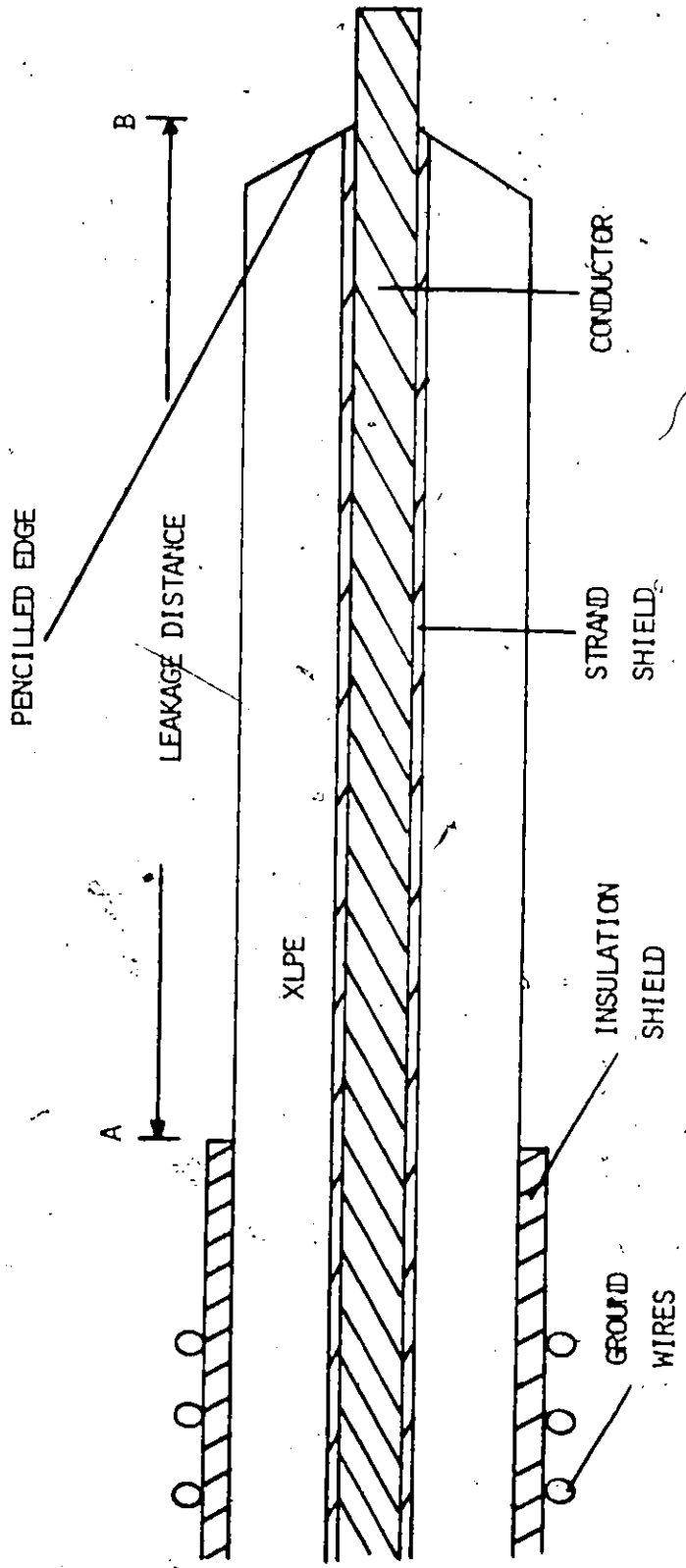

FIGURE 5: - A XLPE INSULATED CABLE PREPARED FOR TERMINATION

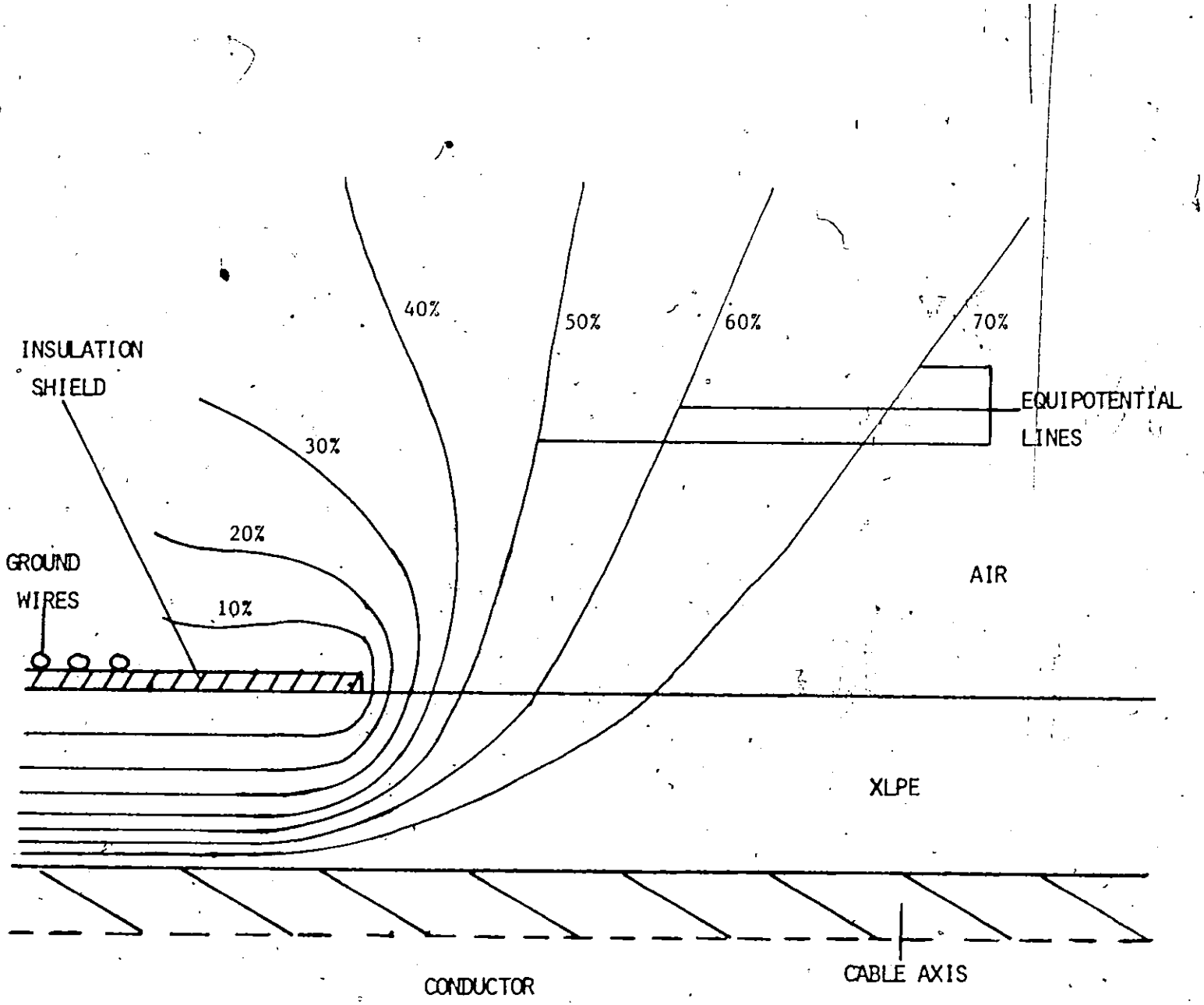

FIGURE 6: - FIELD DISTRIBUTION IN A-CABLE PREPARED FOR TERMINATION

the shield edge would cause a deterioration and finally a failure of the cable insulation if the cable were operated in this unterminated condition.

3.3 Termination by a Capacitive Cone

3.3.1 Stress Control by a Capacitive Cone

The common method of controlling electric stresses is by adding a "capacitive cone" over the insulation as shown in Figure 7. After the cone is installed, the cable insulation shield is extended along one side of the cone surface to the apex by a semi-conducting material. This configuration transfers the shielding edge to a point where the diameter of the insulation is greater than that of the cable insulation itself. The increase in insulation thickness considerably reduces the electric stress at the shield edge, Figure 8. The larger separation between the equipotential lines near the shield edge in Figure 8 than those found in Figure 6 indicates a considerable reduction of the electric stress concentration at the shield edge. The reduction or relief of the electric stress is dependant on the slope of the conducting portion of the cone.

The insulation shield contour in a capacitive termination has a pronounced effect on the electric stress distribution. Too steep a slope introduces abnormally high axial stresses at the shield edge, thus defeating the purpose of the cone. Too shallow a slope produces a negligible improvement in the radial stresses at the shield edge. The stress distribution becomes similar to that in Figure 6.

For maximum reduction of the electric field intensity, the ideal shape of the extended insulation shield has been calculated to be a double logarithmic curve given by [3]

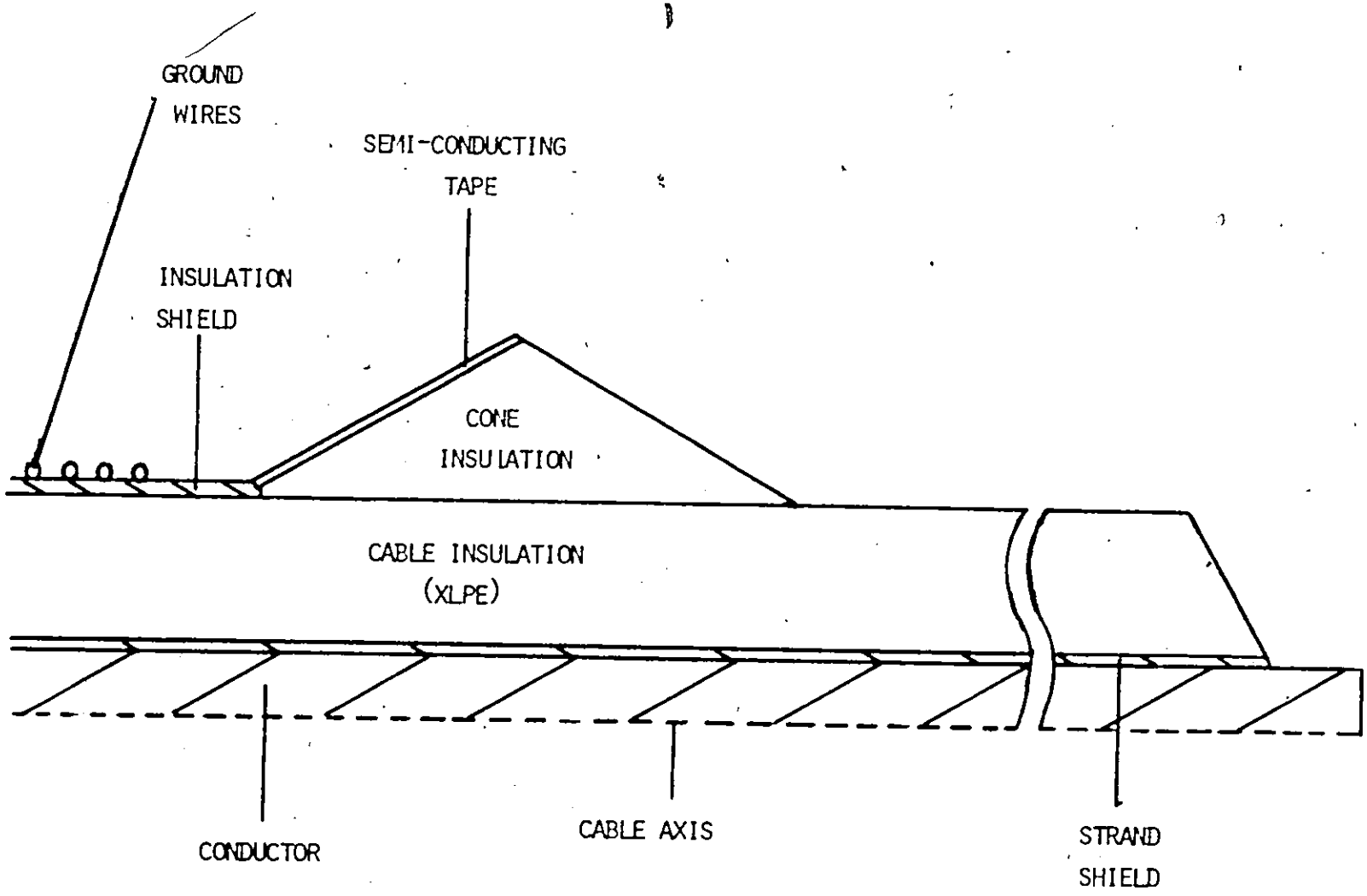

FIGURE 7: - CABLE TERMINATION UTILIZING CAPACITIVE CONE FOR STRESS CONTROL

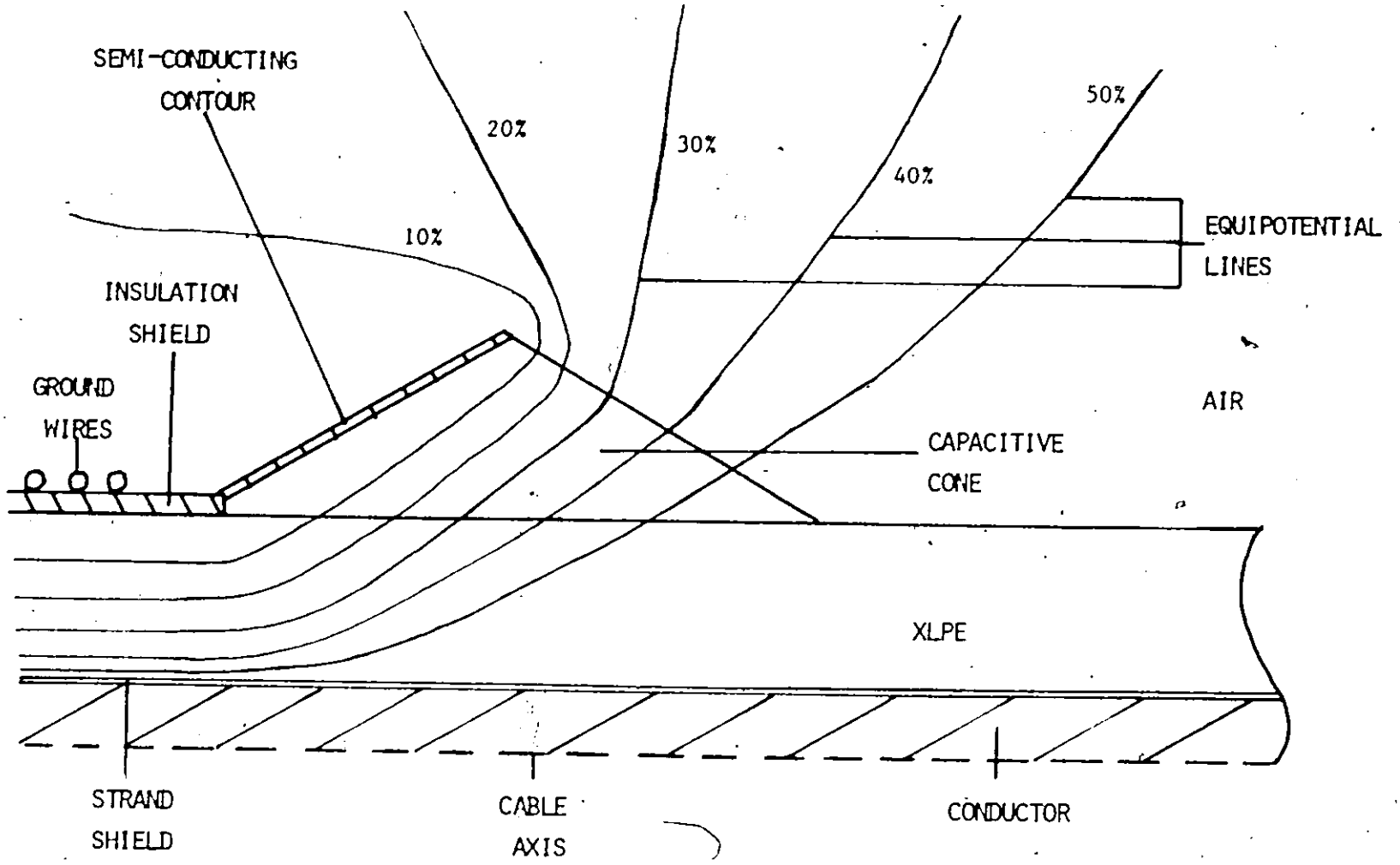

FIGURE 8: - FIELD DISTRIBUTION IN A CAPACITIVE CONE TERMINATION.

$$\log D = \frac{(\varepsilon_A/\varepsilon_B)\ \log_{10}\ (d_b/dc)}{\frac{V}{gL} - 1} + \log_{10} d_b \quad (2)$$

where d_b is the cable insulation diameter,

dc is the conductor diameter,

g is the potential gradient along the cable surface,

L is the distance from the end of the insulation shield,

ε_B is the dielectric constant of the cable insulation,

ε_A is the dielectric constant of the cone insulation,

V is the operating voltage to ground

and D is the diameter of the cone at a distance L from the insulation shield edge.

The resulting curve, equation 2, provides a low angle at the base, thus ensuring that the electric field intensity in this critical region is reduced.

For most applications, a straight-line slope is an adequate practical approximation. This, however, does not provide the high degree of stress relief as does the double logarithmic slope.

3.3.2 Practical Terminations Using a Capacitive Cone

Several types of capacitive cone constructions are presently available. In the conventional method, the cone is made by hand. An insulation tape is wrapped till the ideal shape is approximated. A less tedious method involves the use of a triangular, pennant-shaped sheet of insulating tape. When wrapped around the insulated cable, it forms a cone of pre-determined size. The cone contour, near the cable insulation shield, is claimed to be in accordance with the mathematical relationship expressed by equation (2).

A simpler process is the molded, pre-formed cone, Figure 9, which requires no taping. This cone consists of insulation which is bonded to the conductive shielding, thereby eliminating air pockets from high stress regions along the conducting slope. When slipped on to the cable, the conducting portion is firmly connected to the insulation shield and flares out with a double logarithmic slope. In addition, silicon grease is applied to the cable insulation/molded insulation interface. This provides easy assemblage and eliminates voids that may be formed at the insulation due to an imperfect fit.

3.4 Stress Control by Dielectric and Resistive Methods

3.4.1 Introduction

When a cable is unterminated, that is, the shield is removed, Figure 6, page 16, the potential across the insulation between the ground shield at zero potential and the core is equal to the operating voltage. A high potential gradient exists at the shield edge which forms a discontinuity. The shield has now both radial and tangential components as compared to only a radial component in a continuous cable. The radial component presents no problem because the bulk breakdown strength is much larger than the surface breakdown strength of the insulation. On the contrary, the tangential component of the gradient is especially harmful as it initiates corona discharges leading to surface tracking and insulation deterioration. These harmful effects could be avoided if some means could be found to reduce the tangential gradient.

Two methods exist which extend the ground shield so that a new edge is formed at a higher potential than ground. Hence, at the new edge, the field is reduced as compared to the unterminated condition. In

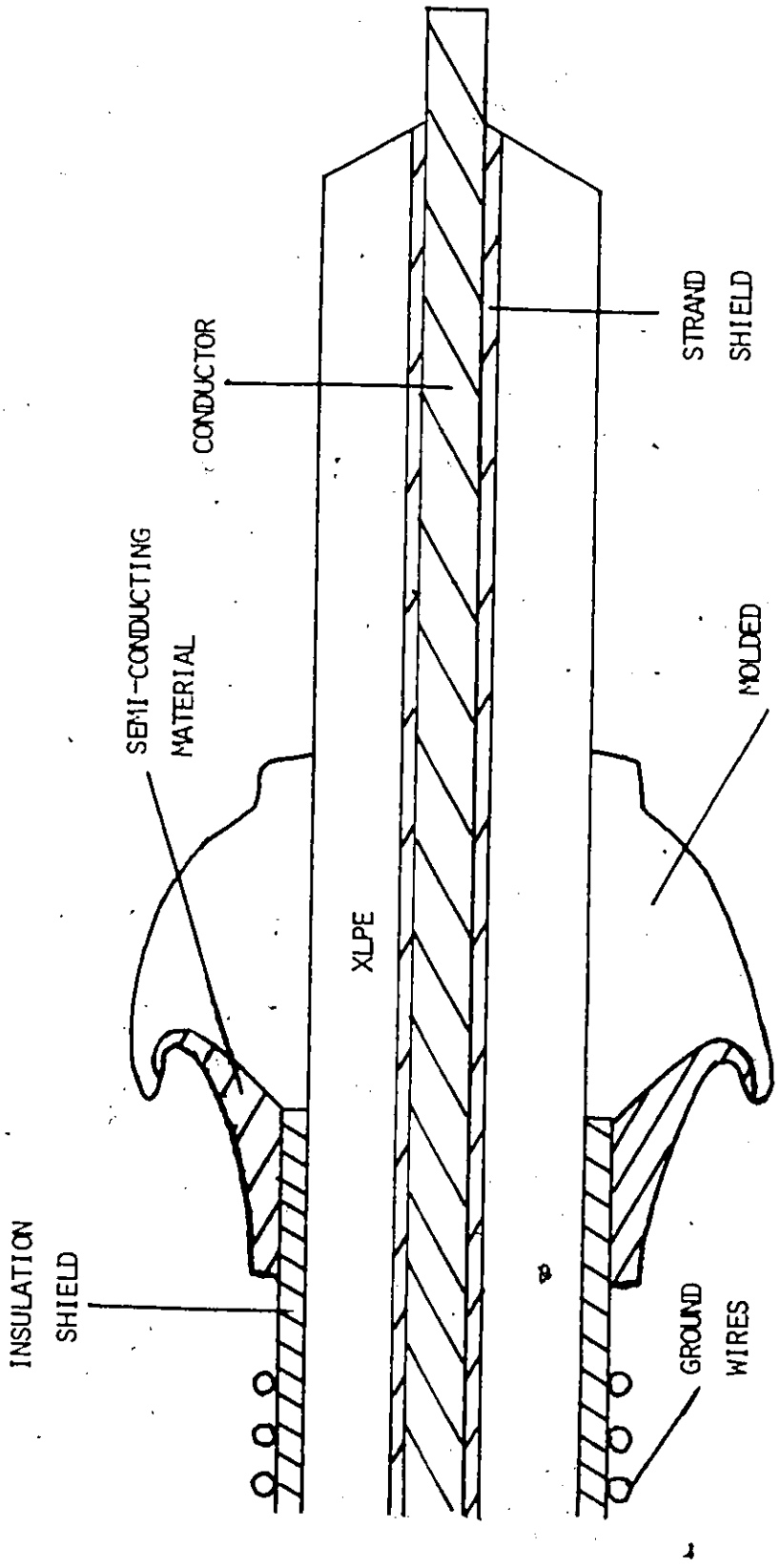

FIGURE 9: - MOLDED CAPACITIVE CORE TERMINATION

one method, the bare insulation is covered by a high dielectric constant tape. In the other method, a high resistance material is applied to the exposed cable insulation. Both methods can be explained best by a distributed parameter ladder network.

3.4.2 The High Dielectric Constant-Capacitive Method

This method utilizes a tape having an apparent high dielectric constant in the tangential direction; namely, along the cable insulation surface. The effect of such an arrangement is similar to a distributed C-C parameter ladder network, Figure 10(a). ΔC and C_x represent the distributed capacitances of the cable insulation and high dielectric constant tape, respectively. The capacitance, ΔC, is much smaller than C_x, hence, the displacement currents through the ladder network are limited to a low value by the capacitance, ΔC.

The displacement current causes a distributed potential rise along the high dielectric constant tape so that the potential at the far edge of the tape is closer to the potential of the core. The field at the new edge is reduced since the core to edge potential, $b \cdot V$, is much lower than the operating potential. It has to be noted that if an unbalanced condition existed, the high dielectric constant tape is not a part of the ground return power circuit, so that the rising potential along the tape is affected only by the displacement current.

Figure 10(b) illustrates this reduction of the field as a new edge at higher potential is established. The graph illustrates that the potential, $b \cdot V$, to the core at the new edge is now about 50% of the operating voltage, V. The electric field intensity at the new edge of the high dielectric constant tape is also reduced in proportion to the decrease in voltage. Since the operating voltage at this new

10B

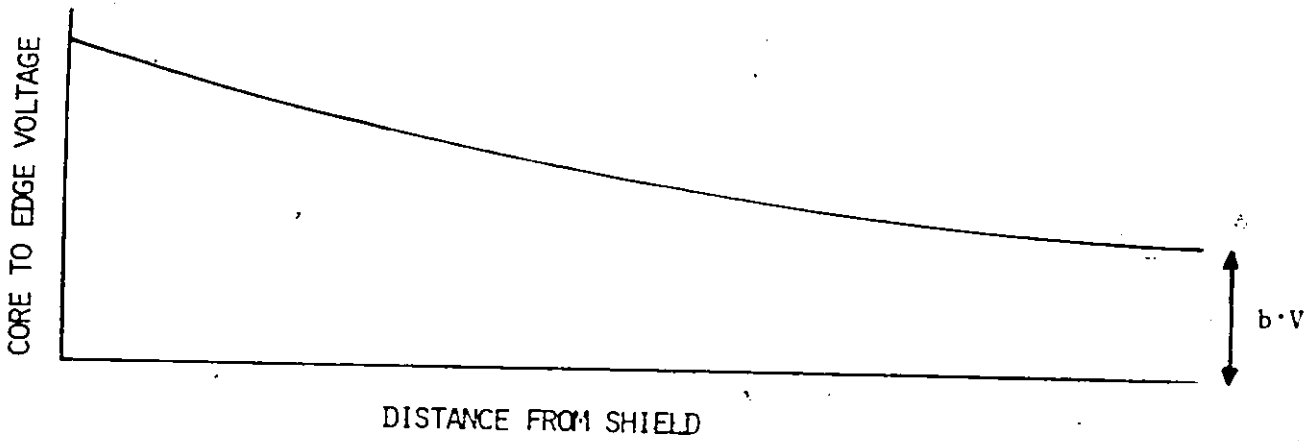

10A

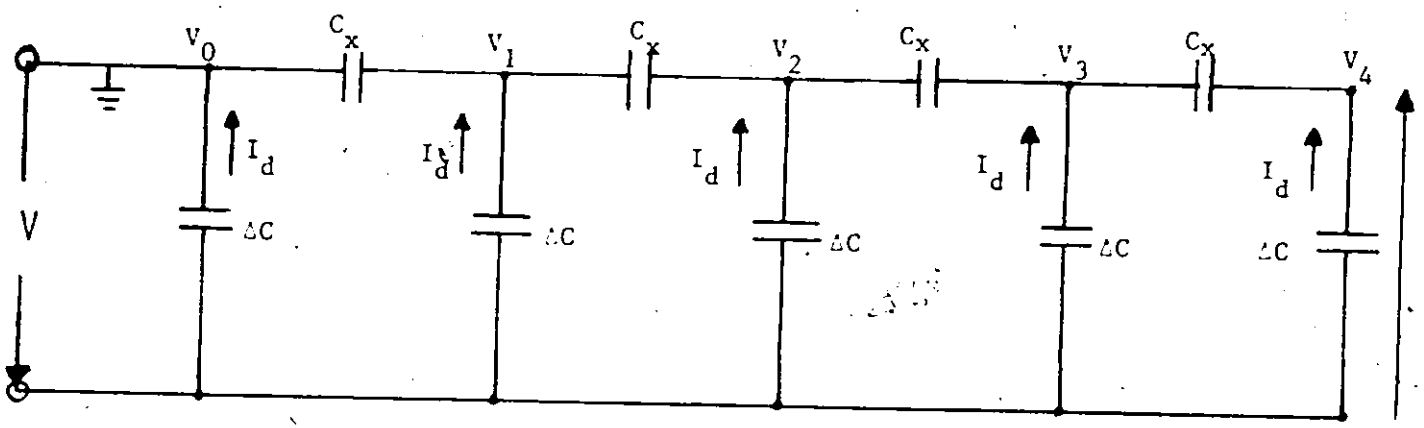

FIGURE 10A: - DISTRIBUTED C_x-ΔC PARAMETER EQUIVALENT OF HIGH DIELECTRIC CONSTANT TAPE TERMINATION

FIGURE 10B: - EDGE TO CORE POTENTIAL DISTRIBUTION ALONG DIELECTRIC SURFACE

edge is now less than the corona inception voltage, no discharges or surface tracking can occur.

3.4.3 The Anisotropic Dielectric

As noted in the previous section, a material with a high dielectric constant can be used to control electric stresses. There exists an anisotropic material that apparently has two dielectric constants, one of which is much larger than the other. The material is produced by compounding an elastomer with embedded microscopic aluminum flakes. Two views of such an imbedded array of flakes are shown in Figure 11. The apparent increase in dielectric constant caused by the insertion of an array of oriented conducting discs (flakes) was first proposed by Estrin.[4] The following theoretical considerations, bring out the principle involved in the above effect.

Neglecting end effects, consider a condenser consisting of two parallel plates with a dielectric interposed between the plates. If an electric field is applied perpendicular to the disc faces, the equipotential lines become oriented along the planes (x and y directions) of the discs, as in Figure 12. The flux lines, which are normal to the equipotential lines, are aligned perpendicular to the plate surfaces. The total capacitance of this condenser is given by

$$C = \frac{\varepsilon A}{s} \quad , \tag{3}$$

where A is the area of the plates,

S is the plate separation

and ε is the dielectric constant of the elastomer.

The apparent dielectric constant, ε, of the condenser becomes that of the filler medium, ε_f, as though the discs did not exist.

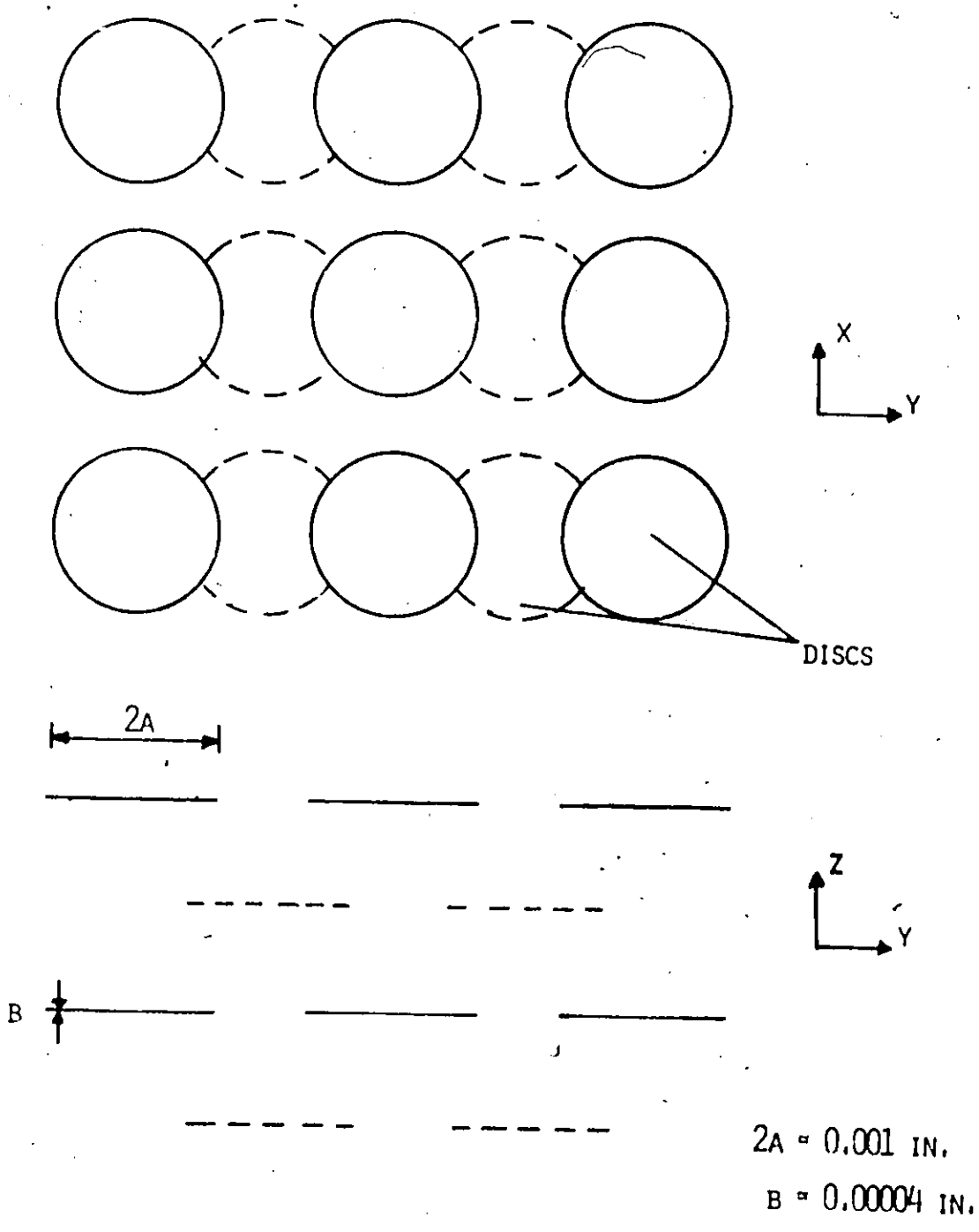

FIGURE 11: - ARRAY OF CONDUCTING DISCS (FLAKES)

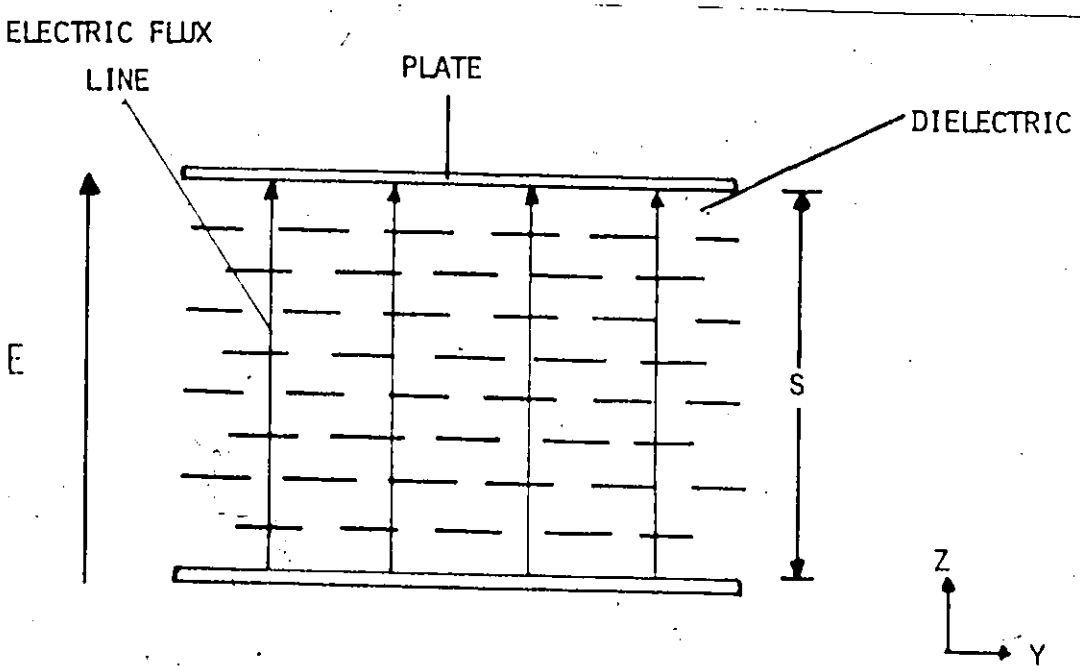

FIGURE 12: - FIELD DISTRIBUTION IN AN ANISOTROPIC DIELECTRIC WITH THE APPLIED FIELD NORMAL TO THE DISC FACES

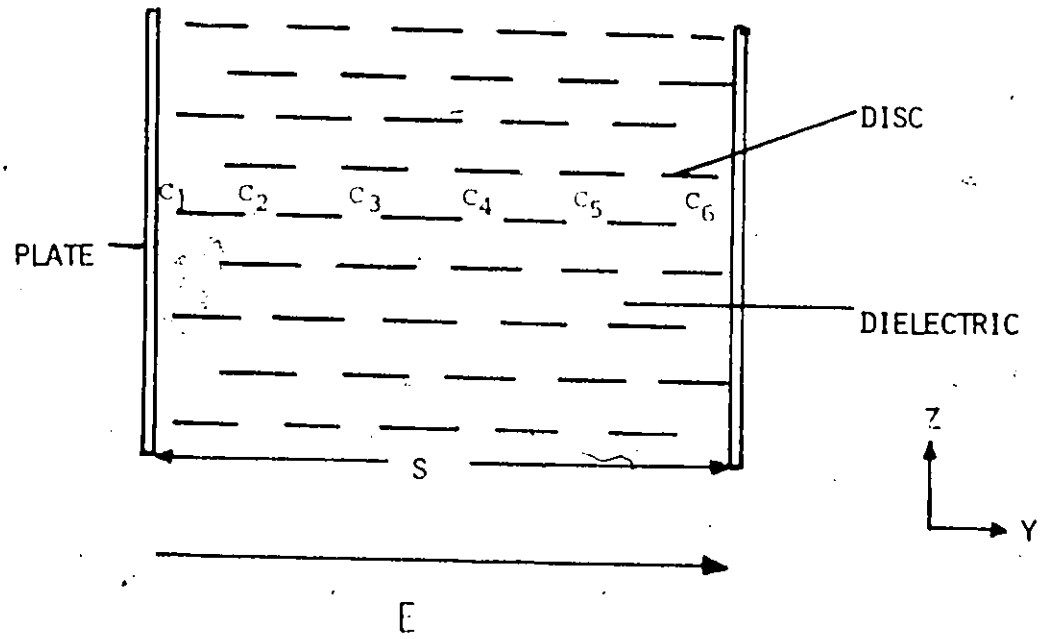

FIGURE 13: - ARRANGEMENT OF THE ANISOTROPIC DIELECTRIC WITH THE APPLIED FIELD PARALLEL TO THE DISC FACES

Now, consider the condenser arranged as in Figure 13, with the electric field parallel to the disc faces. The total capacitance of the condenser, C^1, is now represented by a parallel combination of several large series capacitances, C_1 to C_6, where $C_1 \simeq C_2 \simeq \ldots \simeq C_6$ so that

$$C^1 = \varepsilon \frac{A}{S} \quad , \tag{4}$$

where A and S are the same as in (10).

Since $C^1 >> C$, the apparent dielectric constant ε must increase in order to justify the large value of C^1. The increase in ε is proportional to the corresponding increase in C^1.

For a randomly oriented electric field, the dielectric constants have been found to be determined by[5]

$$\varepsilon_y = \varepsilon_x = \varepsilon_f \left(1 + \frac{16Na^3}{3}\right) \quad , \tag{5}$$

where ε_x, ε_y are the dielectric constants parallel to the plane of disc orientation,

ε_z is the dielectric constant perpendicular to the plane of disc orientation,

N is the number of discs per unit volume,

a is the radius of the discs

and ε_f if the dielectric constant of the filler medium.

Large dielectric constants are possible, in the range of 70 or over, but factors such as breakdown strength of the dielectric restrict the dielectric constant values at operating voltages to the range of 20 to 40.

3.4.4 Practical Termination with an Anisotropic Dielectric

Electric stress control by an anisotropic dielectric can be applied

to high-voltage cable terminations. Figure 14 illustrates a cable end prepared for termination with a high dielectric constant material. The material is a tape wrapped contiguous to the cable insulation and extending over the cable insulation shield. The physical dimensions of the dielectric tape vary according to the operating voltage and tension applied during taping. Increasing the tape tension, and hence its elongation, causes a corresponding decrease in the dielectric constant of the tape.

The electric field distribution of a typical termination using high dielectric constant stress control is shown in Figure 15. Electric flux lines, originating from the conductor, are refracted at the boundary between the cable insulation and the high dielectric constant tape. The anisotropic dielectric is assumed to have a dielectric constant of 30, so that the electric flux lines are totally retained in the dielectric as they approach the shield. The electric stresses in the anisotropic material are considerably reduced. The normal electric field intensity component, E_N, is negligible as the equipotential lines are perpendicular to the interface, Figure 15. Only the E_t component contributes to the electric stresses, as indicated by the spacing of the equipotential lines parallel to the interface. A comparison of Figures 6 and 15 reveals a substantial reduction of the electric field intensity at the shield edge in the anisotropic material.

3.4.5 The High Resistance Method

The second method utilizes a high resistance material in place of the high dielectric constant tape. As before, the ground shield is extended so that a new edge along the material is at a higher potential than zero. At this edge, the potential to core is smaller than the

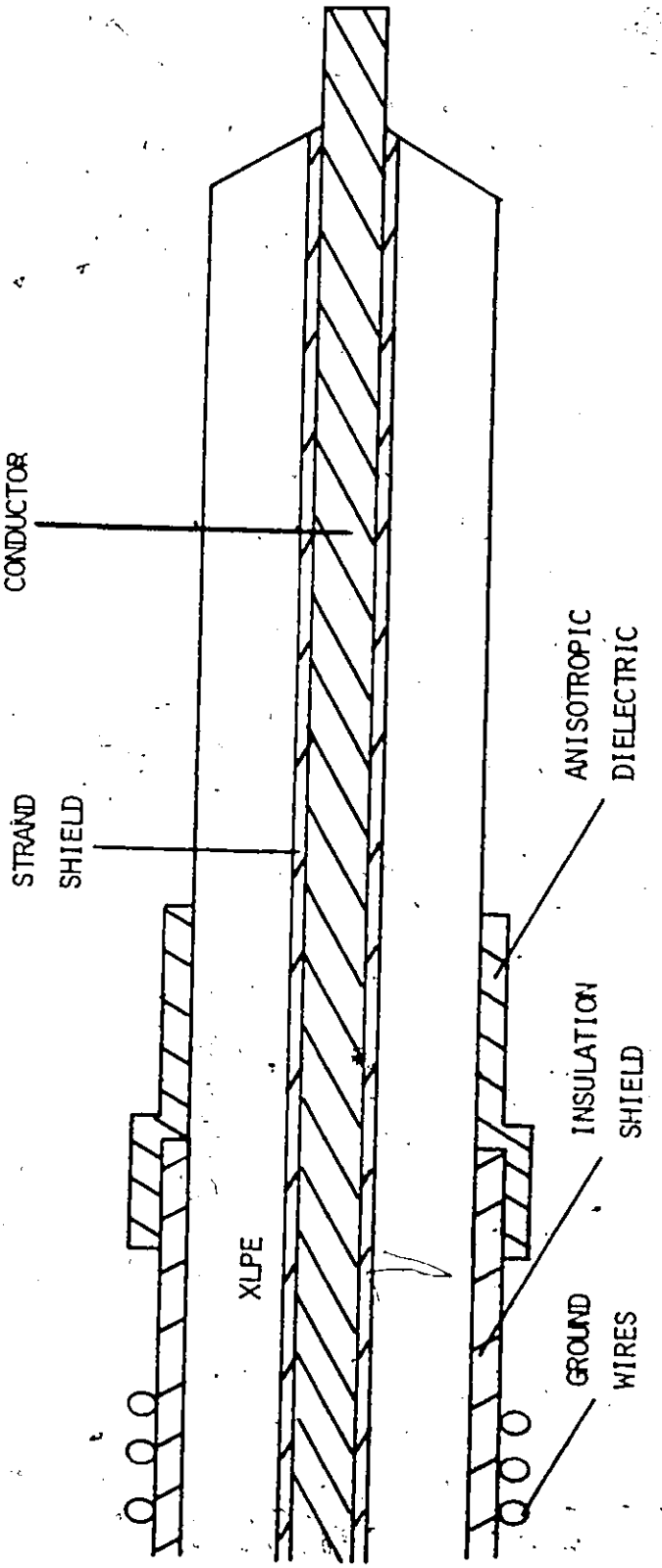

FIGURE 14: - CABLE TERMINATION EMPLOYING ANISOTROPIC DIELECTRIC

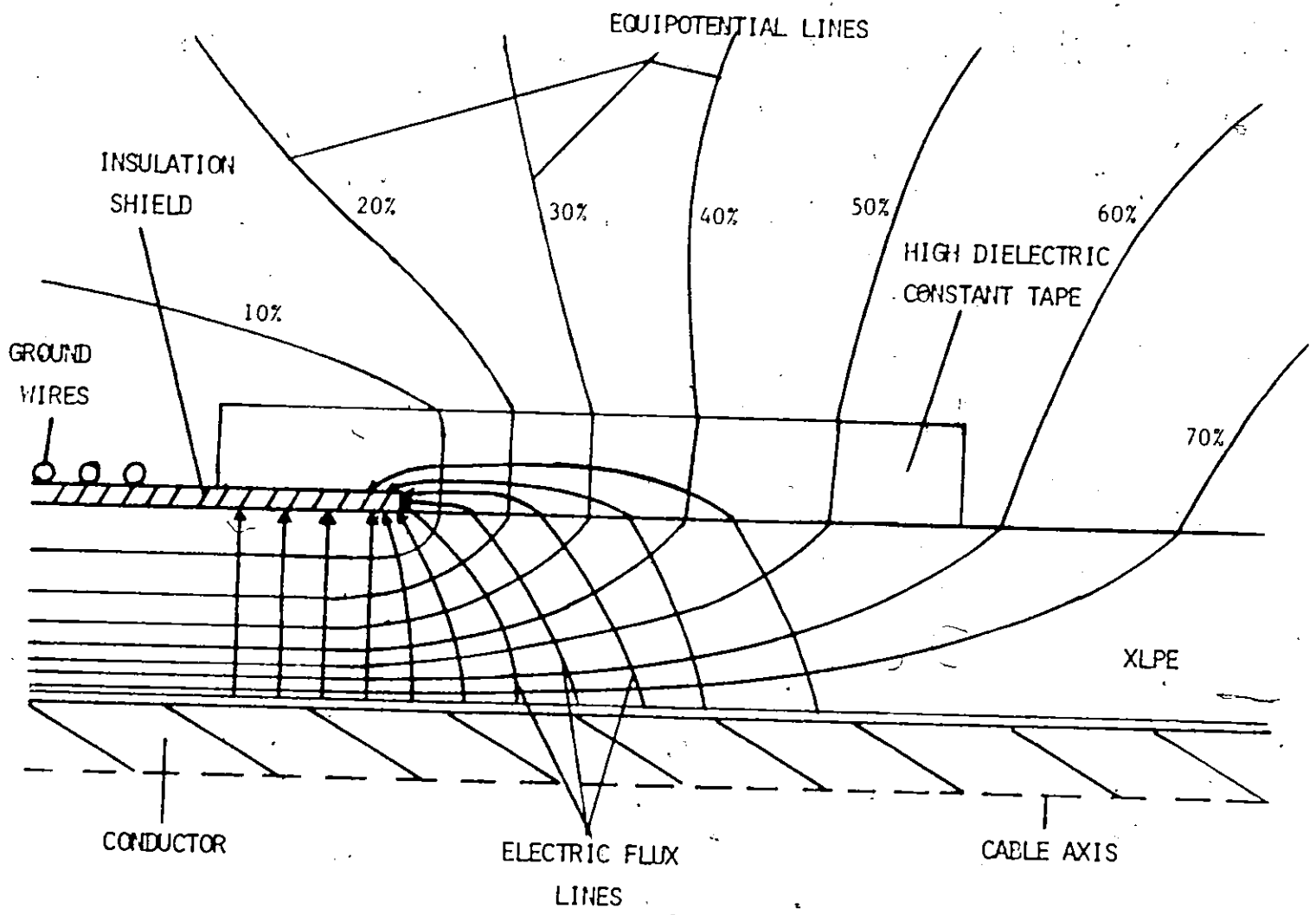

FIGURE 15: - ELECTRIC FIELD DISTRIBUTION IN A CABLE TERMINATION WITH AN ANISOTROPIC DIELECTRIC

operating voltage, hence, the field intensity at this point is reduced proportional to the decrease in potential. This arrangement can be explained by a distributed R - C parameter network.

3.4.6 Non-Linear Resistance Stress Control

The equivalent circuit of a resistive layer, applied on the cable insulation surface and in direct contact with the cable shield is shown in Figure 16(a). If the resistive layer's characteristics are linear, the resistance of each section is equal, namely,

$$\Delta r_1 = \Delta r_3 = \Delta r_3 = \Delta r_4 = \Delta r_x \tag{6}$$

The potential drop across the last terminating section is proportional to the displacement current flowing through the last section of the cable insulation.

$$\Delta U_1 = I_1 \Delta r_x \tag{7}$$

As the shield is approached, however, the potential drops increase because the displacement currents of each section combine. Near the shield,

$$\Delta U_4 = 4\Delta r_x (I_1 + I_2 + I_3 + I_4) >> \Delta U_1 \tag{8}$$

The potential drop across this section is much larger than across the sections further from the shield. A typical potential distribution along the linear resistance layer is shown in Figure 16(b). It can be seen that the potential distribution is non-uniform along the layer surface.

Consider a layer that exhibits non-linear voltage current characteristics. In such a layer, an increase in current is not accompanied by a proportional increase in voltage. A saturation effect is exhibited so that the increased current flow is accomodated

16B

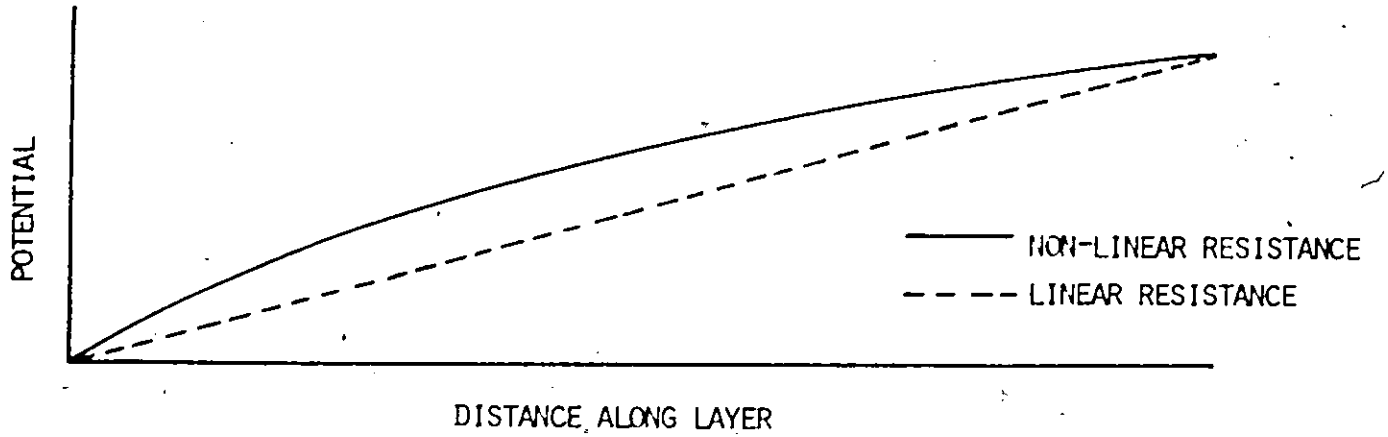

16A

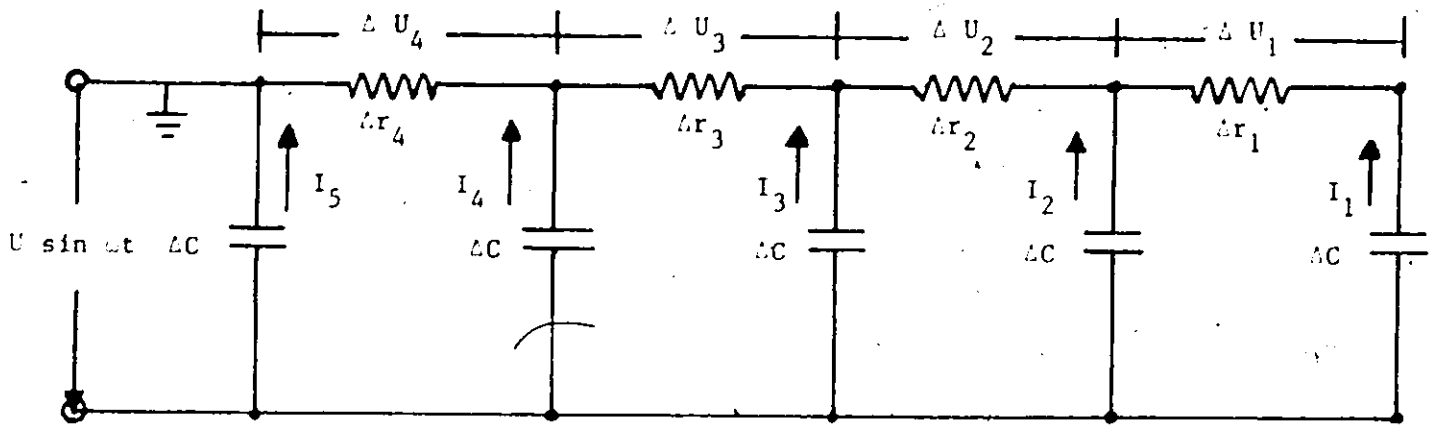

FIGURE 16A: - DISTRIBUTED PARAMETER EQUIVALENT OF RESISTIVE MATERIAL TERMINATION

FIGURE 16B: - VOLTAGE DISTRIBUTION ALONG LINEAR AND NON-LINEAR RESISTANCE MATERIAL

by a decrease in the resistivity of the layer.[6]

In Figure 16(a), the potential drop across the terminated section of the non-linear resistive layer is that given by equation (10). As the cable shield is approached the increasing displacement current through the insulation causes a corresponding decrease in resistivity of each successive section, so that

$$\Delta r_1 > \Delta r_2 > \Delta r_3 \rightarrow \Delta r_4 \qquad (9)$$

The potential drop across each resistive section is a function of the displacement current through the insulation. Consequently, the product of increasing current and decreasing resistivity toward the shield results in a potential distribution, such that

$$\Delta U_1 \simeq \Delta U_2 \simeq \Delta U_3 \simeq \Delta U_4 \qquad (10)$$

The potential distribution along the layer is now uniform, Figure 17(b) as, more or less, equal potential drops occur across each section of the layer.

3.4.7 Non-Linear Resistance Material

The material that exhibits non-linear resistivity consists of small silicon carbide particles in a resinous binder. The conducting silicon carbide is of the high resistivity type; namely, the volume resistivity , which decreases with the current density, varies from a few ohm-cm to several million ohm-cm. The resinous binder, has the property when exposed to air, to shrink so that the silicon carbide particles contact each other.

The current-voltage relation for the non-linear resistance material is described by[7]

$$I = KV^N \qquad (11)$$

where I is the current flowing through the material,

V is the applied voltage,

and K and N are constants.

K depends on the size and shape of the material while N depends only on the material. When N = 1, there is a linear relationship between V and I; namely, Ohm's Law. When N >1, a non-linear voltage-current relation exists.

The relation expressed in equation (14) applies for high current densities. Over the entire current range, the current-voltage relation of the material is

$$I = K^1V + KV^N \tag{12}$$

Typical values of N are in the range 4 to 8. Also, $K^1 >> K$. The added term is the linear Ohm's Law and predominates at low current densities, and hence, very high resistivity range. In the experimental investigation that follows only the second term is considered.

3.4.8 Experimental Determination of Non-Linear Resistivity

Resistivity measurements were conducted on two materials that are supposed to equalize the potential gradients along the surface of cable insulation. Both compositions consist of silicon carbide particles, one, Sikronil, being in a paste form and the other a paint, Coronux.

Thin layers of each composition were deposited by hand on cylindrical plexiglass (polymethyl methacrylate) tubes. After drying, a varying voltage was applied to the sample. The test circuit diagram is shown in Figure 17. The source used is a variable, regulated high-voltage A.C. supply. Current measurements are taken from the potential drop across the 10 kilohm resistor. Since the currents are of small order

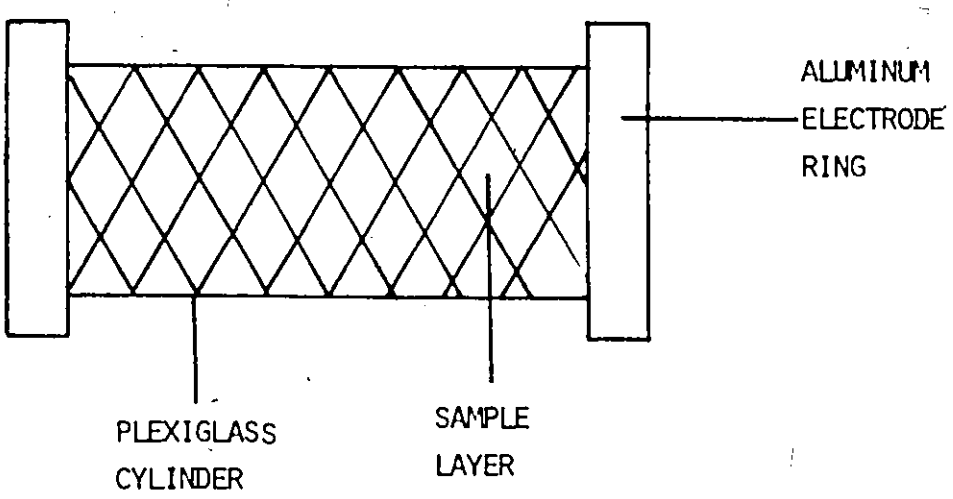

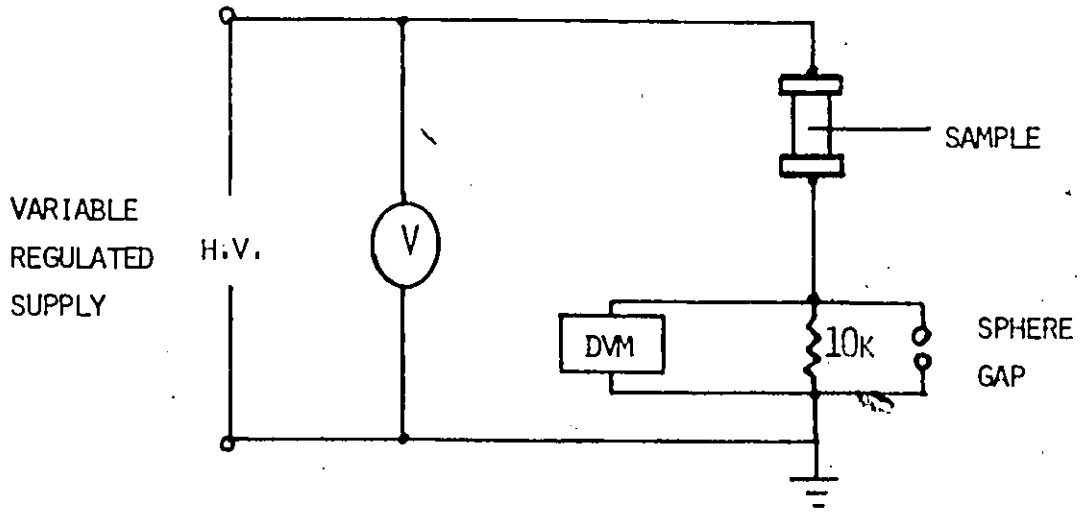

FIGURE 17: - TEST SAMPLE AND CIRCUIT FOR DETERMINING THE RESISTIVITY OF THE NON-LINEAR RESISTANCE PASTE AND PAINT

(10^{-6} amps), a highly sensitive digital voltmeter (DVM) was utilized. Current was assumed to flow only through the resistive sample layer, as the surface and volume resistivity of plexiglass is of a much larger magnitude. The non-linear portions of the surface resistivity of the samples are illustrated in Figure 18. The resistivity values, as obtained by measurements, are contained in two bands, the upper band for Coronux and the lower band for Sikronil. The bands represent the expected range of the resistivity when the layer is hand-applied. The scatter in resistivity is attributed to the non-uniform deposition of the respective layers. The bands illustrate effectively the non-linear voltage-current characteristics of the two resistive materials. It must be noted that the scale of the ordinate, Figure 18, is logarithmic.

3.4.9 Termination Using Non-linear Resistance Layer

Figure 19 shows a cable termination with a non-linear resistance layer. The layer is applied directly to the cable insulation surface and is connected to the insulation shield by means of a semi-conducting tape. Direct contact is avoided with the shield to prevent the formation of air pockets at the layer/cable insulation interface near the shield edge.

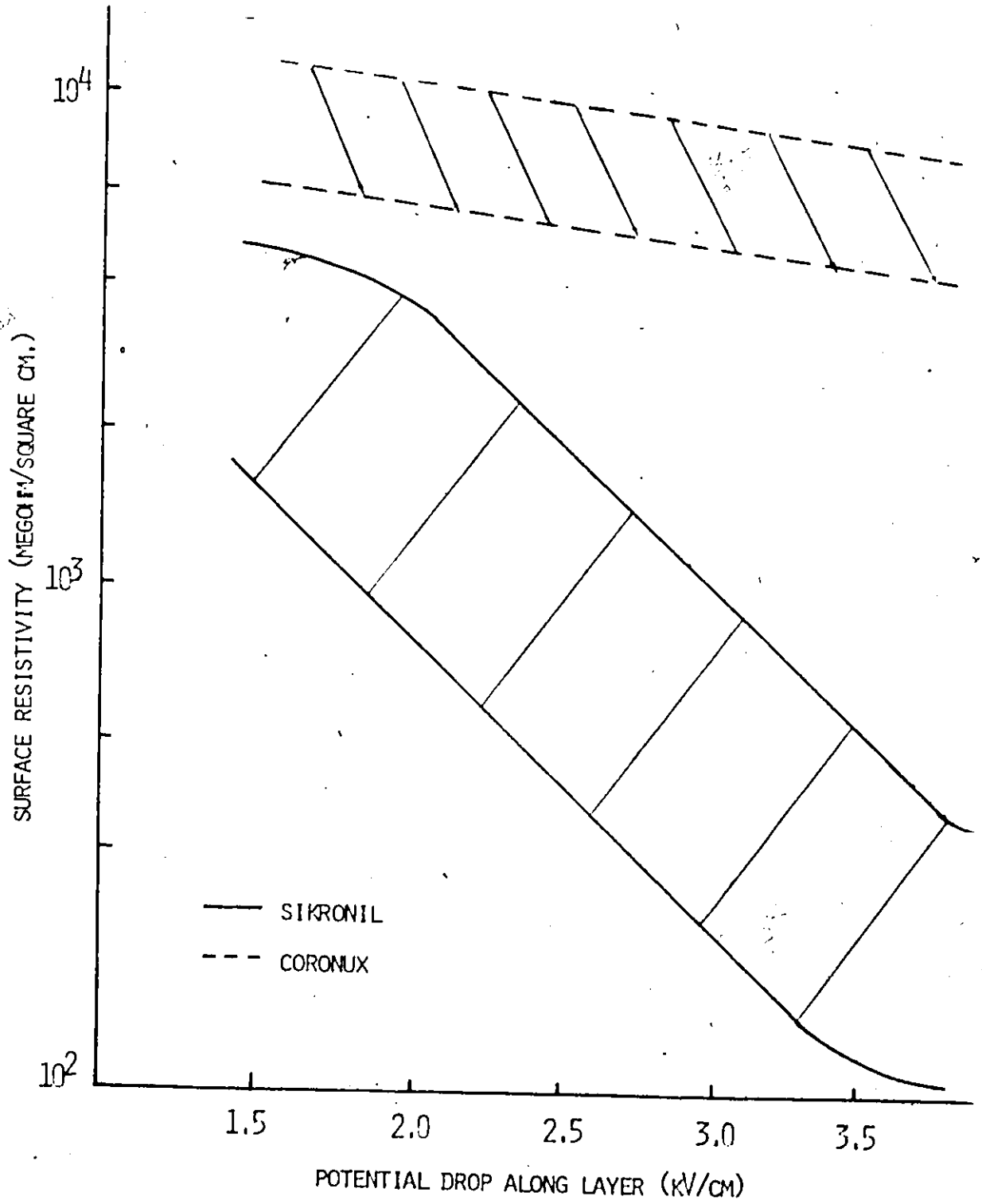

FIGURE 18: - RESISTIVITY VS. FIELD STRENGTH FOR SIKRONIL AND CORONUX

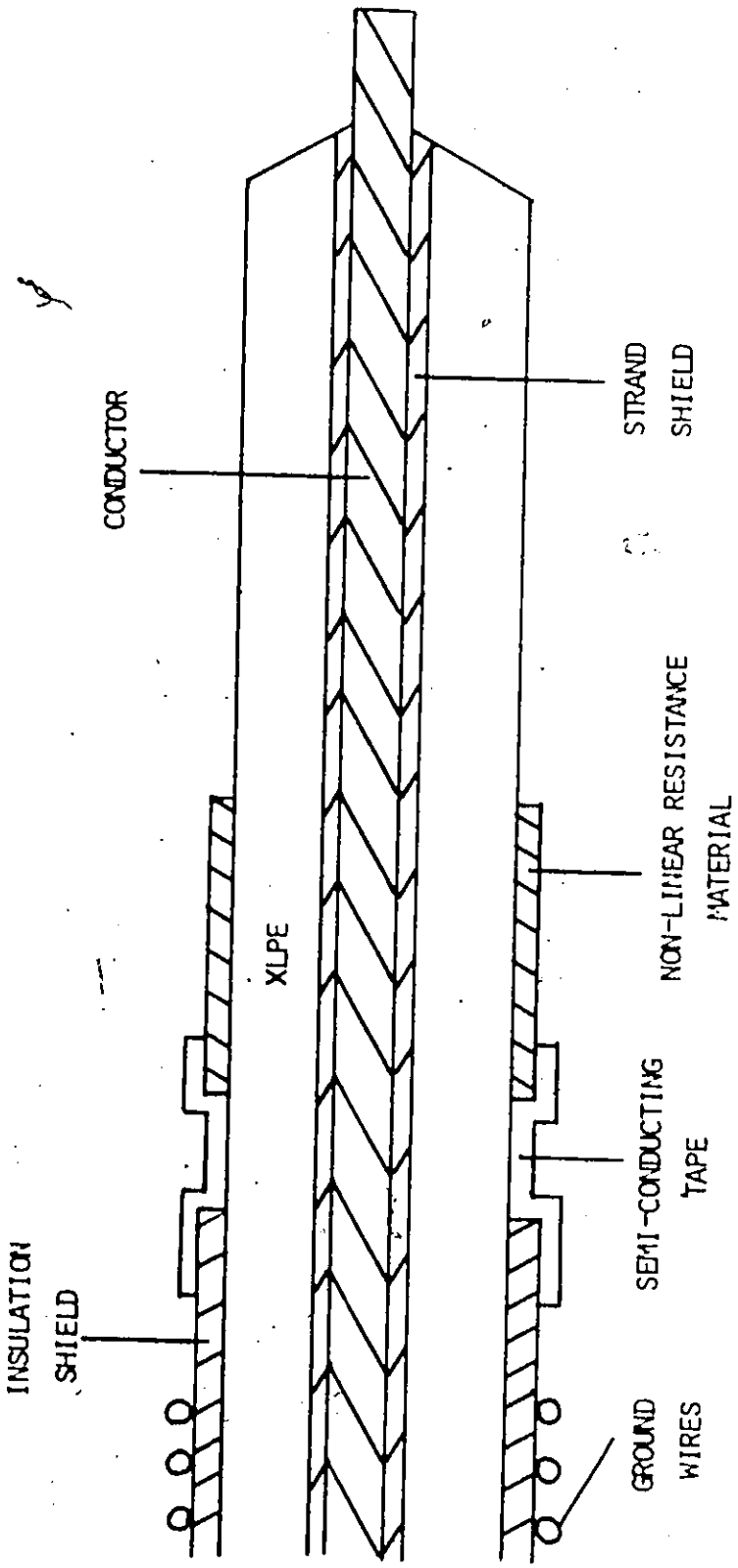

FIGURE 19: - CABLE TERMINATION UTILIZING NON-LINEAR RESISTANCE LAYER

CHAPTER 4

DETERIORATION OF INSULATION IN CABLES, SPLICES AND TERMINATIONS

4.1 Introduction

Satisfactory performance and life of cables, splices and terminations can be expected if electric stresses in the insulation do not exceed certain limits. However, manufacturing defects and poor workmanship often preclude a long-life operation. These factors introduce abnormally high electric stresses which can gradually deteriorate the insulation by chemical, electrical and mechanical actions. This deterioration of the insulation can ultimately lead to failure of the cable itself.

The deterioration of polymeric insulation in cables, splices and terminations is divided into two categories: bulk and surface phenomena.

4.2 Bulk Phenomena in Polymeric Insulation

4.2.1 Ionization

One of the most important electrical agents that enhances insulation deterioration is ionization manifested by electrical discharges. Any insulation, when subjected to certain voltages, exhibits effects of ionization. At low voltages, this may be a characteristic leakage current associated with foreign matter in the insulation. At higher voltages ionization is manifested by internal discharges or corona which may eventually cause dielectric breakdown. This failure is considered to be a function of the degree and duration of ionization.

The occurrence of ionization during service operation is the main concern in the problem of insulation deterioration. At normal operating voltages, ionization occurs because of unequal electric stress distributions in the cable insulation. This may be due to irregularities

on the conductor surface which result in localized high electric field intensities. The existence of air pockets or voids in these high stress regions is especially dangerous.

Air pockets and voids are subject to localized higher electric stresses or gradients, because of a lower dielectric constant than that of the surrounding insulation. At a critical value of the potential gradient or electric field intensity, ionization is initiated. This ionization may not cause an immediate breakdown, but a slow gradual deterioration of the insulation.

The effects of ionization in air pockets cause electro-chemical changes in the surrounding insulation. These changes are manifested by a concentration of highly ionized materials which, under high electric stresses, enhance further ionization. Chemical reactions, such as, oxidation, and the formation of water, acids and gases are the main agents of increasing deterioration of the insulation.

Oxidation reactions, produced by the ionization process, are especially harmful. These processes evolve ozone and atomic oxygen, which deteriorate the insulation through chemical reactions. The main chemical reactions associated with this type of deterioration are [9]

$$
\begin{aligned}
&O_2 + e \xrightarrow{K_1} 2\dot{O} + e \\
&\dot{O} + O_2 + M \underset{K_3}{\overset{K_2}{\rightleftarrows}} O_3 + M \\
&O_3 + \dot{O} \xrightarrow{K_4} 2O_2 \\
&O_3 + e \xrightarrow{K_5} O_2 + \dot{O} + e
\end{aligned}
\qquad (13)
$$

where M is a catalyzer molecule,

$K_1 \rightarrow K_5$ are the reaction rate constants

and $\cdot$ signifies free or reactive.

Ozone (O_3) is a powerful oxidant which attacks the main polymeric chain (carbon-to-carbon bonds) resulting in a scission of the chain [8]

$$R_1 \cdot \dot{C}H_2 + R_2 \cdot \dot{C}H_2 \xrightarrow{2O} R_1 \cdot \overset{\Omega}{C}H + R_2 \cdot \overset{\Omega}{C}H + 2H \quad (14)$$

where R represents the main chain of the polymer.

The hydrogen combines with oxygen to form water.

(15)

The presence of atomic oxygen causes the evolution of highly ionizable materials.

$$R \cdot CH = CH_2 + 2O \rightarrow HCOH + R \cdot COH \quad (16)$$

These aldehydes react with oxygen to form carboxylic acid, water and CO_2

$$HCOH + 2O \rightarrow H_2O + CO_2 \quad (17)$$

$$R \cdot COH + O \rightarrow R \cdot COOH \quad (18)$$

Secondary reactions also introduce other re-agents such as nitrogen oxides [9]

$$\begin{aligned} N_2 + e &\rightarrow 2\dot{N} + e \\ \dot{N} + \dot{O} + M_2 &\rightarrow NO + N_2 \\ \dot{N} + NO &\rightarrow N_2 + \dot{O} \\ \dot{O} + NO &\rightarrow NO_2 \\ \dot{N} + \dot{N} + M_3 &\rightarrow N_2 + M_3 \end{aligned} \quad (19)$$

The concentration of highly ionizable products as oxygen, NO_2 and NO enhance further reactions that produce heat and active oxidants. The end result is chemical degradation of the insulation leading to a possible breakdown.

4.2.2 Shrinkback

When splices and terminations are subjected to heat cycling, thermal expansion and contraction of the cable insulation occurs. The resultant longitudinal relieval of mechanical stresses, built up during the extrusion process, causes a shrinkback of the cable insulation. The extent of this potentially harmful phenomenon depends on temperature changes and the value of internal mechanical stresses. Shrinkback has been known to cause failures in splices or joints.

The effect of shrinkback on the geometry of a splice is illustrated in Figure 20a. The cable insulation recedes axially from the exposed conductor (ferrule), thus tearing the taped insulation. The air-voids at the interstices of the conductor strands are no longer covered by the semi-conducting tape. Mechanical stresses may force the voids into the taped insulation or the pencilled interface. High local electric field gradients at the conductor surface can cause ionization in the voids and subsequent deterioration of the surrounding insulation.

A new design, illustrated in Figure 20b, has been proposed by Mr. M. Kurtz of the Ontario Hydro, to eliminate the effects of shrinkback. A one-half inch of cable insulation (1/8 inch thick) is left exposed past the pencilled edge. Semi-conducting tape is applied up to point A, Figure 20b. If shrinkback does occur, the interstitial voids near the conductor are still covered by conducting tape and not exposed to high gradients.

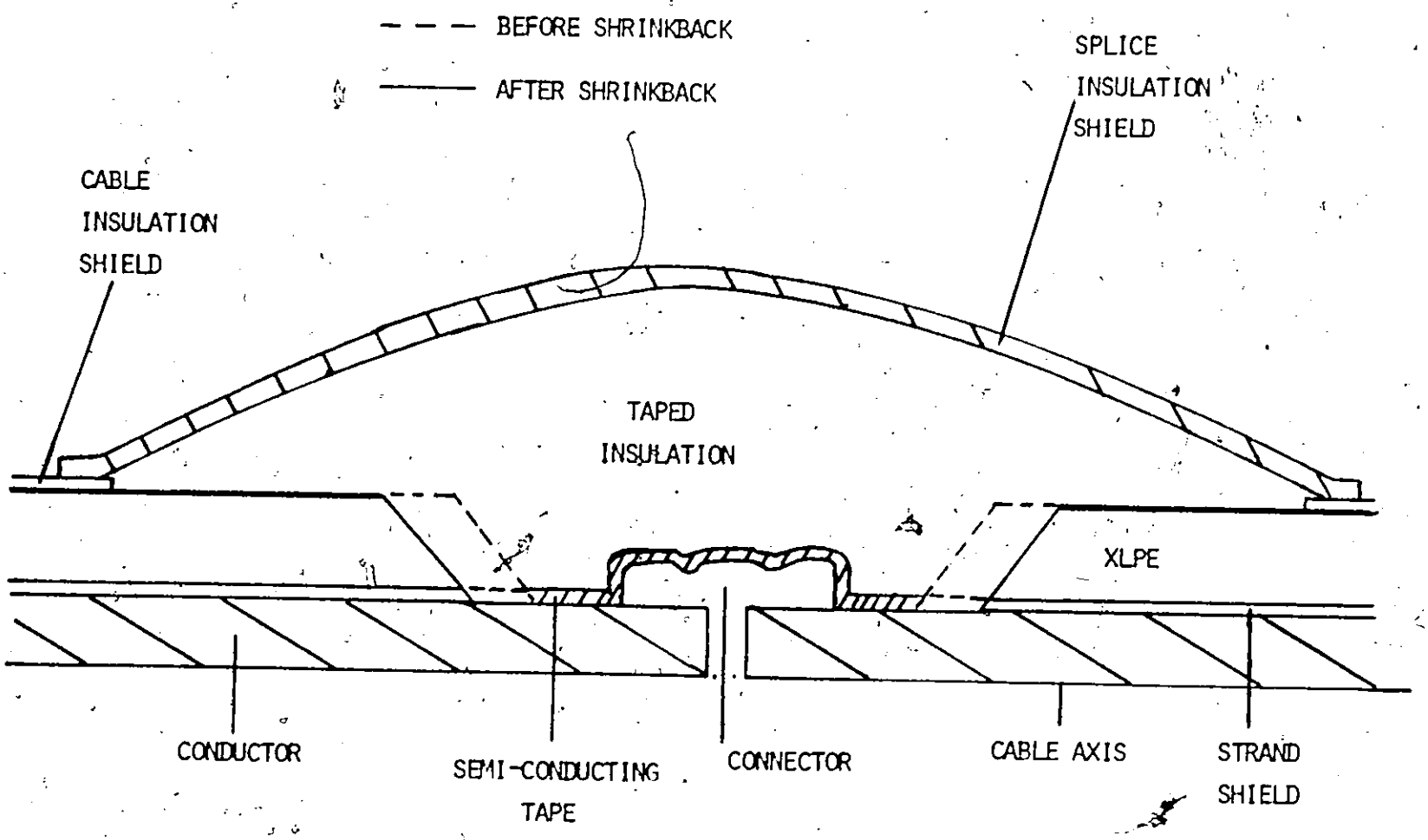

FIGURE 20A: - EFFECT OF SHRINKBACK IN A SPLICE

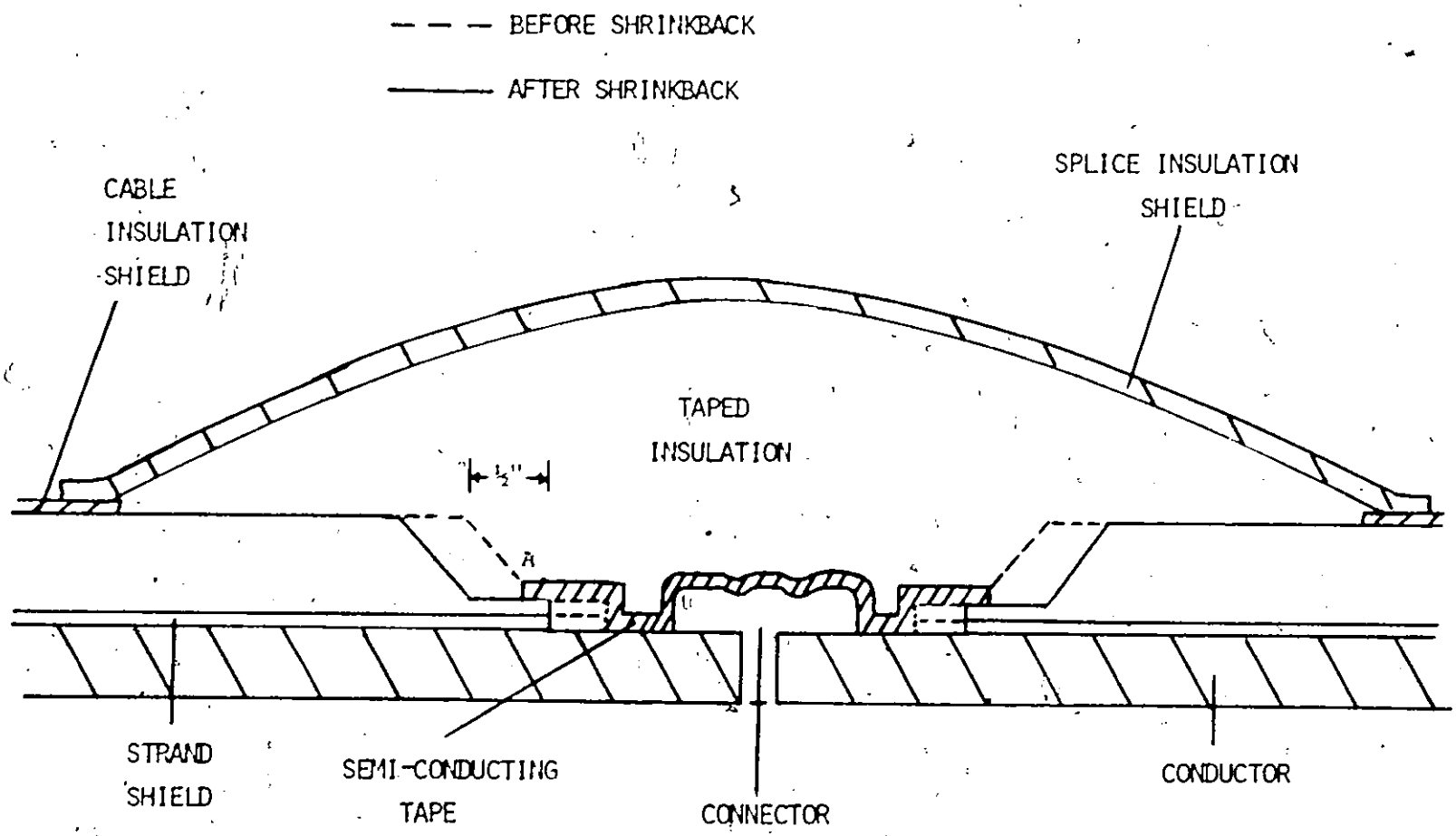

FIGURE 20B: - EFFECT OF SHRINKBACK IN A MODIFIED SPLICE

4.2.3 Treeing in Insulation

Treeing in insulation is recognized as a form of electrical and chemical deterioration which has been observed in nearly all types of insulation. The term "trees" describes fine branch-like microscopic channels which extend though the insulation and orient themselves in the direction of the applied electric field. Trees initiate from sharp irregularities on the conductor or shield and foreign particles, such as, conducting carbon contamination in the insulation. When extremely high localized stresses occur in these areas, microscopic breakdowns (bond scissions) are produced. An accumulation of such partial breakdown forms a long tree-like channel with little branches. Eventually the tree traverses the entire insulation and breakdown results.

Much research has been performed to clarify the treeing mechanism. Mason[10], studying corona breakdown in artificially created voids, has reported the propagation of fine channels that caused insulation failure. Kitchin and Pratt[11] have investigated the occurrence of several types of trees. They conclude that trees originate from surface contamination and impurities in the insulation.

Miyashita,[12] in studying polyethylene-insulated cables in water, found treeing at very low voltages. He ascribed tree growth to the interaction of water and the electric field and concluded that it was independent of corona discharges.

4.3 Surface Phenomenon in Organic Insulation

Surface tracking is a form of electrical breakdown, characterized by progressive deterioration of the dielectric surface by minute local discharges or arcs which may lead to breakdown. Surface tracking is classified into two types: conduction at operating voltage and

discharges that occur at higher voltage surges.

When an insulation surface is exposed to moisture and pollution contaminants, the surface resistivity decreases leading to excessive local surface current densities and dry bands are formed. The potential gradient across the dry band may be sufficient to cause an arc to be struck along this dry band. The arcing and the resultant heat generation can cause local carbonization and carbon tracks. Over an extended time period, surface tracking may proceed to a flashover.

At high surge voltages, tracking may be initiated by localized corona discharges at various points on the insulation surface. These discharges deteriorate the surface by evolving highly ionizable materials, such as, ozone and nitrogen oxides which in turn produce carbon. The accumulation of carbon causes tracks which decrease the effective insulation surface length, and a total surface breakdown takes place.

CHAPTER 5

ELECTRIC FIELD DISTRIBUTIONS IN SPLICES AND TERMINATIONS

5.1 Introduction

A study of the electric field distribution is an essential tool in the improving of existing and assessing of new satisfactory designs of splices and terminations. When analyzed, the distribution predetermines, to some extent, the life and performance of practical splices and terminations.

The two-dimensional axially-symmetric field distributions, can be determined by analytical and analogue methods. The analytical method utilizes numerical techniques and, hence, requires computer programming. Resistive networks, electrolytic tanks and conductive paper are most commonly employed in the analogue studies.

In the present investigations, at first, the conductive paper Teledeltos was used to form the analogue for the study of the electric field distribution. This analogue evidenced unacceptable inaccuracies due to plotting errors and inability to simulate different dielectric media. Since similar differences would be encountered in electrolytic tanks, the analogue method was discarded in favour of a suitable computer aided numerical solution.

5.2 Finite-Difference Techniques

The field in splices and terminations is defined by Laplace's equation in three dimensions with one axis of symmetry, hence, it is reducible to a two-dimensional problem. The solution of the electric field distribution by finite-differences involves three steps:

1) superimposing a square grid network over the entire region of interest,

2) replacing Laplace's partial differential equation by finite-

-difference equations in terms of the field at each grid intersection or node point,

3) solving the finite-difference equations for values at each node.

Any numerical method provides only an approximate solution to the exact field distribution. The degree of accuracy depends on the computation time.

Iterative methods have been successfully utilized to decrease the computation time and, hence the cost. By using Successive-Over-Relaxation (S.O.R.), the node potentials are continuously updated after each iteration. When the difference between the node potentials between subsequent iterations of node potentials is less than a predetermined value, the solution is considered to be final.

The development of the preceeding finite-difference techniques and application to the determination of the field distribution in splices and terminations is described in Appendix A. A general digital program, including a flow chart, utilizing the S.O.R. numerical method is presented in Appendix B.

5.3 Practical Splice and Termination Field Computations

Numerical techniques, with the aid of a digital computer, enable the plotting of field distributions; namely, equipotential and electric flux lines. From the plots, the location and, hence, reduction of localized high field gradients are possible. The gradient or the field intensity is inversely proportional to the distance between the equipotential lines. Hence, where the lines are most crowded are the regions of the highest gradient.

The magnitude of the potential gradients indicates the electric stresses to which the insulation and voids in the insulation are subjected.

When a critical gradient value is reached, electrical discharges are initiated in the insulation even without the presence of a void. With a void, however, corona discharges will occur at a lower gradient value which is determined by the electric stress distribution. Figure 21 illustrates the field distribution of an insulated cable with a void situated at the surface of the current carrying conductor. The introduction of the void causes a distortion of the field as shown by the bending of the equipotential lines toward the void. The higher concentration of equipotential lines in the void indicates higher local gradients in the void. The concentration of these gradients is an inverse function of the dielectric constant.

It must be noted that the concentric neutral type cable has been used exclusively in the splice and termination designs investigated in Chapter 5 and 6. The specifications of the cable are:

Operating Voltage: 27.6 kV phase-to-phase

Conductor: No. 1/0 stranded aluminum (19 strands)

Strand Shielding: extruded semi-conducting polyethylene

Insulation: 0.280 inch wall of XLPE

Insulation Shielding: extruded semi-conducting polyethylene

Concentric Conductor (shield): 15 No. 14 AWG tinned copper wires wound helically over the insulation shield

5.3.1 Analysis of Field Distribution in a Splice

An electric field study has been made of a cable splice designed by the Windsor Utilities for the 27.6 kV underground distribution system. An analysis of the field distribution has revealed three critical areas, A, B and C in Figure 22a. These are located on the conductor surface and near connector irregularities, where local field gradients are high.

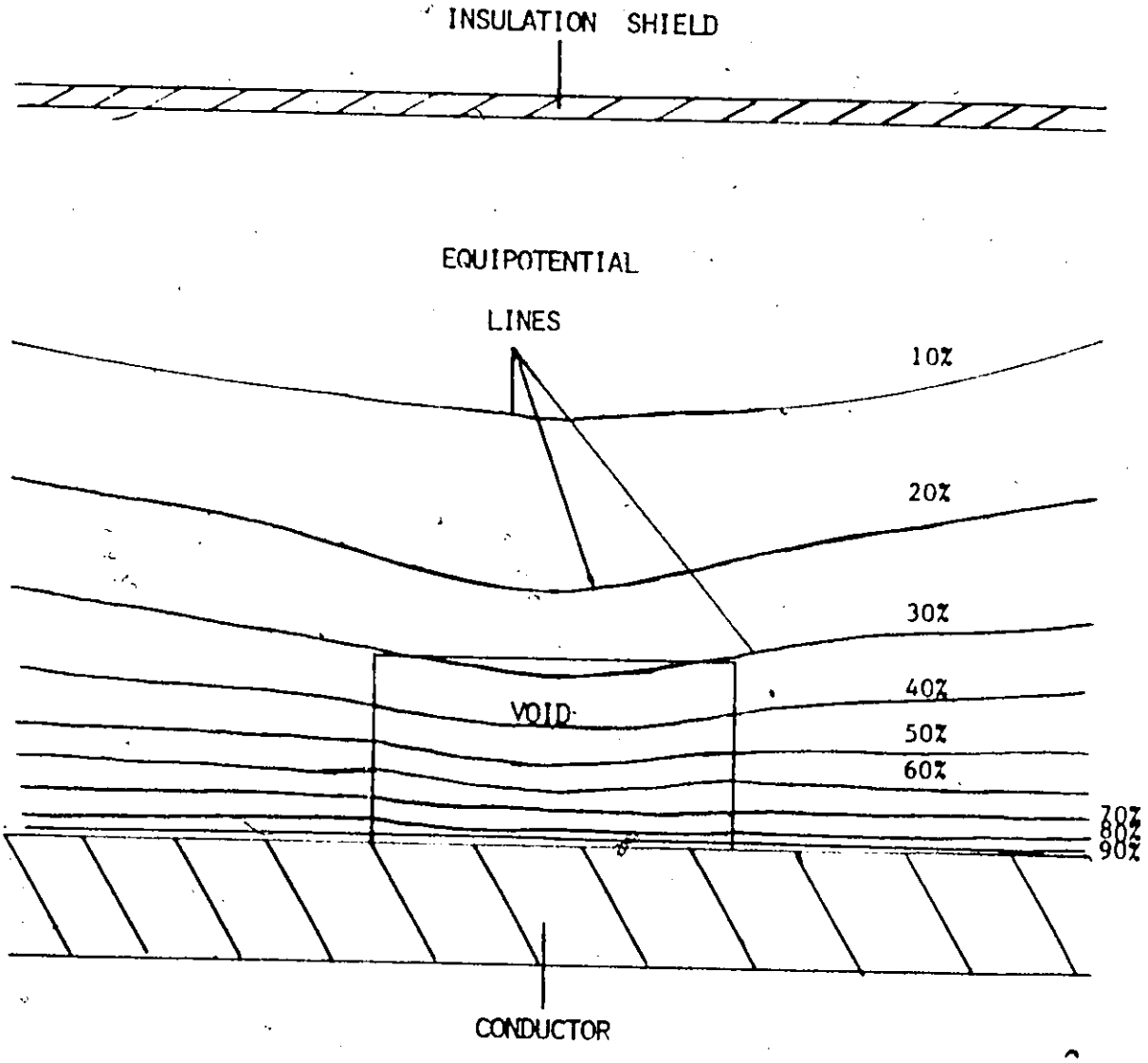

FIGURE 21: - EFFECT OF VOID NEAR THE INSULATED CONDUCTOR ON THE ELECTRIC FIELD DISTRIBUTION

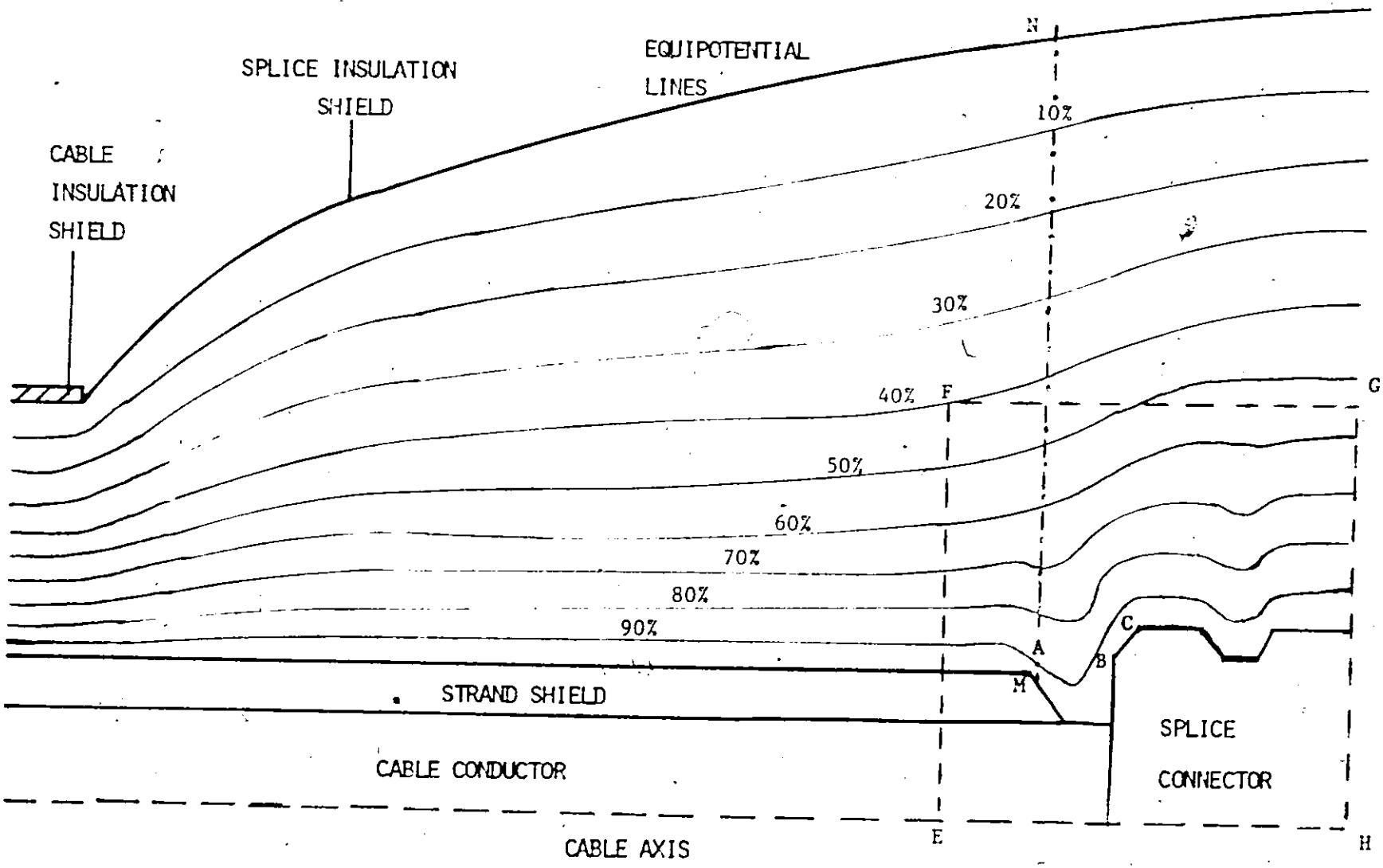

FIGURE 22A: - FIELD DISTRIBUTION IN A WINDSOR UTILITY SPLICE DESIGN

A distortion of the normally uniform radial field introduces a large tangential or axial gradient component.

An enlarged model was constructed to study accurately and in detail the small regions where the potential gradients are high. The field distribution of such a model is illustrated in Figure 22b. The boundary of this model, EFGH in Figure 22a, consists of fixed potentials obtained from a field solution of the larger model. Intermediate potentials along the boundary were fixed by linear interpolation from the known potentials in the larger model.

When insulating tape is used to build up the splice insulation, air pockets or voids may be formed at the exposed conductor and connector surface. These voids may ionize, causing insulation damage, if the potential gradients are of a sufficient magnitude. The effect of such voids on the potential gradient distribution in the three critical regions, A, B and C in Figure 22a is shown in Table I. The voids were assumed to be rectangular and 0.0125 by 0.05 inches in size. The term "RATIO" in the first column of the table represents the ratio of the maximum potential gradient in insulation with a void to that without a void.

Examination of the table reveals that the maximum gradients in regions A, B, C of Figure 22b are all near or above the gradient value required to ionize air; namely 70 peak kV/inch. If voids were introduced in these regions, the maximum potential gradients increase by 30 to 35%. At these increased values, the voids will ionize and cause insulation deterioration.

The effect of a void on the potential gradient distribution in a splice is shown in Figure 23. The gradients plotted are those along a

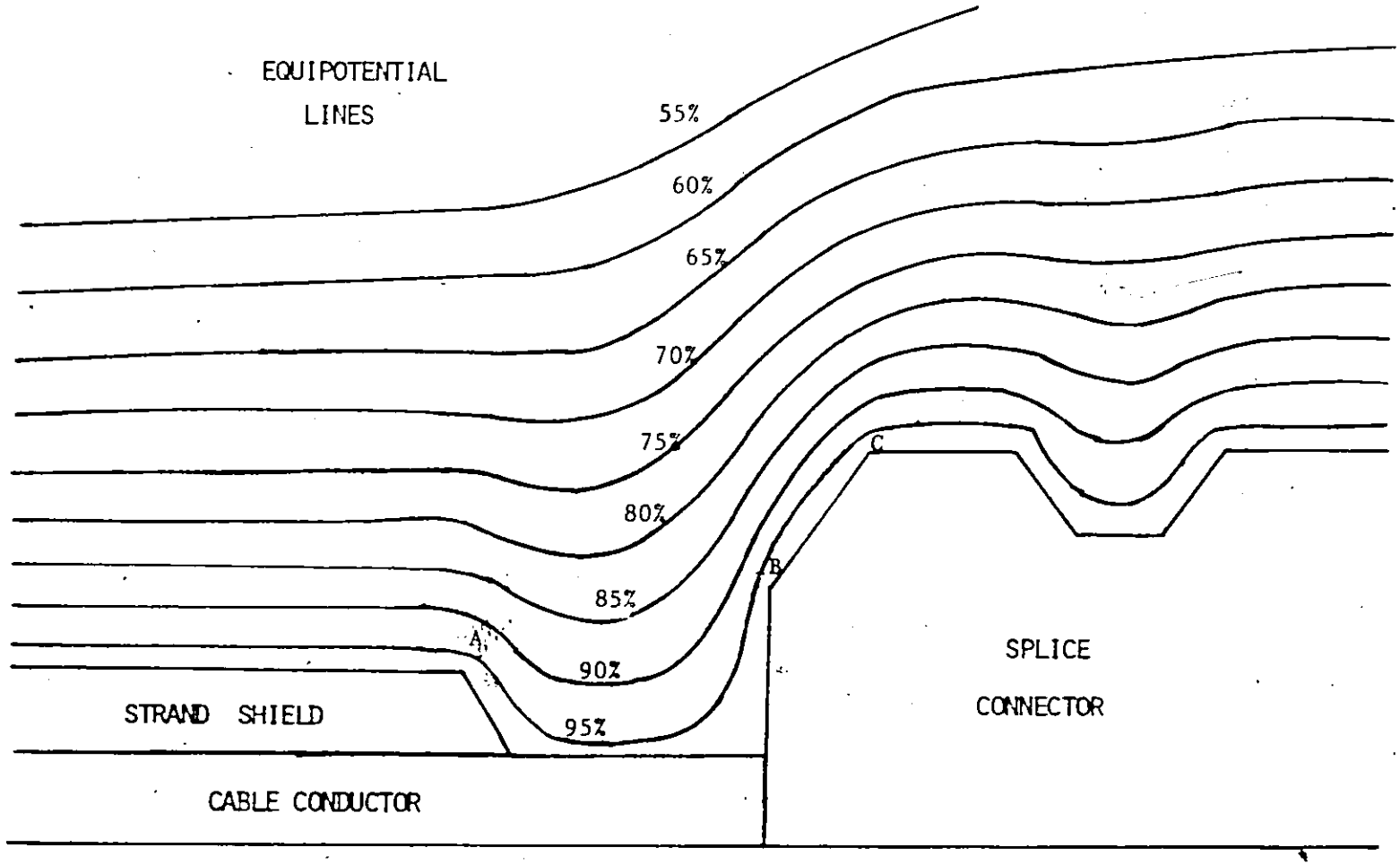

FIGURE 22B: - FIELD DISTRIBUTION IN THE ENLARGED REGION OF THE WINDSOR UTILITY SPLICE DESIGN

TABLE I:

EFFECT OF VOIDS ON GRADIENTS IN CRITICAL HIGH STRESS REGIONS IN A WINDSOR UTILITY SPLICE

GRADIENT (KV/IN)	PRESENCE OF VOID IN REGION	GRADIENTS (KV/IN) IN REGION OF INTEREST		
		A	B	C
MAXIMUM	NO VOIDS	78.8	67.8	69.4
AVERAGE		53.9	49.2	55.8
RATIO		1.0	1.0	1.0
MAXIMUM	VOID IN REGION A	107.2	67.8	69.4
AVERAGE		64.0	49.2	56.3
RATIO		1.36	1.0	1.0
MAXIMUM	VOID IN REGION B	78.8	88.3	69.4
AVERAGE		53.9	62.0	56.3
RATIO		1.0	1.30	1.0
MAXIMUM	VOID IN REGION C	78.8	70.9	94.6
AVERAGE		53.9	50.4	67.0
RATIO		1.0	1.05	1.36

NOTE: THE OPERATING VOLTAGE IS 16.0 KV PHASE-TO-GROUND.

radial line, MN in Figure 22a, from the conductor surface, through a void in region A and through the splice insulation to the insulation shield. At the conductor surface, the void causes a 35% increase in the gradient, point Z, as compared to the gradient if the void were not present. The splice insulation immediately adjacent to the void experiences a decrease in gradient as indicated by the sudden drop of the gradient curve at point X. The peaking of the gradient in the voidless insulation, point Y in Figure 23, is attributed to the non-uniform field near the connector. If the field were uniform, as in a continuous cable, the gradient curve would decrease exponentially.

5.3.2 Field Distribution in a Cable Prepared for Termination

A comparison was made of the electric field distribution in a continuous cable and that of a cable end prepared for termination. A high localized potential gradient exists at the shield edge discontinuity, Figure 24. It can be seen from the figure that approximately 70% of the operating voltage (16 kV phase-to-ground) appears along the first 3/8 inch of exposed cable insulation. The high tangential component of the field intensity at the shield edge, can initiate surface tracking as the breakdown strength along the surface is much less than through the bulk. In the continuous cable, however, only the radial component of the field intensity exists, hence, no tangential gradients are present near the external shield.

At the operating voltage, the potential gradient at the shield edge, region W in Figure 24, was found to be approximately 116 kV/inch if the cable described in section 5.3, page 50 were prepared for termination. As this value is well above the critical gradient, approximately 70 peak kV/inch, required to ionize the air, corona

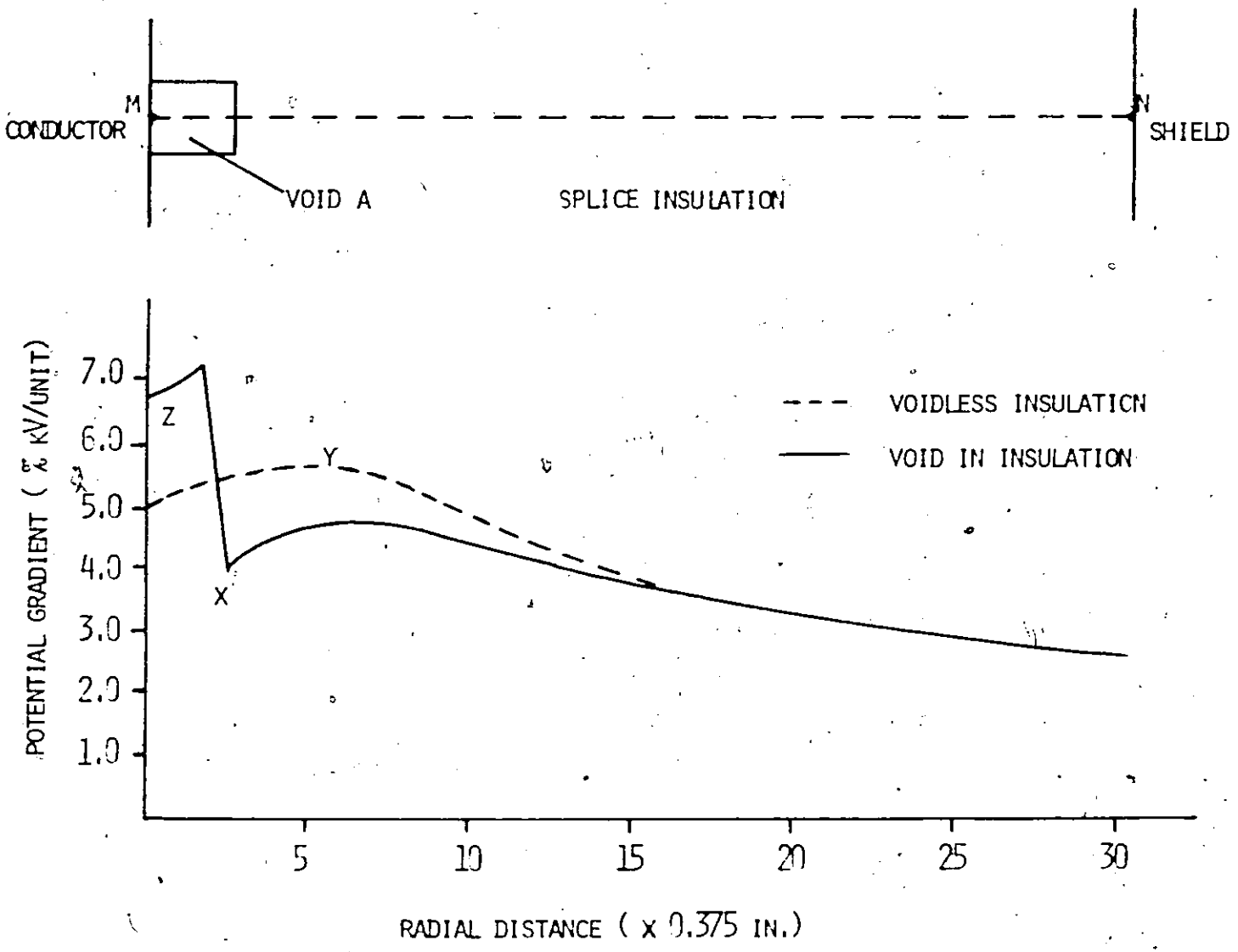

FIGURE 23: - EFFECT OF VOID ON THE POTENTIAL GRADIENT DISTRIBUTION THROUGH THE SPLICE INSULATION

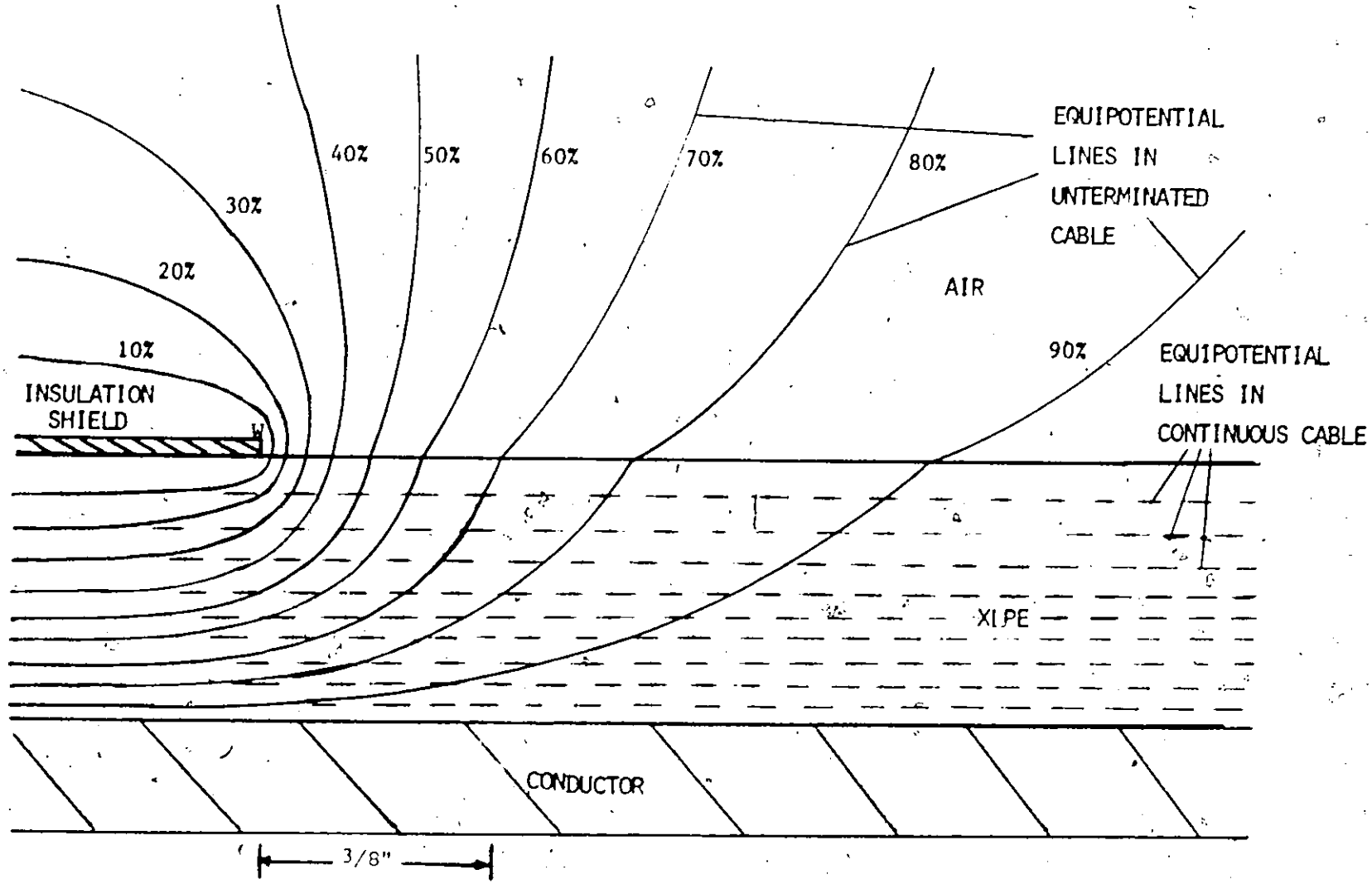

FIGURE 24: - FIELD DISTRIBUTION IN CONTINUOUS CABLE AND CABLE PREPAPED FOR TERMINATION

discharges will occur at the shield edge during normal operation.

5.3.3 Field Distribution of Capacitive Cone Termination

For comparison purposes, the electric field distribution of two capacitive cone terminations of different designs was analyzed. One cone has been designed by the Windsor Utilities and the other by the Ontario Hydro. The field patterns were found to be almost identical, within 5%, hence, only the Windsor Utilities field distribution is discussed. The results also apply to the Ontario Hydro design.

Figure 25 illustrates the potential distribution of a capacitive cone termination utilized by the Windsor Utilities. Analysis has shown that the largest gradients occur at the surface of the conductor and at the terminating point of the conducting slope. At the termination point, point L in Figure 25, the maximum gradient is 54.5 kV/inch, which is a reduction of more than 50% compared to the shield edge in the unterminated cable. This reduction in the potential gradient is attributed to the slope of the conducting portion of the cone and the increased insulation diameter. The slope of the stress cone reduces the axial component of the gradient while the increased radius of the insulation decreases the radial component.

Because the cone is built-up by wrapping tape, voids may be formed at the cone/cable insulation interface and along the conducting slope, regions I, J and K in Figure 25. If the potential gradient exceeds a critical value in these regions, the voids may ionize and deteriorate the insulation. The effect of these voids on the potential gradient discribution is summarized in Table II. The rectangular voids are 0.05 by 0.1 inches in size. Examination of Table II reveals that a void in region J causes a 46% increase in the potential gradient, while

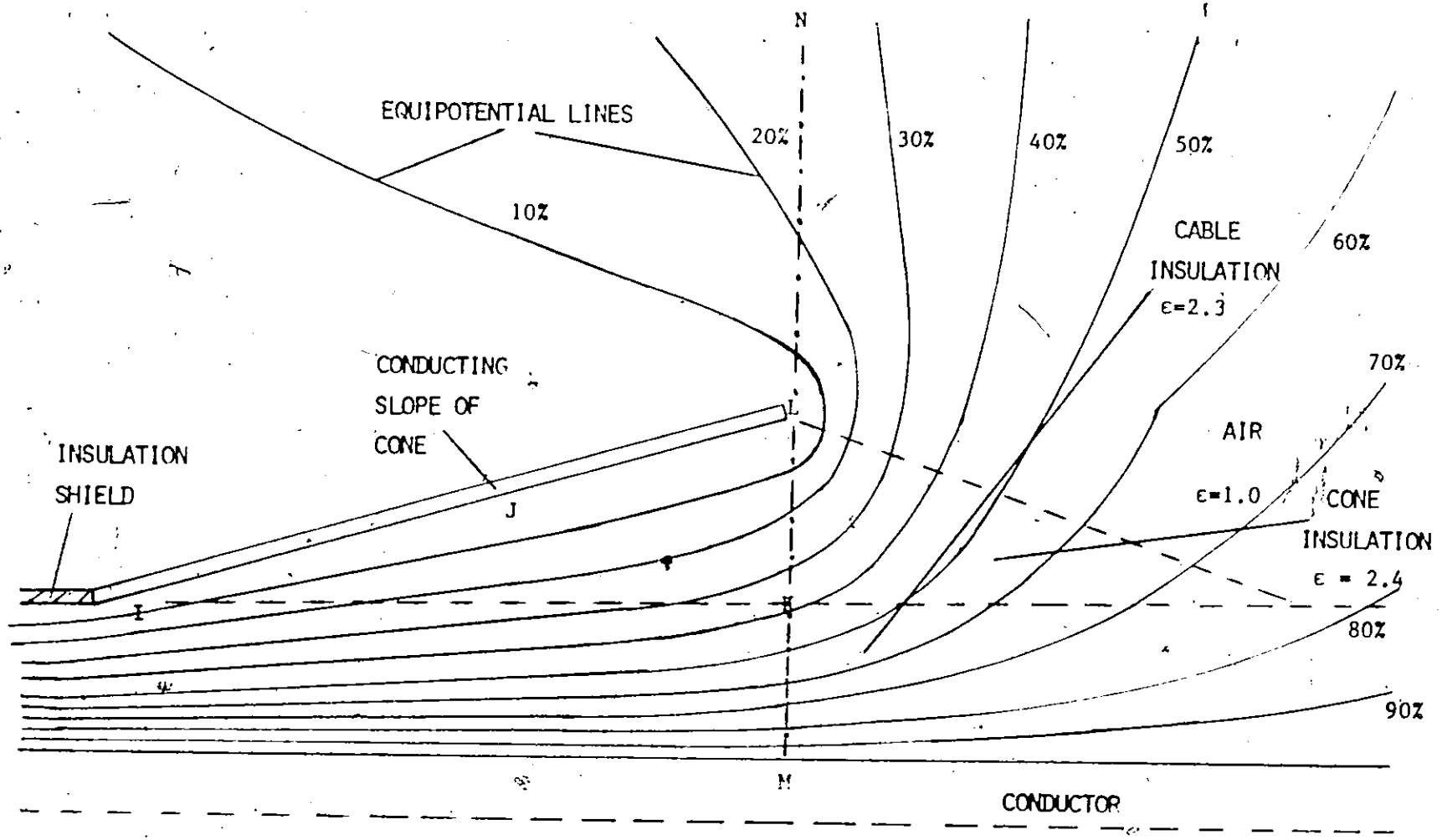

FIGURE 25: - FIELD DISTRIBUTION OF WINDSOR UTILITY TERMINATION DESIGN

TABLE II

EFFECT OF VOIDS ON GRADIENTS IN CRITICAL REGIONS IN WINDSOR UTILITY CAPACITIVE CONE TERMINATION

GRADIENT (KV/IN.)	PRESENCE OF VOID IN REGION	GRADIENTS (KV/IN) IN REGION OF INTEREST		
		I	J	K
MAXIMUM	NO VOIDS	30.2	22.5	20.7
AVERAGE		26.6	20.7	16.8
RATIO *		1.0	1.0	1.0
MAXIMUM	VOID IN REGION I	32.9	22.5	20.7
AVERAGE		27.4	20.7	16.8
RATIO		1.09	1.0	1.0
MAXIMUM	VOID IN REGION J	32.2	32.9	20.7
AVERAGE		32.2	25.8	16.7
RATIO		1.0	1.46	1.0
MAXIMUM	VOID IN REGION K	30.2	22.5	26.6
AVERAGE		32.2	20.7	25.1
RATIO		1.0	1.0	1.28

NOTE: OPERATING VOLTAGE IS 16.0 KV PHASE-TO-GROUND

* RATIO INDICATES THE RATIO OF THE MAXIMUM GRADIENT WHEN A VOID IS PRESENT IN INSULATION TO THE MAXIMUM GRADIENT IN UNIFORM INSULATION WITHOUT A VOID

in region K the increase is only 28%.

Figure 26 illustrates the distribution of potential gradients which can also be shown as a graph of potential gradient versus distance along a selected radial line through the insulation, MN in Figure 25. In the graph, the gradient distribution in uniform insulation against insulation with a void is compared. From Figure 26, it can be seen that the potential gradient decreases at the void/insulation interface nearest the conductor, point D, and is largest within the void, point E. The gradient rise at point F is due to the proximity of the stress cone tip and the high local gradient associated with it.

5.3.4 High Dielectric Constant Tape Termination

The field distribution of a termination utilizing a high dielectric constant tape ($\varepsilon = 30$), is shown in Figure 27. The potential gradient at the shield edge was found to be 18 kV/inch, which is a reduction of 85% as compared to the unterminated cable. The gradient reduction is attributed to a decrease of the radial component to a negligible value. In addition, the tangential gradients have been more uniformly distributed along the cable insulation surface as compared to the unterminated condition. This is indicated by the increased spacing between the equipotential lines.

The wrapping of the high dielectric constant tape, may form voids at the tape/cable insulation interface. The effect of voids in two regions, G and H in Figure 27, along this interface is illustrated in Table III. The rectangular voids are 0.025 by 0.05 inches in size. The presence of a void near the shield edge, region G, increases the potential gradient threefold whereas a void in region H, raises the gradient by only 33%.

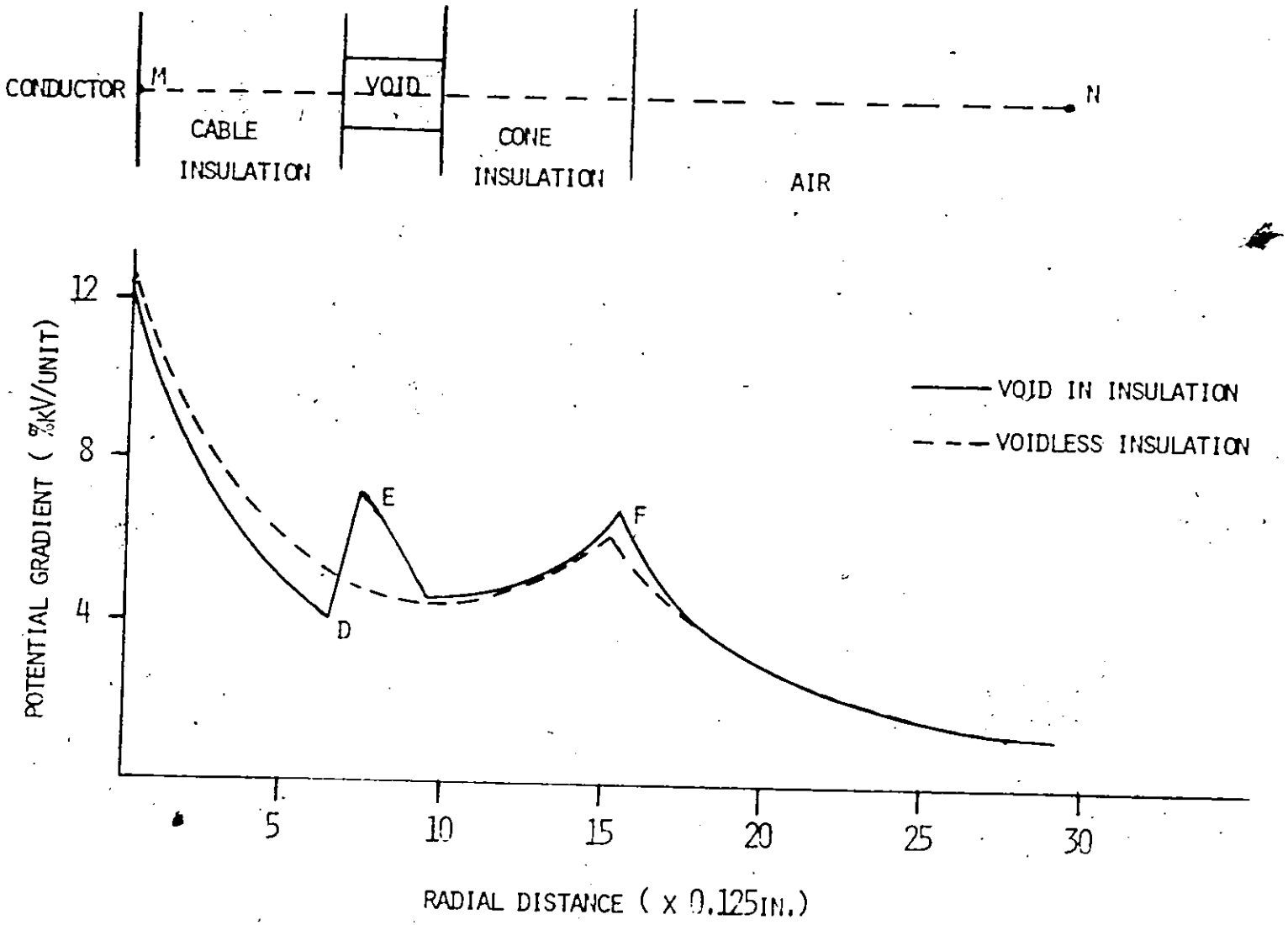

FIGURE 26: - EFFECT OF VOID ON FIELD DISTRIBUTION IN A WINDSOR UTILITY TERMINATION DESIGN

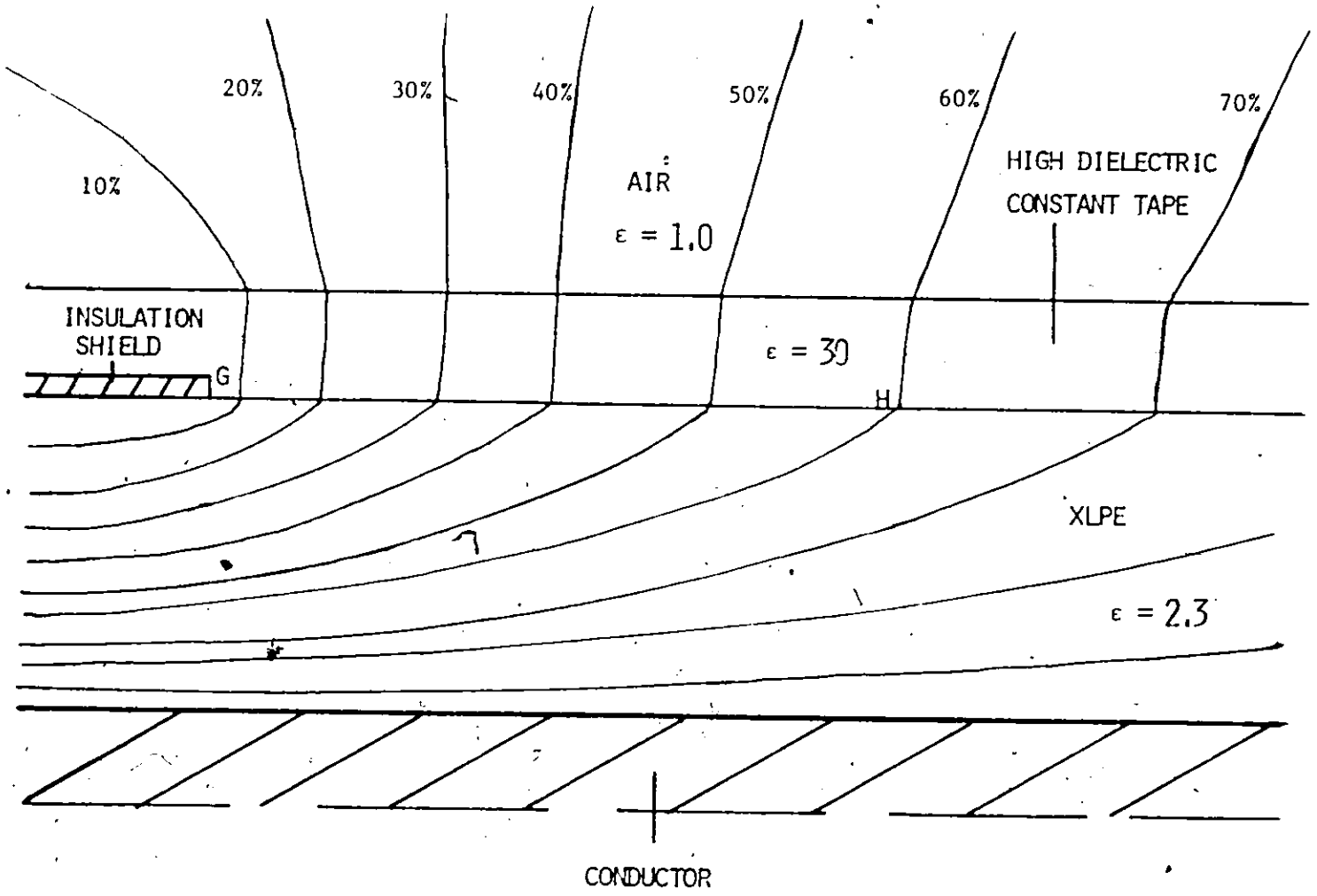

FIGURE 27: - FIELD DISTRIBUTION IN HIGH DIELECTRIC CONSTANT TAPE TERMINATION

TABLE III:

EFFECT OF VOIDS ON GRADIENTS AT CRITICAL REGIONS IN A HIGH DIELECTRIC CONSTANT TAPE TERMINATION

GRADIENT	PRESENCE OF VOIDS	REGION OF INTEREST (GRADIENTS KV/IN)	
		G	H
MAXIMUM	NO VOIDS	18.02	8.11
AVERAGE		16.82	4.43
RATIO		1.0	1.0
MAXIMUM	G	56.78	2.7
AVERAGE		28.85	2.7
RATIO		3.15	.33
MAXIMUM	H	18.02	10.81
AVERAGE		16.82	4.96
RATIO		1.0	1.33

NOTE: APPLIED VOLTAGE IS 16.0 KV PHASE-TO-GROUND

The dimensions of the built-up high dielectric constant insulation have a pronounced effect on the gradients distributed along the tape/cable insulation interface. Figures 28 and 29 show the dependence of the gradient on the number of layers and length of tape in regions G and H of Figure 27, respectively. From the graph of Figure 28, a two inch length of four layers of high dielectric constant tape would be optimum in minimizing the potential gradient at the shield edge.

5.3.5 Non-Linear Resistance(Sikronil) Termination

A cable employing a non-linear resistance layer for voltage distribution purposes can be approximated by the equivalent circuit in Figure 30. The potential distribution along the layer from right to left is defined by the following system of differential equations.[6]

$$\frac{dU_o}{dt} = \omega U^1 \cos\omega t - \frac{2N}{CL} \cdot S_R \left[\frac{N}{L \cdot E_R}\right]^{\beta} \left(U_o - U_1\right)^{\beta}$$

$$\frac{dU_1}{dt} = \omega U^1 \cos\omega t - \frac{N}{CL} \cdot S_R \left[\frac{N}{L \cdot E_R}\right]^{\beta} \left(U_1 - U_2\right)^{\beta} - \left(U_o - U_1\right)^{\beta}$$

$$\frac{dU_{N-1}}{dt} = \omega U^1 \cos\omega t - \frac{N}{CL} \cdot S_R \left[\frac{N}{L \cdot E_R}\right]^{\beta} \left[\left(U_{N-1}\right)^{\beta} - \left(U_{N-2} - U_{N-1}\right)^{\beta}\right] \quad (20)$$

where L is the total length of the layer (m.),

b is the outer circumference of the cable insulation (m),

O, 1...N are points on the layer,

U_o, U_1, U_N are corresponding potentials at the points with respect to ground (V),

C is the specific capacitance between the conductor and the layer (F/m^2),

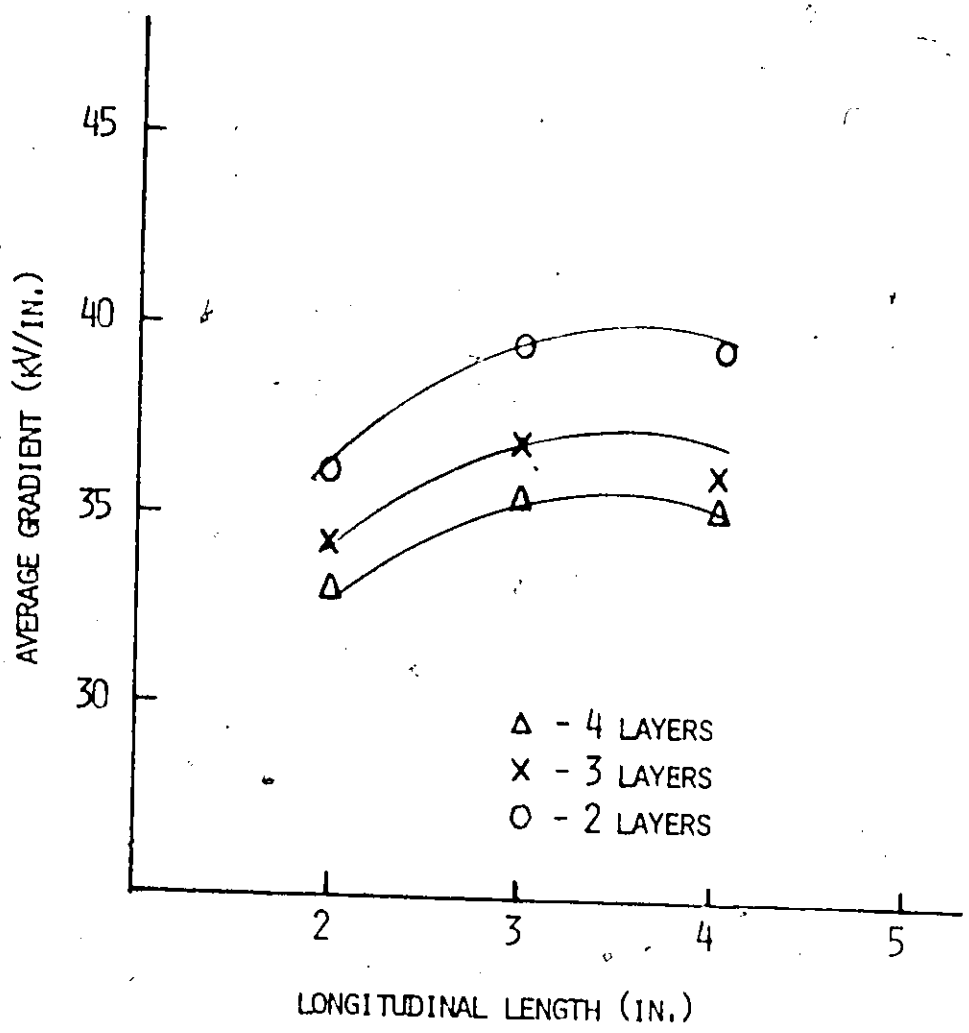

FIGURE 28: - EFFECT OF BUILT-UP HIGH DIELECTRIC CONSTANT TAPE DIMENSIONS ON THE AVERAGE GRADIENT IN REGION G

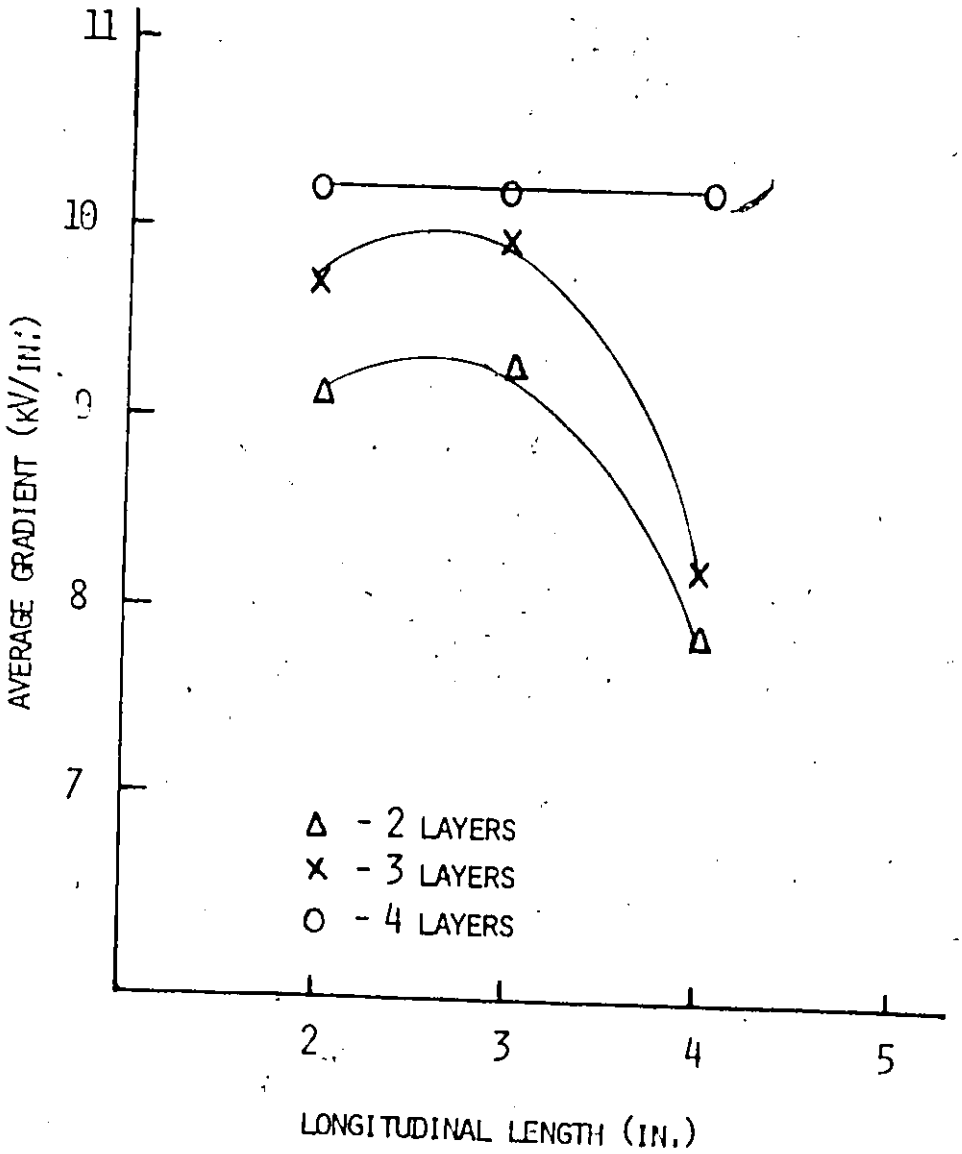

FIGURE 29: - EFFECT OF BUILT-UP HIGH DIELECTRIC CONSTANT TAPE DIMENSIONS ON THE AVERAGE GRADIENT IN REGION II

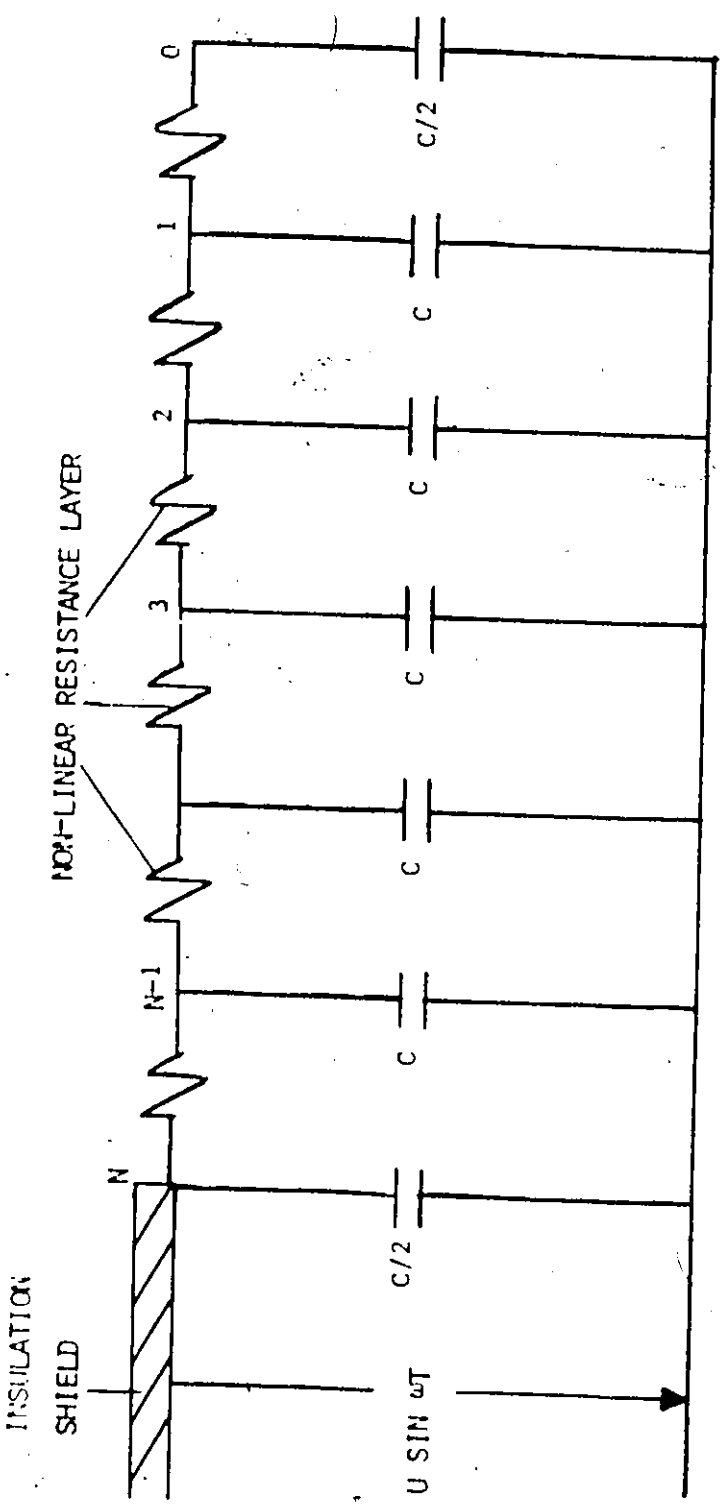

FIGURE 30: - EQUIVALENT CIRCUIT OF NON-LINEAR RESISTANCE TERMINATION

$$C = \frac{NC^1}{L \cdot b},$$

C^1 is the capacitance of the insulation between two succesive points 0 1...N,

U^1 is the voltage between the conductor and shield (peak value (V)),

W is the angular frequency (1/S),

E_R and S_R are the reference field strength and current density that define the non-linear charcteristic (V/m) and (A/m) and β is the non-linearity characteristic, N of equation (12) (assumed constant).

The equations represent the derivatives of the potential with respect to time for various equidistant points along the layer. Using the Runge-Kutta iteration method, the voltage distribution can be determined by a digital computer. Figure 31 illustrates the operation of the non-linear resistance layer for different applied voltages and β equal to 4 in equation 20. A voltage of 22.5 kV peak represents the normal service operation of a termination in a 27.6 kV phase-to-phase distribution system. As the operating voltage increases, a larger part of the layer becomes active in the uniform distribution of the voltage. The exponent β, which represents the slope of the characteristic current-voltage curve of the non-linear resistance layer, has been assumed constant. β actually varies, being approximately unity at voltages much below the operating voltage and between 6 and 7 at voltages higher than the operating voltage. The effect of increasing β on the voltage distribution along the layer is shown in Figure 32. As β increases, a more uniform voltage drop per unit becomes distributed along the layer.

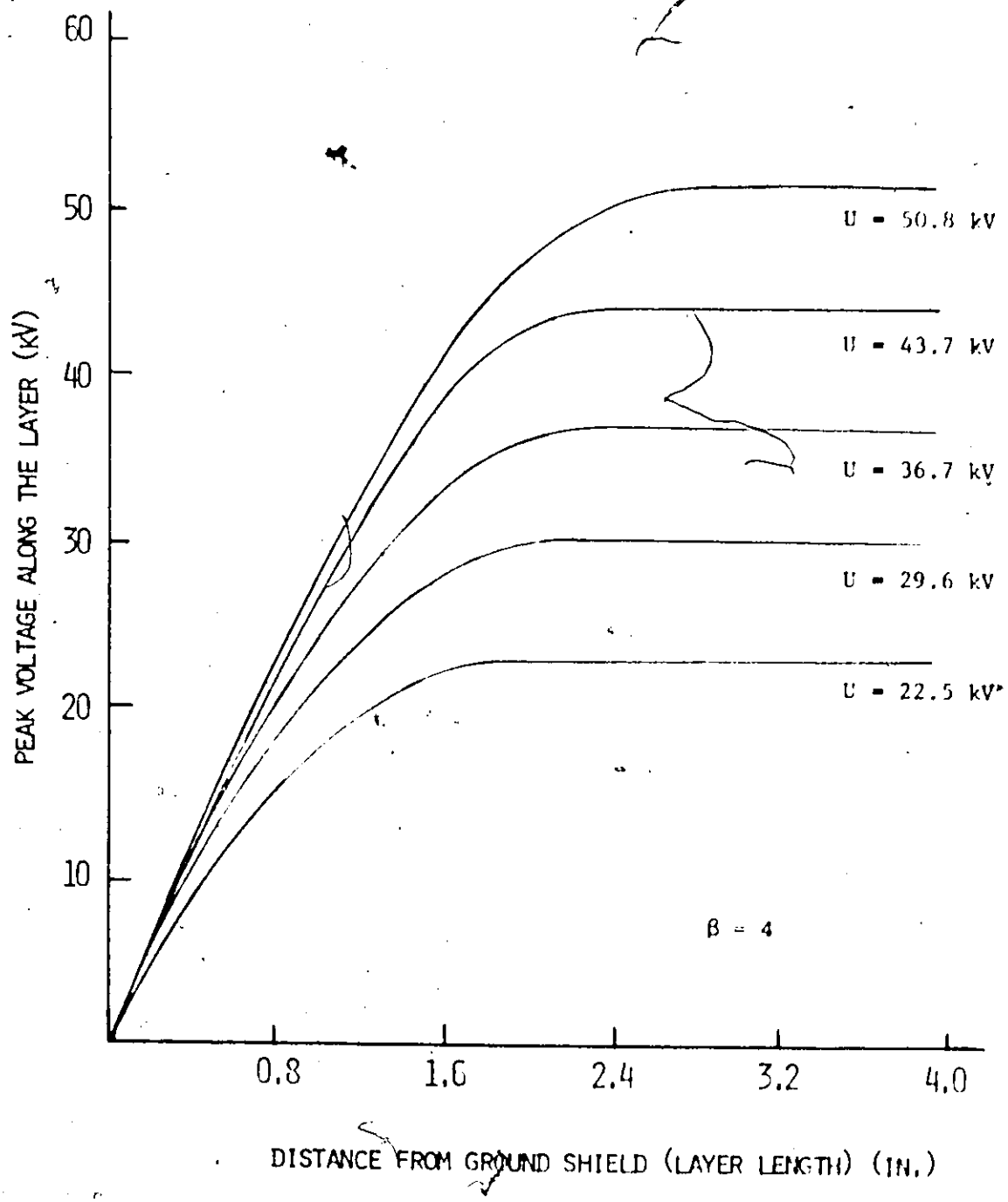

FIGURE 31: - POTENTIAL DISTRIBUTION ALONG NON-LINEAR RESISTANCE LAYER FOR DIFFERENT OPERATING VOLTAGES

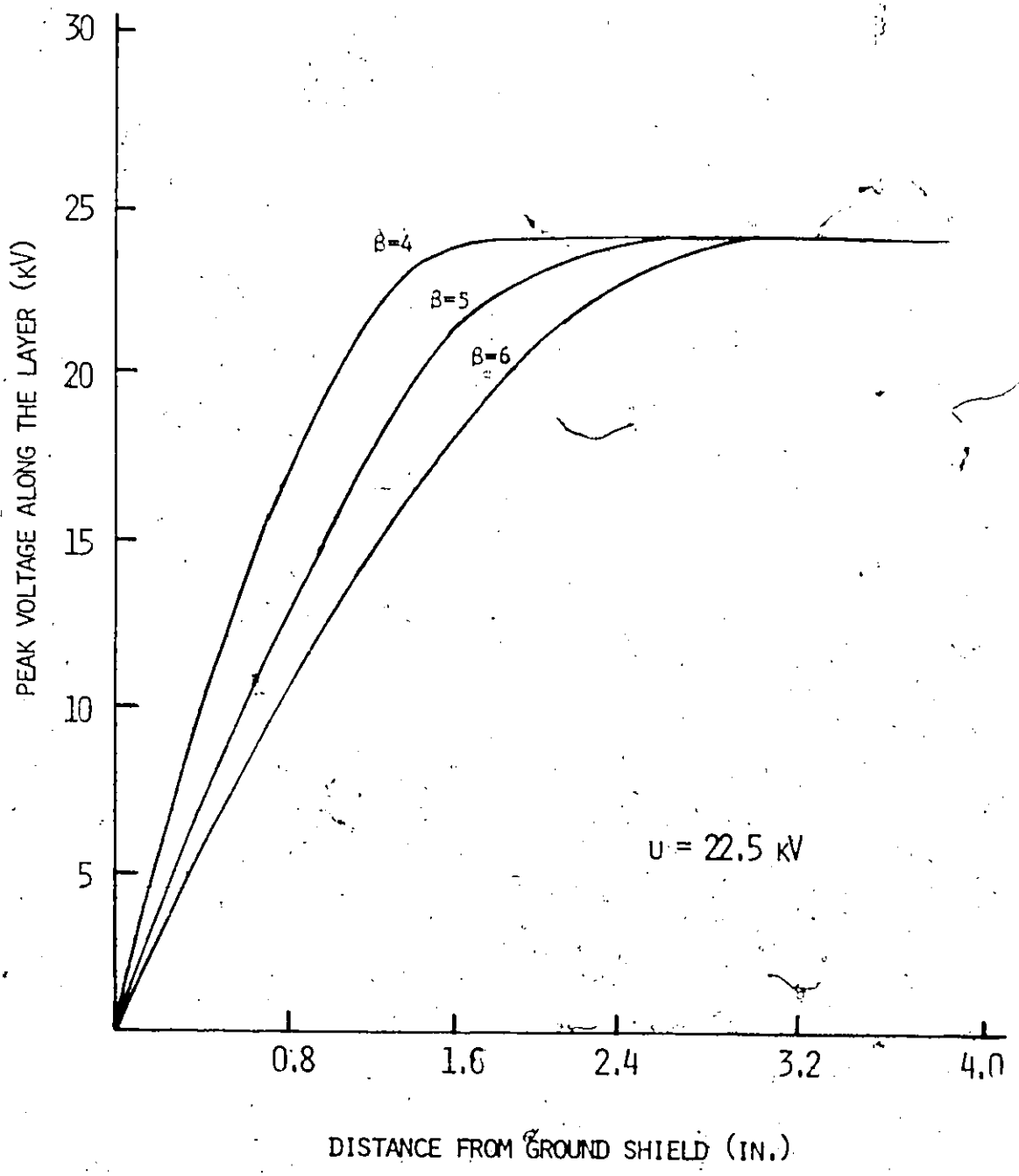

FIGURE 32: - EFFECT OF β ON THE POTENTIAL DISTRIBUTION ALONG THE NON-LINEAR RESISTANCE LAYER

CHAPTER 6

EXPERIMENTAL INVESTIGATION OF TERMINATIONS

6.1 Experimental Studies

The success of any operational testing depends on establishing testing procedures to estimate expected service life. In this study, corona inception, C.I.V. and extinction voltage, C.E.V. levels, and standard high-voltage tests were performed. The laboratory set-up and equipment to perform these tests are illustrated in Figure 33.

6.1.1 Laboratory Set-up and Test Equipment

The source consisted of a variable and regulated high-voltage 3 KVA, single-phase, 220v/150 kV transformer that was corona free to 120 kV. A control panel was provided with over-voltage and over-current protective arrangements. Also, an automatic timer was available. When the sample under test broke down, the high-voltage supply was automatically disconnected and the time of breakdown recorded.

A 250 kΩ wirewound resistor was inserted in series with the high-voltage bus to limit the short-circuit current and to prevent the corona currents from being short-circuited. This inductive resistor was wound on a 3" diameter ceramic pipe. Copper fittings were attached at the ends of the resistor to prevent corona formation.

The test sample consisted of a 27.6 kV cable with corona-free cone terminations at both ends of the cable. In addition, two anti-corona spheres were fixed to the cable conductor ends.

The impedance of the cable is very large, about j 30 megohms. The resulting small current through the cable sample causes a voltage drop across the 250 kΩ resistor. At 90 kV, this voltage drop was less than 1 kV and nearly the full source voltage was applied across the tested sample.

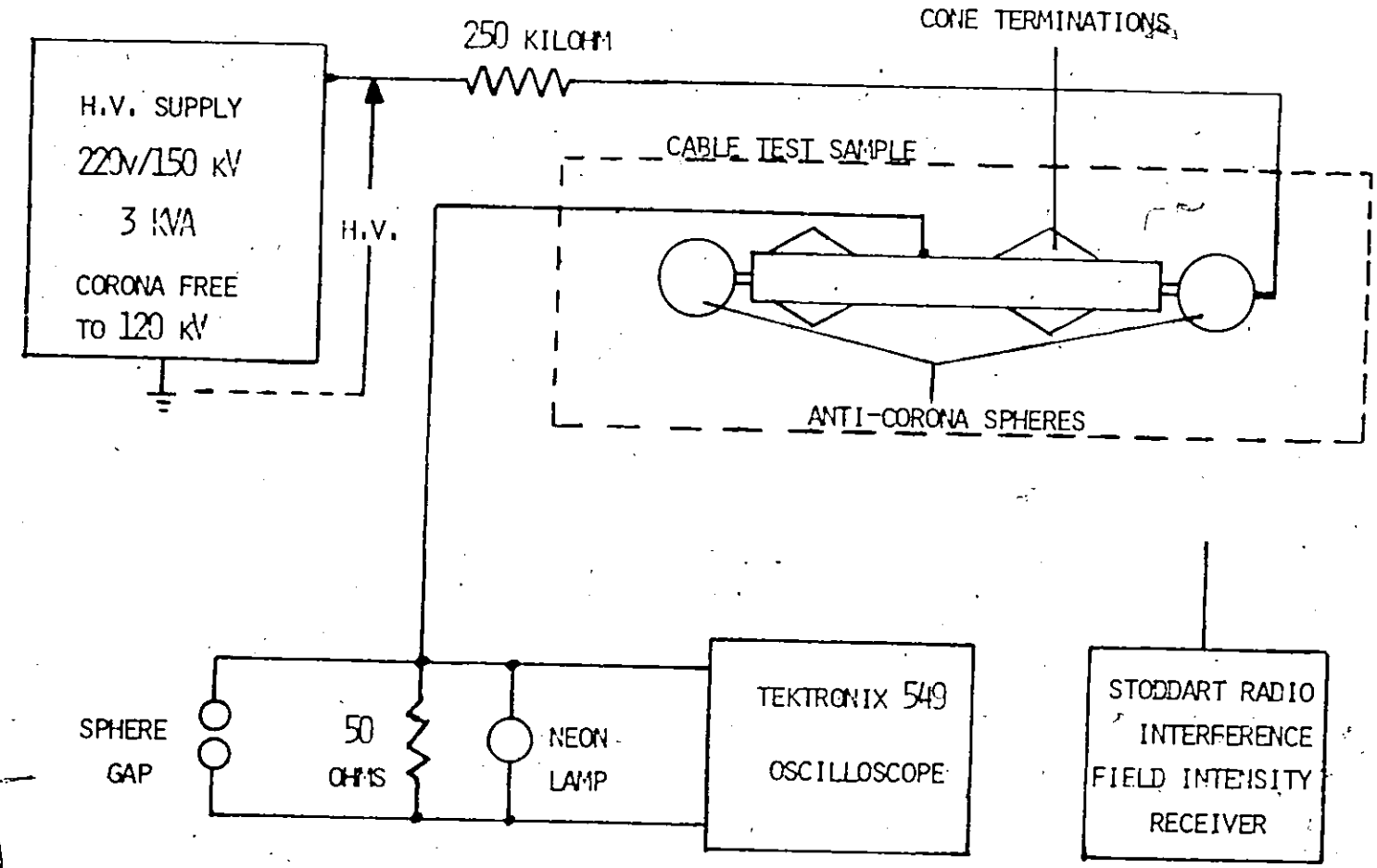

FIGURE 33: - THE LABORATORY TEST CIRCUIT

The corona detector consisted of a Tektronix Type 549 storage oscilloscope for the photographing of corona discharges. A 50 Ω resistor was inserted in series with the test sample. The voltage across the resistor, caused by the corona current, was measured by the differential amplifier plug-in unit of the oscilloscope. This amplifier measures voltages as low as 10 microvolts and has a variable bandwidth from DC to 1 MH_Z. In addition to the oscilloscope, a Stoddart Radio Interference-Field Intensity Receiver, tuned to 1 MH_Z, was employed to detect corona.

Several safety devices were provided in case of breakdown of the main automatic protective devices. These included a sphere gap with a breakdown voltage of 600 V and a neon lamp with a starting voltage of about 80 V, Figure 33.

6.1.2 The Measurement of Corona Levels

In this report, the "corona level" refers to the cable voltage at which corona discharges are below measurable values. The presence of corona indicates impurities within or at the surface of cable insulation, splices and terminations.

A variety of methods are available for detecting corona discharges: audible, visual, power factor measurements, oscilloscope etc. All are based on measuring the corona inception voltage (C.I.V.) and corona extinction voltage (C.E.V.). The C.I.V. is the voltage level at which corona discharges can be detected. The C.E.V. level is the voltage level at which the corona discharges, upon decrease of the applied voltage, disappear.

As suggested by the Insulated Power Cable Engineers Association (I.P.C.E.A.), the minimum acceptable C.E.V. level is 150 percent of the

normal operating voltage. This standard establishes a guideline for determining the suitability of the test sample for field operation. Most manufacturers and utilities generally accept this criterion.

Three corona level measurements were taken within a short time interval (3 minutes). The reason for this is the varying nature of corona; that is, at a given voltage, the corona discharges usually taper off with time. This phenomenon is attributed to two factors. First, a space charge formation within the voids of the insulation alters the electric field configuration and contributes to the extinction of the discharges. Secondly, the discharges within the voids initiate chemical reactions that carbonize the void surface and provide a conductive path. (Ref. section 4.2.1.)

6.1.3 Accelerated High-Voltage Measurements

At voltages higher than the normal operating voltage, test results indicate the ability of the test sample to withstand the action of ionization. Moreover, tests under accelerated high-voltages reduce testing time to produce a failure, hence, enabling examination of the nature and cause of breakdown. To a large extent, these tests indicate the expected service life of the tested sample.

At present, there are no industrial standards for high voltage tests of 27.6 kV terminations and splices. The Standard High-Voltage Test for Potheads (A.I.E.E. No. 48, Revised May 15, 1962), however, suggests some tests that could be considered adequate for evaluating the performance and expected life of terminations and splices. The test voltages referred to in this standard have been extrapolated for testing terminations rated at 27.6 kV phase-to-phase. The tests include the following withstand voltages.

1) One minute, 60 H_z, dry - 75 kV RMS

2) Six hours, 60 H_z, dry - 60 kV RMS

Samples which passed these two tests without failures were subjected to the step-voltage tests. This consisted of applying an initial 60 H_z voltage of 60 kV RMS and increasing the applied voltage every hour by 5 kV, up to 90 kV RMS.

6.2 Test Terminations and Test Results

Initially, the experimental investigation concentrated on testing a splice model similar to that in Figure 3, page 10. For proper stress relief, two stress cone terminations of the Windsor Utility type were installed at both ends of the splice under test. These cones were used to prevent flashovers at the cable ends and ensure that the detected corona originates only in the splice under test. It was found, however, that these capacitive cone terminations, exhibited corona discharges at voltages near or below the normal operating voltage. As a result, the true corona levels in the splice were masked by the corona discharges in the end terminations. In consequence, a more immediate priority was attached to the investigation of terminations which would assure a high corona inception voltage.

6.2.1 Tests on Non-Linear Resistance Terminations

The non-linear resistance method of stress control is typified by terminations using Sikronil (paste) and Coronux (paint). For 15 kV (phase-to-phase) operation, a three-inch layer of Sikronil is recommended by the manufacturer. However, at the higher operating voltage of 27.6 kV, a four-inch layer was applied as a safety precaution against high stress concentrations in the non-linear resistance layer. Detailed dimensions of these terminations are illustrated in Figure 34.

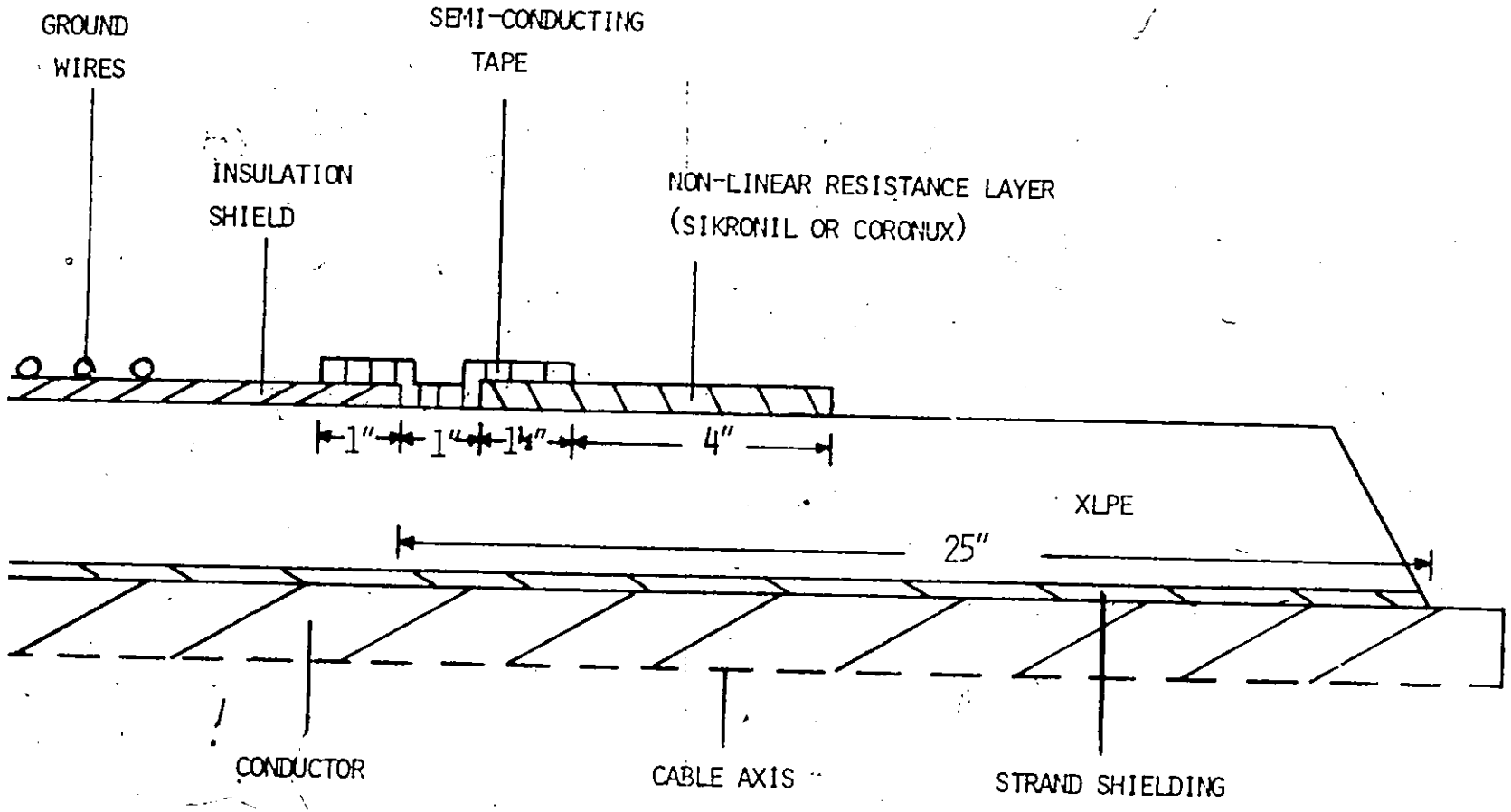

FIGURE 34: - CABLE TERMINATION UTILIZING A NON-LINEAR RESISTANCE LAYER (SIKRONIL OR CORONUX)

The results of corona and high-voltage tests on both resistive type terminations are summarized in Table IV. Column one of the table indicates the types of terminations used at both ends of the cable. The Sikronil terminations displayed corona extinction voltage levels well above the I.P.C.E.A. standard. The Coronux terminations, on the other hand, showed C.E.V. values just a little above the standard. Table IV shows that both the Coronux and Sikronil terminations passed the high-voltage tests. The Sikronil layer did exhibit a cracking or splitting of the resistive layer, attributed to heat build-up. However, these terminations passed successfully a second high-voltage test and no change in results could be observed.

6.2.2 Tests on High-Dielectric Constant Tape Terminations

The termination in Figure 35, designated as 3M-K, is an example of stress control by employing a high dielectric constant tape described in Chapter 3. As yet, dimensions of the built-up tape have not been finalized by the manufacturer for 27.6 kV operation. Hence, corona and high-voltage tests were made on terminations using various combinations of layer length and number of layers.

Table V illustrates the results of corona and high-voltage tests on various dimensions of the built-up high dielectric constant tape. The best results with respect to corona levels seemed to be four layers of the tape with a three-inch longitudinal length. All the terminations tested met the requirements of the I.P.C.E.A. corona standard and accelerated high-voltage tests.

Examination of the terminations after completion of the tests revealed severe deterioration of the high dielectric tape in some terminations, indicated by an asterisk (*) in Table V. Large ozone

TABLE IV:

CORONA AND HIGH-VOLTAGE TESTS ON CABLE TERMINATIONS WITH NON-LINEAR RESISTANCE LAYER

CABLE TERMINATIONS	CIV (KV)	CEV (KV)	% DEVIATION OF CEV FROM STANDARD IPCEA	HIGH VOLTAGE TESTS		
				75 KV (1 MIN)	60 KV (6 HRS)	STEP VOLTAGE INCREASE
SIK ~ SIK	32.0	31.5	+31.8	P	P	P
SIK ~ SIK	31.0	30.4	+27.2	P	P	P
SIK ~ SIK	30.0	29.0	+21.3	P	P	P
COR ~ COR	25.5	24.5	+ 2.5	P	P	P
COR ~ COR	25.4	24.0	+ 0.4	P	P	P
COR ~ COR	25.1	24.5	+ 2.5	P	P	P

SIK - SIKRONIL

COR - CORONUX

P - TEST PASSED

NOTE: THE IPCEA STANDARD CEV LEVEL IS 23.9 KV RMS PHASE-TO-GROUND

TABLE V:

CORONA AND HIGH-VOLTAGE TESTS ON CABLE TERMINATIONS WITH HIGH-DIELECTRIC CONSTANT TAPE

CABLE TERMINATIONS	HIGH DIELECTRIC TAPE		CORONA		HIGH VOLTAGE TESTS			
	LONGITUDINAL LENGTH (IN)	NUMBER OF LAYERS	CIV (KV)	CEV (KV)	75 KV (1 MIN)	60KV (6 HRS)	STEP VOLTAGE INCREASE	
3M-K ~ 3M-K	2	2	27.0	26.0	P	P	P	*
3M-K ~ 3M-K	2	4	29.5	29.0	P	P	P	*
3M-K ~ 3M-K	3	2	27.0	26.5	P	P	P	
3M-K ~ 3M-K	3	4	31.8	30.4	P	P	P	
3M-K ~ 3M-K	4	2	25.5	24.5	P	P	P	*
3M-K ~ 3M-K	4	4	28.5	28.0	P	P	P	

3M-K - HIGH DIELECTRIC CONSTANT TAPE

P - TEST PASSED

* - INDICATES DETERIORATION OBSERVED

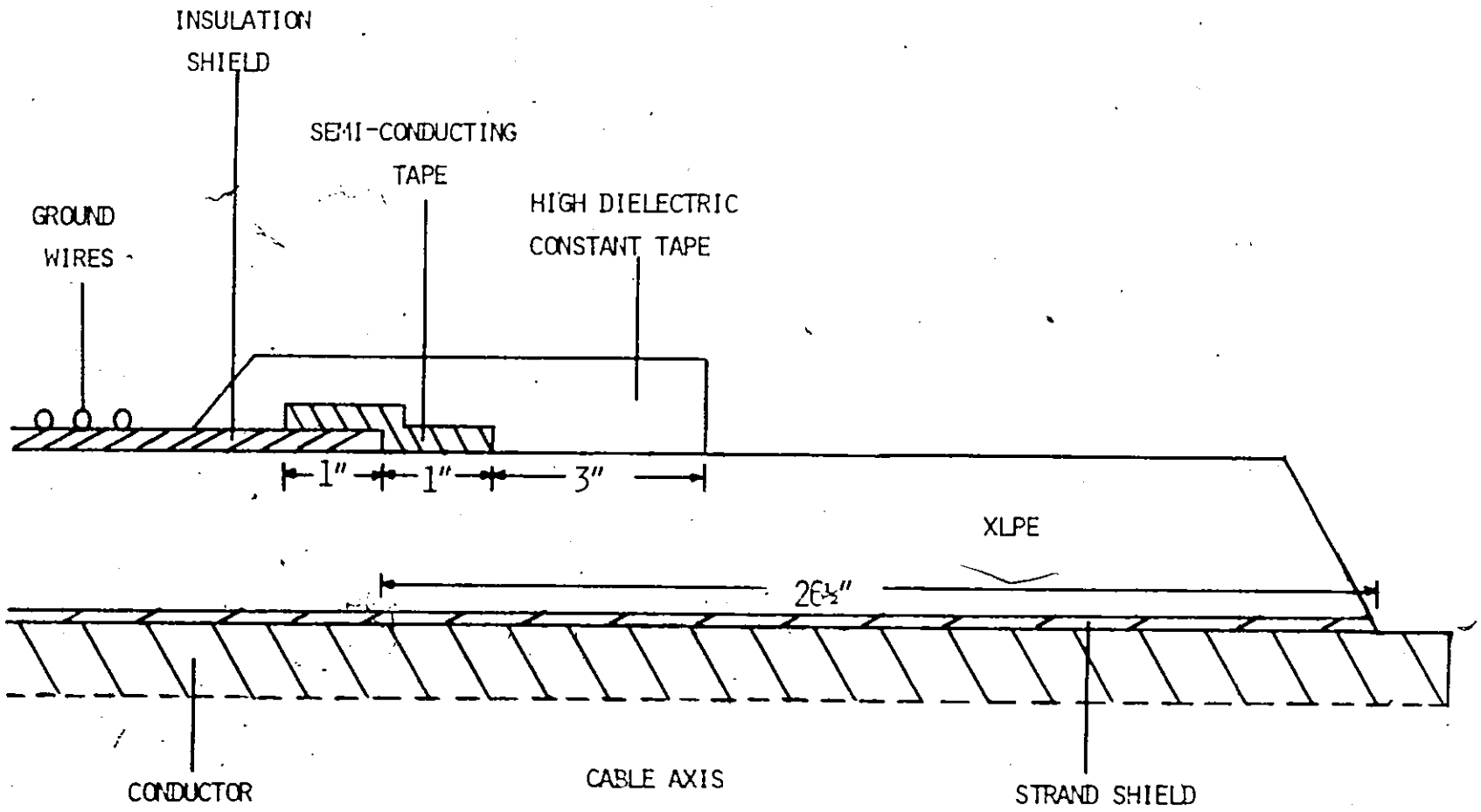

FIGURE 35: - HIGH DIELECTRIC CONSTANT TAPE TERMINATION

pockets and carbonization were located between the cable insulation and the high dielectric tape near the shield edge. These phenomena were the result of severe discharges that occurred during the accelerated withstand tests. At normal operating voltage, this deterioration might be expected over a long time. Further investigation is required before this termination method is accepted as safe.

6.2.3 Tests on Capacitive Cone Terminations

Three different types of terminations, employing capacitive cones to relieve electric stresses at the terminated portion of the cable, were tested.

The Windsor Utilities design, designated W.U-A, incorporates a 15 kV rated, insulating pennant built up with polyisobutylene (P.I.B.) tape, as its stress cone, Figure 36. Slight modifications in the design, referred to as W.U-B and W.U-C will be discussed in detail later in this chapter.

A similar type of taped capacitive cone design for 27.6 kV terminations by the Ontario Hydro, indicated as O.H., was also studied, Figure 37. Different dimensions and the use of highly-stretchable amalgamating tape instead of a pennant constitute the major differences between this type and the W.U-A type.

The final type studied (manufactured by Esna Ltd.) utilizes a pre-molded stress cone designed and pre-tested for operation at 35 kV. The cone insulation is an ethylene-propylene diene modified elastomer (E.P.D.M.), having electrical properties compatible with most solid extruded cable insulation. Molded to the cone insulation is a conducting rubber portion, which when slipped on the cable, connects to the cable shield and flares out to relieve high stress concentration, Figure 38.

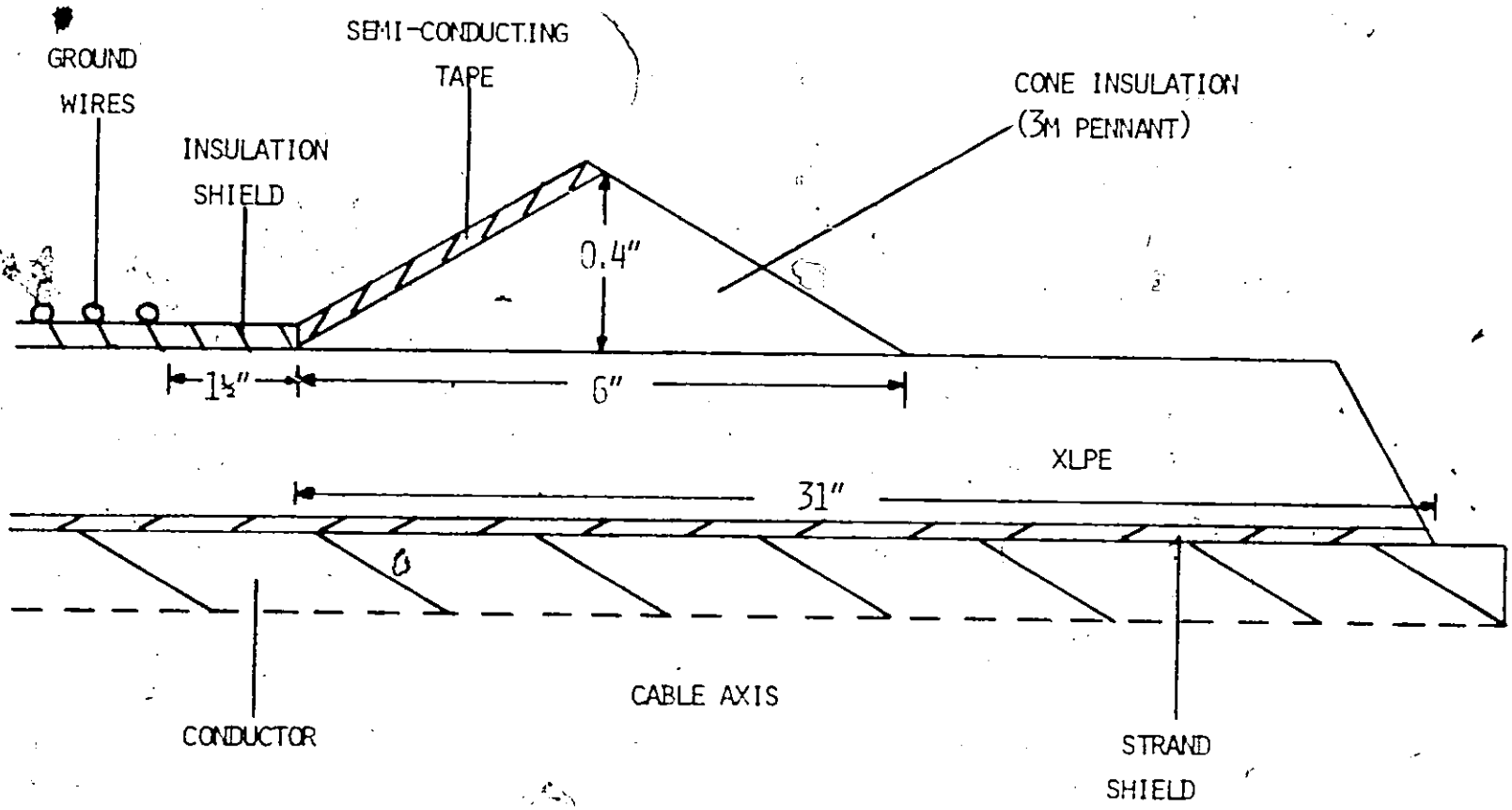

FIGURE 36: - WINDSOR UTILITY CAPACITIVE CONE TERMINATION

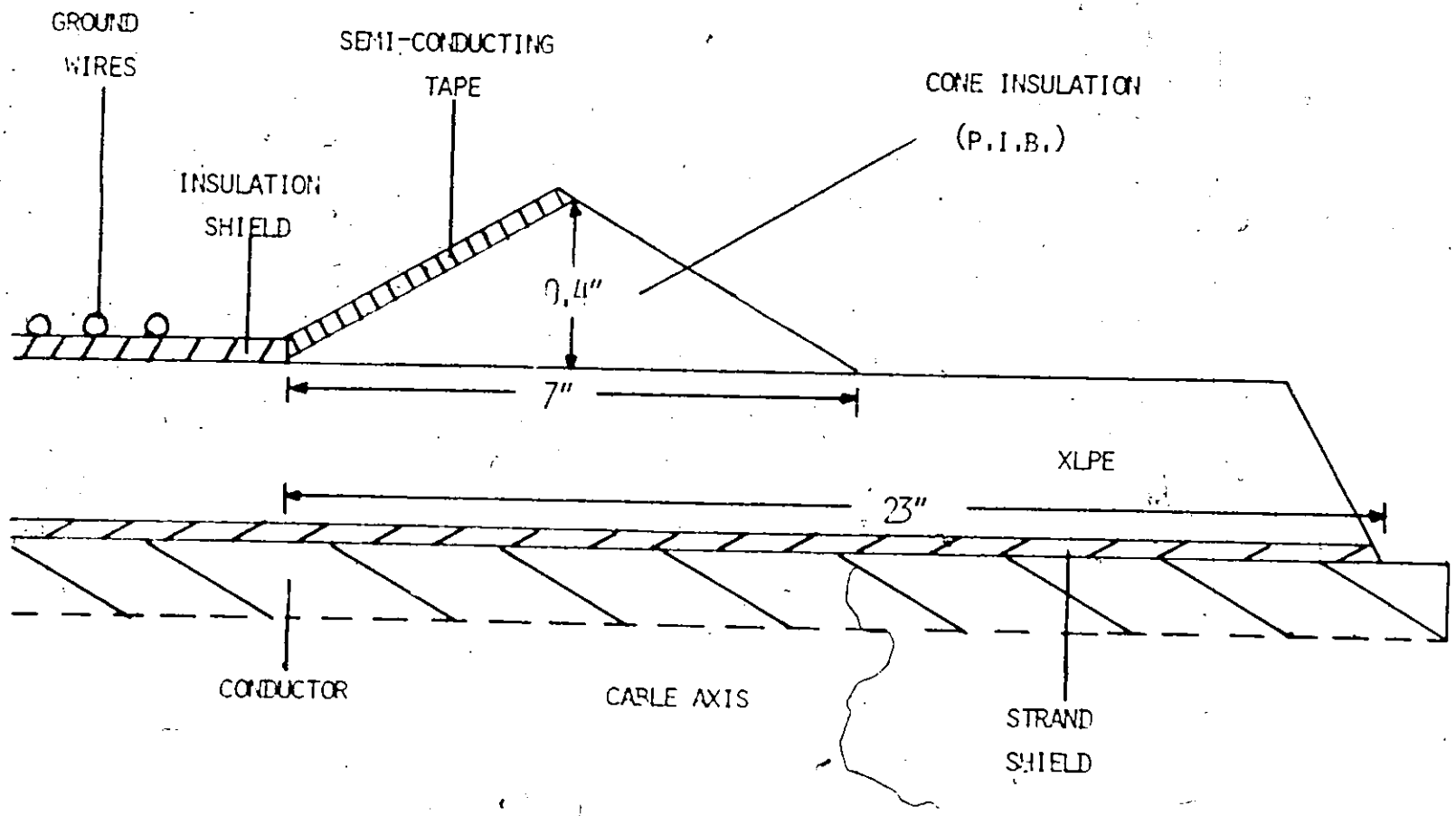

FIGURE 37: - ONTARIO HYDRO CAPACITIVE CONE TERMINATION

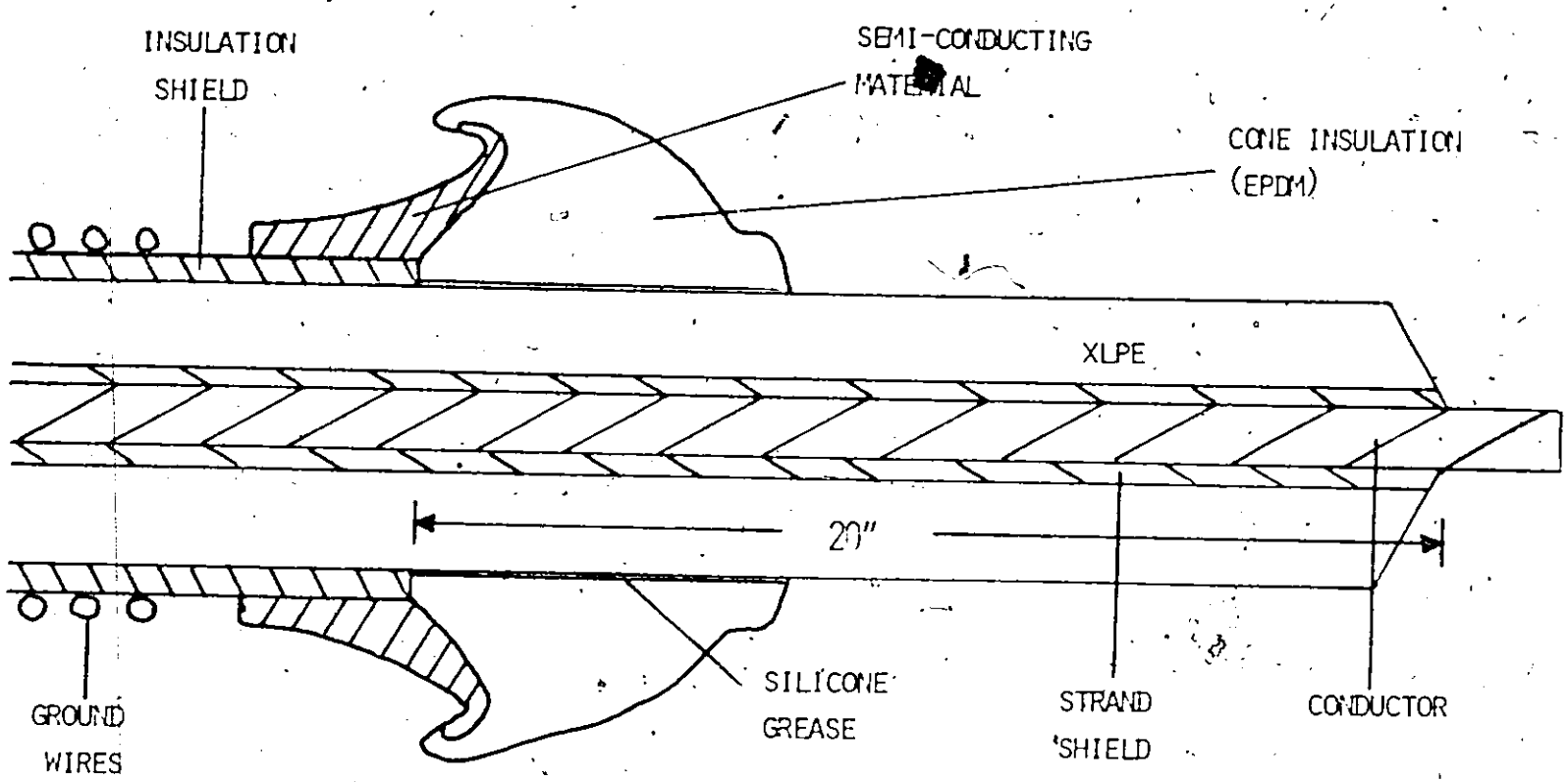

FIGURE 38: - ESNA MOULDED CAPACITIVE CONE TERMINATION

6.2.4 Results of High-Voltage Tests on Capacitive Cone Terminations

The results of the accelerated high-voltage tests are tabulated in Table VI. Six of the W.U-A terminations failed at various stages in the tests while the O.H. and ESNA type terminations passed successfully all the tests.

Physical examination of the failed terminations indicated the existence of a longitudinal void path between the XLPE cable insulation and the cone (pennant). Adjacent to the void, tracking, evidenced by carbonization, was observed along the yellow adhesive tape at the base of the pennant. This yellow tape facilitates the installation of the pennant. All the failures were characterized by puncture of the cable insulation within a distance of 1/4 inch from the shield and yellow tape edges.

In order to ascertain if the failures are caused by the yellow tape, six additional W.U-A terminations, with the yellow adhesive tape removed, were tested. These terminations are referred to as W.U-B in Tables VI and VII. From Table VI, it can be seen that this removal significantly improved performance under the high-voltage tests. No failures occurred nor could any trace of longitudinal tracking be found at the pennant-cable insulation interface.

The 3M Company, manufacturer of the cone-pennant, have reported similar results in their research laboratories. A plausible explanation for the destructive influence of the yellow adhesive tape has been presented by the 3M Company.

Above the corona extinction voltage a chemical reaction occurs between the yellow tape and the XLPE cable insulation. This reaction, initiated by corona discharges, produces ozone and other ionizable

TABLE VI

HIGH VOLTAGE TESTS ON CABLE TERMINATIONS WITH A CAPACITIVE CORE

TEST NO.	CABLE TERMINATIONS	HIGH VOLTAGE TESTS		
		75 KV (1 MIN)	60 KV (6 HRS)	STEP VOLTAGE INCREASE
1	*W.U-A ~ W.U-A	F (15 SEC)		
2	W.U-A ~ W.U-A*	P	F (1 HR)	
3	*W.U-A ~ 3M-K	P	F (3.5 HR)	
4	*W.U-A ~ 3M-K	F (55 SEC)		
5	*W.U-A ~ SIK	P	F (2.5 HR)	
6	*W.U-A ~ SIK	P	P	F (15 MIN. AT 75KV)
7	W.U-B ~ W.U-B	P	P	P
8	W.U-B ~ W.U-B	P	P	P
9	W.U-B ~ 3M-K	P	P	P
10	W.U-B ~ 3M-K	P	P	P
11	W.U-C ~ W.U-C	P	P	P
12	W.U-C ~ W.U-C	P	P	P
13	W.U-C ~ SIK	P	P	P
14	W.U-C ~ SIK	P	P	P
15	O.H ~ SIK	P	P	P
16	O.H ~ SIK	P	P	P
17	O.H ~ SIK	P	P	P
18	O.H ~ SIK	P	P	P
19	ESNA ~ SIK	P	P	P
20	ESNA ~ SIK	P	P	P
21	ESNA ~ SIK	P	P	P

NOTE: * INDICATES THE FAILED TERMINATION

gases at the cable/pennant interface. These gases, including nitrogen oxides, when ionized, cause carbonization of the XLPE cable insulation. Over an extended time period, deterioration of the insulation becomes complete and the cable fails by puncturing. For this and other reasons, 3M does not recommend their pennant for terminations operating above 15 kV phase-to-phase.

Another modification, W.U-C, was made in the W.U-A terminations to minimize the interfacial tracking phenomenum. Several layers of insulating tape were applied directly over the cable insulation and under the pennant construction. As the tape is of the same material, ethylene propylene rubber (EPR), as the pennant, it was felt that a possible better bond would eliminate any interfacial reaction in the termination.

None of the five terminations tested failed during the accelerated high-voltage tests nor could any traces of deterioration be observed when the terminations were dissected. Hence, the detrimental effect of the yellow adhesive tape on the breakdown has been proven and a method of eliminating this effect has been found.

6.2.5 Results of Corona Tests on Capacitive Cone Terminations

Two distinct voltage levels of corona (C.I.V. and C.E.V.) were observed in the tests. Only the lower corona level is tabulated. This corona level, recorded by the oscilloscope, is attributed to internal partial discharges within the termination insulation.

The second higher distinct corona level recorded by the Stoddart is not tabulated. This level is probably caused by discharges of much greater magnitude occurring at the interface between the cable and cone insulation.

It must be noted that Sikronil and 3M-K terminations were employed at one end of the test cable. Since Sikronil and 3M-K were both found acceptable with respect to corona levels and high-voltage tests, they were used as reference standards for comparison purposes.

Examination of test results 1 to 6 in Table VII, shows that the W.U-A terminations had unacceptable low corona inception voltages. The corona level occurred at or very near the operating voltage of the cable; that is, 16.0 kV phase-to-ground instead of above as in the case of the O.H. and ESNA terminations. The modifications in the original W.U-A termination, W.U-B and W.U-C, have little appreciable effect on the corona level; tests 7 to 14. Only a slight increase in the C.I.V. level is noticed.

Tests 15 to 18, performed on the Ontario Hydro design terminations, showed that the recorded corona levels were approximately the same as those recommended by the I.P.C.E.A.

The molded ESNA terminations exhibited corona levels well above the minimum requirements; i.e., tests 19 to 21. No deterioration was observed.

It can be concluded from Tables VI and VII that the best results were obtained with the ESNA termination and, next, with the Ontario Hydro tape-type stress cone. However, it must be pointed out that these terminations were constructed under ideal laboratory conditions. Under field conditions, results may become unacceptable due to environmental and pollution effects.

TABLE VII

CORONA TESTS ON CABLE TERMINATIONS WITH CAPACITIVE TYPE STRESS CONTROL

TEST NUMBER	CABLE TERMINATIONS	C.I.V. (KV)	C.E.V. (KV)	% DEVIATION FROM IPCEA STANDARD
1	W.U-A ~ W.U-A	15.0	14.0	-41.4
2	W.U-A ~ W.U-A	15.5	15.0	-37.2
3	W.U-A ~ 3M-K	16.5	16.0	-33.1
4	W.U-A ~ 3M-K	16.8	16.0	-31.1
5	W.U-A ~ SIK	17.5	16.5	-31.0
6	W.U-A ~ SIK	17.4	16.5	-31.0
7	W.U-B ~ W.U-B	16.0	15.0	-37.2
8	W.U-B ~ W.U-B	16.8	16.0	-33.1
9	W.U-B ~ 3M-K	19.5	18.6	-22.2
10	W.U-B ~ 3M-K	18.3	17.4	-27.2
11	W.U-C ~ W.U-C	17.4	16.5	-31.0
12	W.U-C ~ W.U-C	18.3	17.5	-26.8
13	W.U-C ~ SIK	18.0	17.5	-26.8
14	W.U-C ~ SIK	18.0	17.0	-29.1
15	O.H. ~ SIK	25.0	24.0	+ 0.4
16	O.H. ~ SIK	25.0	24.0	+ 0.4
17	O.H. ~ SIK	24.5	23.5	- 1.6
18	O.H. ~ SIK	24.4	22.5	- 5.8
19	ESNA ~ SIK	29.5	28.5	+19.2
20	ESNA ~ SIK	29.8	29.0	+21.3
21	ESNA ~ SIK	30.4	29.5	+23.4

CHAPTER 7

FINDINGS, CONCLUSIONS AND RECOMMENDATIONS

The investigation of an existing device or part of a real operating system can be divided into several interacting stages. The study of the splices and terminations for a 27.6 kV underground distribution system described in this report, consisted of

a) a preliminary study of the history of splices and terminations, operational problems and the present state of the art;

b) determination of aspects to be investigated;

c) determination of feasible methods of investigation;

d) systematic experimental and theoretical studies;

e) critical interpretation of results and findings, and their practical usage;

f) conclusions.

SPLICES: After a general study of splices and cross-linked polyethylene cables, their construction and component materials, laboratory tests were initiated of the hand-wound tape splices designed by the Windsor Utilities Commission.

It was found that the splice performance tests required corona-free cable terminations. Hence, the investigation of the terminations commenced and its completion constituted the major part of the study.

Computer field mapping investigations revealed the vulnerable regions inside the splice.

One, at the edge of the internal crimped connector, could be improved by increasing the number of semi-conducting tape layers and careful workmanship, paticularily in the field during adverse weather conditions.

The second region is located near the base of the pencil at the outer edge of the extruded semi-conducting core shield. In this region a high voltage gradient exists which may initiate corona discharges and, hence, tracking along the pencilled surface. This would be enhanced by the shrinkback of the cable insulation.

It can be concluded that the hand-wound splices should be further investigated with respect to corona, tracking, shrinkback and chemical compatibility of the materials.

TERMINATIONS: Six original pennant-type terminations have been found unsatisfactory because of corona being initiated near the operating voltage, and failure during the high-voltage tests. The latter can be improved to acceptable test performance by some practical modifications, however, the harmful corona could not be eliminated. Hence, no long service life can be expected even from the improved pennant-type terminations.

The high dielectric constant tape terminations passed all the required corona and high-voltage tests. Upon examination of the terminations after the high-voltage tests, the presence of ozone and carbonization was observed at the tape/cable insulation interface near the shield edge. This is the region where the highest potential gradients exist, as predicted from a computer field mapping. The deterioration in this region, though observed at high test voltages, may be expected to develop over a long time of operation at normal voltage.

Both the non-linear resistance terminations, Sikronil and Coronux, passed the high-voltage and corona tests. It was noticed, however, that extensive fissures or cracks had developed in the resistive layer. A subsequent high-voltage test was performed and the results were found

to be still acceptable. Although the test results are favourable, it can not be concluded that this termination method will perform satisfactorily in service, as surface ageing, temperature and water effects on the resistive layer have not been determined. A hand-wound tape, capacitive cone termination designed by the Ontario Hydro was also investigated. Performance during high-voltage and corona tests proved acceptable and no evidence of insulation deterioration could be observed. During adverse conditions in the field, however, tape wrapping proves time consuming and facilitates void formation and contamination in the insulation. Such conditions would preclude long service life.

Of all the terminations studied, the best performance in the laboratory tests was exhibited by the Esna molded capacitive cone terminations. The high-voltage tests were passed and the corona extinction voltage was well above the I.P.C.E.A. standard. Molded construction and factory pre-testing allows for fast, easy installation and good expected performance.

It must be noted, however, that the results of corona and high-voltage tests are only indicative of expected life and performance. The terminations tested were installed under ideal laboratory conditions and, as such, do not take into account atmospheric and environmental effects. Factors, such as, pollution, temperature changes, moisture, etc. can be expected to produce results less favourable than those obtained in this investigation. It is recommended, therefore, that periodic visual inspections be made of terminations and splices in service to check for corona deterioration.

There are two aspects that perhaps require further study. First, out-door tests and laboratory investigations should be made to investigate the effects of ageing and pollution on the performance of terminations.

This can be facilitated by life tests performed at higher than operating voltage till breakdown and the results extrapolated to normal voltage operation.

Secondly, it would be useful to study the effects of conductor, connector and shield geometry changes on the electric field distribution in splices. It is conceivable that a design might be developed with reduced high local gradients. In such a splice, shrinkback or its harmful effects should also be eliminated.

REFERENCES

1. "A.I.E.E. Number 48 Pothead Standards", A.I.E.E. Trans. P.A.S., Vol. 81, May, 1962, pg. 1072.
2. Swinburne, J., "Methods of Electrical Transformation", Proc. I.C.E., Vol. 38, Pt. IV, 1898, pg. 498.
3. "Rome PSR-1 Pennant", Product Engineering Bulletin, No. PSR-1, March 12, 1963.
4. Estrin, G., "The Effects of Anisotropy in a Three-Dimensional Array of Conducting Disks", Proc. I.R.E., Vol. 39, July 1951, pp. 821-826.
5. Kock, W.E., "Metallic Delay Lenses", Bell Sys. Tech. Journal, Vol. 27, January 1948, pg. 58.
6. Virsberg, L.G., and Ware P.H., "A New Termination for Underground Distribution", I.E.E.E. Trans. P.A.S., Vol. PAS-86, No. 9 1967, pg. 1129.
7. Schwertz, F.A., and Mazenko, J.J., "Non-linear Semi-conductor Resistors", J. Appl. Physics, Vol. 24, No. 8, August 1953, pg. 1015.
8. Kato, Y., and Tsukui, T., "Study of Deterioration Characteristics of Organic Insulating Materials Due to Corona Discharge", E.E. in Japan, Vol. 86, No. 8, 1966, pg. 92.
9. Okamoto, H., and Ikeda, Y., "Study of Mechanisms of Degradation of Polyethylene by Corona", E.E. in Japan, Vol. 85, No. 1, 1965, pg. 1.
10. Mason, J.H., "The Deterioration and Breakdown of Dielectrics Resulting from Internal Discharges", J.I.E.E., Vol. 98, Pt. 1, 1951, pg. 44.

11. Kitchin, D.W., and Pratt, O.S., "Treeing in Polyethylene as a Prelude to Breakdown", I.E.E.E. Trans. P.A.S., 1958, pg. 181.

12. Miyashita, T., and Inoue, T., "Treeing Phenomena in Polyethylene-Coated Wires Immersed in Water", E.E. in Japan, Vol. 90, No. 3, 1970, pg. 83.

13. Storey, J.T., "The Determination of Axially Symmetric Fields By Digital Computation", I.E.E.E. Trans. on Insulation, Vol. EI-4, No. 2, 1969, pg. 23.

14. Storey, J.T., and Billings, M.J., "General Digital-Computer Program for the Determination of Three-Dimensional Electrostatic Axially Symmetric Fields", Proc. I.E.E., Vol. 114, No. 10, October 1967, pg. 1551.

15. Billings, M.J., and Storey, J.T., "Consideration of the Effect of Pollution on the Potential Distribution of Insulation Systems", Proc. I.E.E., Vol. 115, No. 11, November 1969, pg. 1661.

16. Binns, K.J., and Lawrenson, P.J., "Analysis of Computation of Electric and Magnetic Field Problems," Pergamon Press, New York, 1963, pg. 254.

17. Wensley, J.H., and Parker, F.W., "The Solution of Electric Field Problems Using a Digital Computer", Electrical Energy, Vol. 1, 1956, pg. 13.

18. Vitkovitch, D., "Field Analysis", D. Van Nostrand Co. Ltd., London, 1966, pg. 111.

19. Frankel, S.P., "Convergence of Iterative Treatments of Partial Differential Equations", M.T.A.C., Vol. 4, pg. 65.

20. Carre, B.A., "The Determination of the Optimum Accoleration Factor for S.O.R.", Computer Journal, Vol. 4, No. 1, 1961, pg. 73.

APPENDIX A

DETERMINATION OF AXIALLY SYMMETRIC ELECTRIC FIELD DISTRIBUTIONS BY DIGITAL COMPUTER

Numerical methods exist for determining the electric field distributions in multi-dielectric configurations with one axis of symmetry. The implementation of these methods is made easier by using the digital computer.[13,14,15]

A.1 Finite-Difference Approximations

The electrostatic fields of cables, splices and terminations are governed by Laplace's equation,

$$\nabla^2 V = 0 \tag{A1}$$

where V is the potential,

or, in cylindrical co-ordinates, (r,ϕ,z),

$$\frac{1}{r}\frac{\partial}{\partial r}\left(r\frac{\partial V}{\partial r}\right) + \frac{1}{r^2}\frac{\partial^2 V}{\partial \phi^2} + \frac{\partial^2 V}{\partial z^2} = 0 \tag{A2}$$

If axial symmetry exist, $\frac{\partial}{\partial \phi} = 0$. Eq. (A2) then reduces to

$$\frac{1}{r}\frac{\partial V}{\partial r} + \frac{\partial^2 V}{\partial r^2} + \frac{\partial^2 V}{\partial z^2} = 0 \tag{A3}$$

Laplace's equation is solved numerically by converting it to a difference equation which is an approximation to the partial differential equation over small intervals of length.

First, a system of rectangular grids are superimposed over the region of interest. A portion of the grid and associated node points are shown in Figure A1. Boundaries are defined along the grid lines.

Next, a finite difference equation is set up in terms of the potentials at the nodes. This equation is developed by expanding the potential at node 0, Figure A1, in a Taylor's series. Expressions for

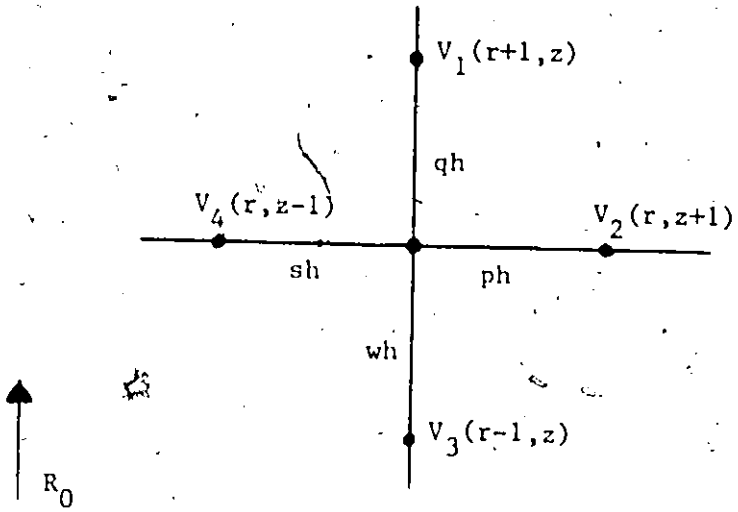

FIGURE A1

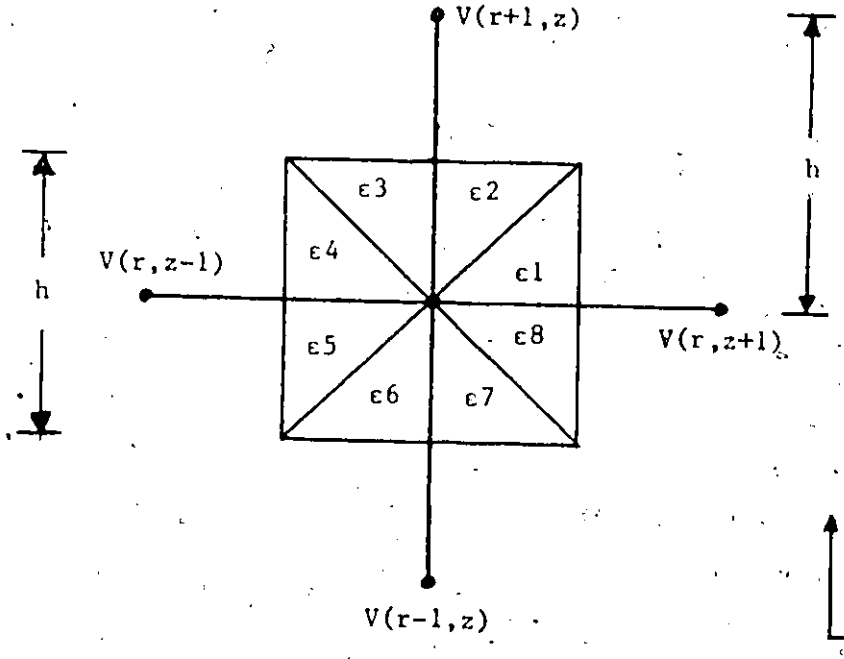

FIGURE A2

$\left(\partial^2 V/\partial r^2\right)$, $\left(\partial^2 V/\partial z^2\right)$ and $\left(\partial V/\partial r\right)$ in terms of the node potentials are derived and substituted into Laplace's equation.[16]

At any node point r_A, situated on the grid line between co-ordinates r-1 and r+1, the potential V can be expanded in terms of the potential V_o at node 0 by using Taylor's series

$$V = V_o + \left(\partial V/\partial r\right)_o \left(r_A - r\right) + \frac{1}{2!}\left(\partial^2 V/\partial r^2\right)_o \left(r_A - r\right)^2 + 1/3!\left(\partial^3 V/\partial r^3\right)_o \left(r_A - r\right)^3 + \ldots . \quad (A4)$$

Substituting into this equation for $r_A = r + qh$ and $r_A = r - wh$, gives the potentials at nodes 1 and 3 as

$$V_1 = V_o + qh\left(\frac{\partial V}{\partial r}\right)_o + \frac{1}{2!} q^2h^2\left(\frac{\partial^2 V}{\partial r^2}\right)_o + \frac{1}{3!} q^3h^3\left(\frac{\partial^3 V}{\partial r^3}\right)_o + \ldots . \quad (A5)$$

and

$$V_3 = V_o - wh\left(\frac{\partial V}{\partial r}\right)_o + \frac{1}{2!} w^2h^2\left(\frac{\partial^2 V}{\partial r^2}\right)_o - \frac{1}{3!} w^3h^3\left(\frac{\partial^3 V}{\partial r^3}\right)_o + \ldots . \quad (A6)$$

Ignoring terms with h^3 and higher powers, multiplying equation (A5) by w and equation (A6) by q and adding, produces

$$V_1 + qV_3 = V_o\,(w+q) + \frac{h^2}{2} wq\,(w+q)\left(\frac{\partial^2 V}{\partial r^2}\right)_o \quad (A7)$$

Rearranging

$$\left(\frac{\partial^2 V}{\partial r^2}\right)_o = \frac{2V_1}{qh^2(w+q)} + \frac{2V_3}{wh^2(w+q)} - \frac{2V_o}{h^2wq} \quad (A8)$$

In a similar manner V is expanded about V_o in a Taylor's series in the Z-direction.

$$\left(\frac{\partial^2 V}{\partial z^2}\right)_o = \frac{2V_2}{ph^2(p+s)} + \frac{2V_4}{sh^2(p+s)} - \frac{2V_o}{h^2 ps} \qquad (A9)$$

Multiplying equation (A6) by q^2 and equation (A5) by w^2 and subtracting, yields

$$w^2 V_1 - q^2 V_3 = V_o (w^2 - q^2) + hwq (w+q) \left(\frac{\partial V}{\partial r}\right)_o$$

Rearranging

$$\left(\frac{\partial V}{\partial r}\right)_o = \frac{wV_1}{hq(w+q)} - \frac{qV_3}{hw(w+q)} - \frac{(w-q)V_o}{hwq} \qquad (A10)$$

Substituting equations (A8), (A9) and (A10) into (A4) gives

$$V_o = \frac{\dfrac{V_1 (1 + wh/2Ro)}{q(w+q)} + \dfrac{V_2}{p(p+s)} + \dfrac{V_3 (1 - qh/2Ro)}{w(w+q)} + \dfrac{V_4}{s(p+s)}}{\dfrac{1}{wq} + \dfrac{1}{sp} + \dfrac{h(w-q)}{2wqRo}} \qquad (A11)$$

When the distance between node points is equal; namely, p=s=q=w=1, a special form of equation (A11) (regular star) results.

Equation A11 then reduces to

$$Vo = 1/4 \left[V_1 (h/2R0 + 1) + V_3 (1 - h/2Ro) + V_2 + V_4\right] \qquad (A12)$$

or

$$V_1 (h/2Ro + 1) + V_3 (1 - h/2Ro) + V_2 + V_4 - 4Vo = 0 \qquad (A13)$$

In terms of the co-ordinates r and z of Figure A1, equation (A13) becomes

$$V(r+1,z)(h/2Ro + 1) + V(r-1,z)(1 - h/2Ro) + V(r,z+1) + V(r,z-1) - 4V(r,z) = 0 \qquad (A14)$$

A.2 Finite-Difference Equations for Dielectric Interfaces

A special form of finite-difference equations is employed when

determining the potentials at nodes on the interface between different dielectric regions. However, in this case, the interface boundary is approximated to fit the nodes of the grid.

Consider a node O, (V(r,z)), surrounded by eight octants each of which may be a different dielectric as in Figure A2.[17]

Laplace's equation in two dimensions with axial symmetry can be written as

$$\text{div } (\varepsilon_R \text{ grad } V) = 0 \tag{A15}$$

where V is the potential

and ε_R is the dielectric constant within the region of interest

By the divergence theorem, eq. (A15) is replaced by

$$\int_Q (K \text{ grad } V)\, dn = 0 \tag{A16}$$

where Q is the square curve surrounding point O

and dn is the incremental vector normal to Q .

If I_i is defined as the integral of equation (A16) taken over all the octants, equation (A16) becomes

$$\sum_{i=1}^{8} I_i = 0 \tag{A17}$$

Therefore

$$I_1 = \int_o^{h/2} \varepsilon_1 (r_o + \xi) \frac{\partial V}{\partial z} \, d\xi \tag{A18}$$

where h is the mesh length,

ro is the distance of point O from the axis of symmetry

and ξ is the incremental change in the Z direction.

If a first order interpolation in h is assumed

$$\frac{\partial V}{\partial Z} = \frac{V(r,Z+1) - V(r,Z)}{h} \qquad \text{(A19)}$$

Equation (A7) becomes

$$I_1 = V(r,Z+1) - V(r,Z) \left[\int_o^{h/2} \frac{\varepsilon_1 r_o}{h} \, d\xi + \int_o^{h/2} \frac{\varepsilon_1 \xi}{h} \, d\xi \right]$$

$$I_1 = [V(r,Z+1) - V(r,Z)] \left[\frac{\varepsilon_1 r_o}{2} + \frac{\varepsilon_1 h}{8} \right]$$

$$I_1 = [V(r,Z+1) - V(r,Z)] \frac{\varepsilon_1 r_o}{2} \left[1 + \frac{h}{4r_o} \right] \qquad \text{(A20)}$$

Similarly for the other octants

$$I_2 = [V(r+1,Z) - V(r,Z)] \frac{\varepsilon_2 r_o}{2} \left[1 + \frac{h}{2r_o} \right]$$

$$I_3 = [V(r+1,Z) - V(r,Z)] \frac{\varepsilon_3 r_o}{2} \left[1 + \frac{h}{2r_o} \right]$$

$$I_4 = [V(r,Z-1) - V(r,Z)] \frac{\varepsilon_4 r_o}{2} \left[1 + \frac{h}{4r_o} \right]$$

$$I_5 = [V(r,Z-1) - V(r,Z)] \frac{\varepsilon_5 r_o}{2} \left[1 - \frac{h}{4r_o} \right]$$

$$I_6 = [V(r-1,Z) - V(r,Z)] \frac{\varepsilon_6 r_o}{2} \left[1 - \frac{h}{2r_o} \right]$$

$$I_7 = [V(r-1,Z) - V(r,Z)] \frac{\varepsilon_7 r_o}{2} \left[1 - \frac{h}{2r_o} \right]$$

$$I_8 = [V(r,Z+1) - V(r,Z)] \frac{\varepsilon_8 r_o}{2} \left[1 - \frac{h}{4r_o} \right]$$

On summing and isolating node potentials, equation (A17) becomes

$$V(r,Z+1)\,C_1 + V(R+1,Z)\,C_3 + V(r,Z-1)\,C_5 + V(r-1,Z)\,C_7 + V(r,Z)\,C = 0 \qquad \text{(A21)}$$

where $C = C_1 + C_3 + C_5 + C_7$,

$$C_1 = \left[1 + \frac{h}{4r_o}\right]\varepsilon_1 + \left[1 - \frac{h}{4r_o}\right]\varepsilon_8 ,$$

$$C_3 = \left[1 + \frac{h}{2r_o}\right](\varepsilon_2 + \varepsilon_3) ,$$

$$C_5 = \left[1 + \frac{h}{4r_o}\right]\varepsilon_4 + \left[1 - \frac{h}{4r_o}\right]\varepsilon_5$$

and $C_7 = \left[1 - \frac{h}{2r_o}\right](\varepsilon_6 - \varepsilon_7)$.

A.3 Boundary Conditions

The solution of Laplace's partial differential equation is contingent on specified boundary conditions. In the particular case of cables, terminations and splices, the outer boundaries are governed by the Dirichlet and Neumann boundary conditions.

The Dirichlet condition defines the values of potential at all points or segments of the boundary so that

$$V = V_o$$

where V_o is some defined potential at the boundary.

The Neumann condition fixes the outer boundary at a sufficient distance so that the field distribution in the region of interest will not be affected. This condition sets the gradient of the potential normal to the boundary at some value; namely

$$\frac{\partial V}{\partial n} = 0$$

A.4 Numerical Solution by Digital Computer

The finite-difference equations (A14) and (A21) are satisfied only when the potentials in these equations are assigned their exact values. However, should there be some error in the value of one or all of the potentials, then equations (A14) and (A21) are not exact due to the introduction of a residual. The residual, denoted by R, is given by

$$V_1 (h/2R_o + 1) + V_3 (1 - h/2R_o) + V_2 + V_4 - 4V_o = R \qquad (A22)$$

The relaxation method reduces this residual to zero by repeated variation of the potentials at the nodes. Practically, it is not possible to reduce the residual identically to zero. It is sufficient to reduce the value of the residual to a low fixed value. As a rough estimate, to achieve an accuracy of 1 to 5%, the residuals at individual nodes should be reduced to 0.1% of the mean of all the potentials. Likewise, the sum of the residuals of all the nodes could be reduced to a corresponding similar size.[18]

In order to accelerate the computation and rate of convergence of the iterative process, the Successive-Over-Relaxation (S.O.R.) or extrapolated Liebmann method is used. The general S.O.R. iterative equation is given by

$$V(r,Z)^{n+1} = V(r,Z)^{n} + \alpha f(R) \qquad (A23)$$

where $f(R)$ is related to the residual,

n is the order of the iteration,

and α is the accelerating factor.

The updated potential is calculated as the sum of the previous potential value plus the difference between the potential value given in equation (A14) and the previous potential value times some factor α.

For equations (A14) and (A21), the S.O.R. equations are written, respectively, as

$$V(r,Z)^{n+1} = V(r,Z)^{n} + \frac{\alpha}{4}\left[V(r+1,Z)^{n}(h/2R_o + 1) + V(r-1,Z)^{n+1}(1 - h/2R_o) + V(r,Z+1)^{n} + V(r,Z-1)^{n+1} - 4V(r,Z)^{n}\right] \quad (A24)$$

$$V(r,Z)^{n+1} = V(r,Z)^{n} + \frac{\alpha}{K^1}\left[V(r,Z+1)^{n} K1 + V(r+1,Z)^{n} K3 - V(r,Z-1)^{n+1} K5 + V(r-1,Z)^{n+1} K7 - V(r,Z)^{n} K^1\right] \quad (A25)$$

where $K^1 = \frac{1}{wq} + \frac{1}{sp} + \frac{h(w-q)}{2wq R_o}$,

$$K1 = \frac{1}{p(p+s)},$$

$$K3 = \frac{1 + wh/2R_o}{q(q+w)}$$

$$K5 = \frac{1}{S(p+S)},$$

$$K7 = \frac{1 - qh/2R_o}{w(q+w)}$$

n = order of iteration

and α = accelerating factor.

Both equations are applied at the appropriate nodes till the error criterion (sum of residuals) is satisfied, as

$$\sum_{r,Z} \left| V(r,Z)^{n+1} - V(r,Z)^{n} \right| \leq b \quad (A26)$$

where b is some small value.

The S.O.R. method is highly convergent when the accelerating factor, α, is between 1 and 2. There exists a value of α which reduces the computation time to an optimum value. This optimum value can be calculated by complex mathematical techniques but two simple expressions have been found to determine an approximate α for a rectangular grid n by m. These are

$$\alpha \text{ opt} = 2[1 - \Pi \left[\frac{1}{(n-1)^2} + \frac{1}{(m-1)^2}\right]^{16}] \qquad \text{(A27)}$$

where n and m are greater than 15.

and

$$\alpha \text{ opt} = \frac{2}{1 + \sqrt{1 - \lambda^2}}$$

where $\lambda^2 = \frac{[\cos \pi/n + \cos \pi/m]^2}{4}$ 19,20 (A28)

n and m are the dimensions of the grid.

A.5 Errors

The difference equations used to represent Laplace's equation are only approximations to the field equation. Third order terms and higher have been neglected, leading to what is called a truncation error. This error, dependent on h, can be made negligibly small if h is small. The reduction of h or the grid size in the region of interest results in a more accurate solution of the field distribution.

Two other types of error, due to computer limitations, also affect the accuracy of solution. One is roundoff error because of the limited number of available significant digits. The other, called computation error, is affected by the finite number of iteration cycles available.

APPENDIX B

In the following pages, a flow chart and program listing are given. The program determines the electric field distribution of a splice.

FLOW CHART

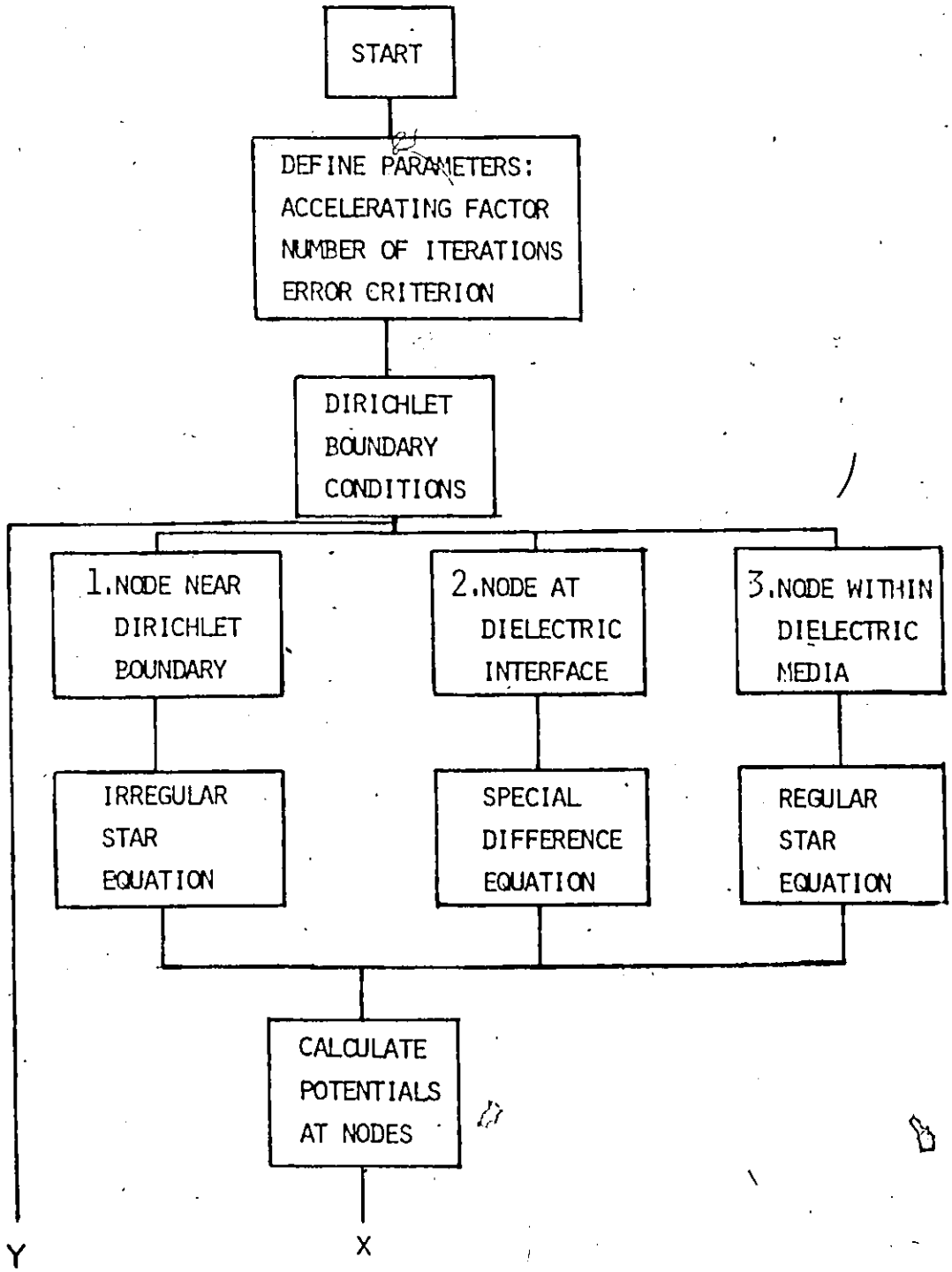
START
DEFINE PARAMETERS:
ACCELERATING FACTOR
NUMBER OF ITERATIONS
ERROR CRITERION
DIRICHLET
BOUNDARY
CONDITIONS
1.NODE NEAR
DIRICHLET
BOUNDARY
2.NODE AT
DIELECTRIC
INTERFACE
3.NODE WITHIN
DIELECTRIC
MEDIA
IRREGULAR
STAR
EQUATION
SPECIAL
DIFFERENCE
EQUATION
REGULAR
STAR
EQUATION
CALCULATE
POTENTIALS
AT NODES
Y
X

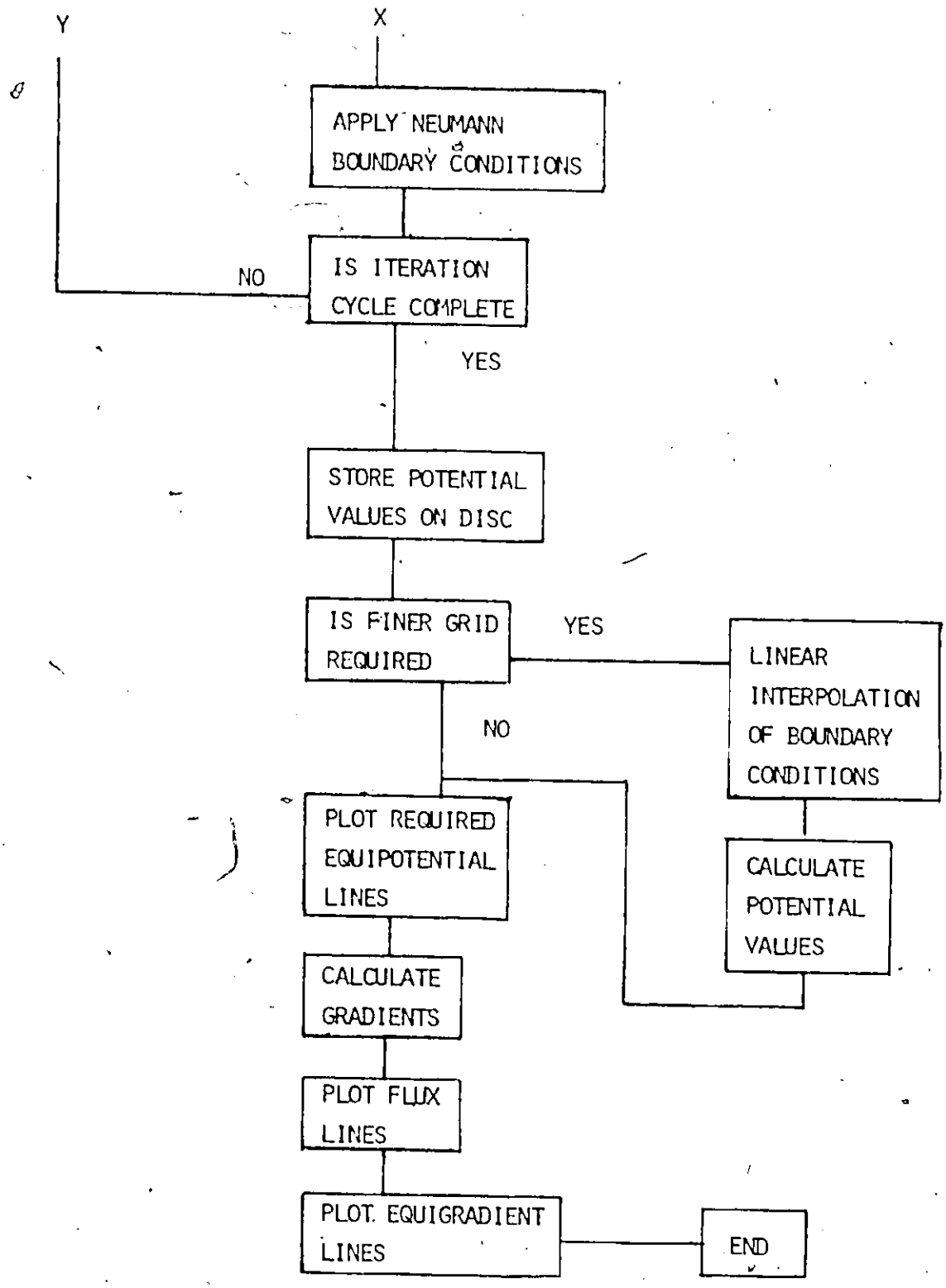
Y
X
APPLY NEUMANN BOUNDARY CONDITIONS
NO
IS ITERATION CYCLE COMPLETE
YES
STORE POTENTIAL VALUES ON DISC
IS FINER GRID REQUIRED
YES
LINEAR INTERPOLATION OF BOUNDARY CONDITIONS
NO
PLOT REQUIRED EQUIPOTENTIAL LINES
CALCULATE POTENTIAL VALUES
CALCULATE GRADIENTS
PLOT FLUX LINES
PLOT EQUIGRADIENT LINES
END

```
C     [illegible] SYM[illegible] [illegible]
C     [illegible]
C     [illegible] [illegible]
C     [illegible]
C     [illegible]
C
C     DESCRIPTION OF PARAMETERS
C         [illegible]
C         MAXIT = MAXIMUM [illegible] ITERATION NUMBER
C         [illegible] SYSTEM [illegible]
C         [illegible]
C         [illegible]
C         [illegible]
C         OPTAP = OPTIMUM ACCELERATION PARAMETER [illegible]
C                 [illegible])
C         [illegible] = [illegible] FOR WHICH THE SUM OF SQUARES
C                 [illegible]
C         [illegible] = VECTOR CONTAINING COEFFICIENTS OF THE
C                 POLYNOMIAL
C
C     SUBROUTINES
C
C         [illegible] = LEAST SQUARES CURVE FITTING. FITS POINTS TO
C                 [illegible]Y POLYNOMIAL CURVE.
C
C         [illegible] = CALCULATES [illegible] AT IRREGULAR NODES
C                 ADJACENT TO DIRICHLET BOUNDARY.
C
      DIMENSION [illegible](21,155),[illegible](6)
      [illegible]
      DOUBLE PRECISION [illegible] Y(100),X(100),YCALC(100),S[illegible](100),A(11),S(11),
     1V1,V2,[illegible],XV,Z(100)
      [illegible]/[illegible]/ Y,X,[illegible],YCALC,V1,V2,[illegible],XV
      [illegible]
      [illegible]
      DIMENSION [illegible]X(100),[illegible]Y(100),[illegible](18),[illegible](18)
      INTEGER [illegible] F,FF,FFF,FFFF
      [illegible]=[illegible].0
      [illegible] = [illegible].0
      MAXIT = 100
C
C     CALCULATE THE OPTIMUM ACCELERATION PARAMETER
C
      R2=21
      R1=165
      OPTAP=2./(1.+SQRT(1.-((COS(3.142/R2)+COS(3.142/R1))**2/4.)))
C
C     SET ALL NODES TO INTERMEDIATE VALUE,MIDWAY BETWEEN MAXIMUM AND
C     MINIMUM
C
      DO 2 I=1,21
      DO 2 J=1,165
    2 U(I,J)=50.0
C
C     DIRICHLET BOUNDARY CONDITIONS
C     DEFINE DIRICHLET BOUNDARIES
C
      N=4
```

```
      DO 3 J=1,165
      IF(J.EQ.144.OR.J.EQ.157)M=M-1
      IF(J.EQ.150)M=M+2
      IF(J.EQ.152.OR.J.EQ.160)M=M+1
      DO 3 I=1,M
    3 U(I,J)=100.
      I=10
      DO 4 J=1,22
    4 U(I,J)=0.0
C
C     SET ITERATION COUNTER
      ITN=1
C
C     FIT POINTS DEFINING BOUNDARY TO A FOURTH ORDER POLYNOMIAL.
C
      CALL LSCF
   70 SUM=0.0
C
C     POTENTIALS WITHIN XLPE CABLE INSULATION (E=2.3 )
C
      M=9
      DO 180 J=2,142
      IF(J.EQ.127.OR.J.EQ.132.OR.J.EQ.138.OR.J.EQ.142)M=M-1
      DO 180 I=5,M
      RES =OPTAP*((U(I,J+1)+U(I,J-1)+U(I+1,J)*(1.+1./(2.*FLOAT(I)))+U(I-
     11,J)*(1.-1./(2.*FLOAT(I))))/4.-U(I,J))
      U(I,J)=U(I,J)+RES
  180 SUM=SUM+ABS(RES)
      DO 519 I=1,5
  519 AA(I)=SNGL(A(I))
C
C     POTENTIALS WITHIN APPLIED INSULATION ( E=2.4 )
C     IF NODE IS REGULAR USE FORM OF LAPLACE'S EQUATION FOUND IN
C     STATEMENT 8 . IF NODE IS IRREGULAR USE FORM FOUND IN SUBROUTINE
C     ELECT
C
      M=5
      N=10
      DO 11 J=23,164
      IF(J.EQ.26)N=N+1
      IF(J.EQ.127.OR.J.EQ.132.OR.J.EQ.138.OR.J.EQ.142.OR.J.EQ.143.OR.J.E
     10.157)N=N-1
      IF(J.EQ.144)N=N-2
      IF(J.EQ.150)N=N+2
      IF(J.EQ.152.OR.J.EQ.160)N=N+1
      DO 111 I=N,20
      F=0
      FF=0
      FFF=0
      FFFF=0
      YY=I+1
      XX=J
      ZZ=YY-(A(1)+A(2)*XX+A(3)*XX**2+A(4)*XX**3+A(5)*XX**4)
      IF(ZZ.GE.0.0)F=1
      YY=I
      XX=J-1
      ZZ=YY-(A(1)+A(2)*XX+A(3)*XX**2+A(4)*XX**3+A(5)*XX**4)
      IF(ZZ.GE.0.0)FF=1
      YY=I
      XX=J+1
```

```
      ZZ=YY-(A(1)+A(2)*XX+A(3)*XX**2+A(4)*XX**3+A(5)*XX**4)
      IF(ZZ.GE.0.0)FFF=1
      YY=I-1
      XX=J
      ZZ=YY-(A(1)+A(2)*XX+A(3)*XX**2+A(4)*XX**3+A(5)*XX**4)
      IF(ZZ.GE.0.0)FFFF=1
      IF(F.EQ.0)GO TO 9
    7 CALL ELECT(I,J,U,M,ZZ,XX,YY,AA,MM,F,FF,FFF,SUM,OPTAP,FFFF)
      GO TO 11
    8 RES =OPTAP*((U(I,J+1)+U(I,J-1)+U(I+1,J)*(1.+1./(2.*FLOAT(I)))+U(I-
     11,J)*(1.-1./(2.*FLOAT(I))))/4.-U(I,J))
      U(I,J)=U(I,J)+RES
      SUM=SUM+ABS(RES)
  111 CONTINUE
   11 CONTINUE
C
C     POTENTIALS AT INTERFACE BETWEEN XLPE AND APPLIED INSULATION
C
      READ (5,900) E1,E2,E3,E4,E5,E6,E7,E8
  900 FORMAT(8F3.1)
      DO 12 J=26,125
      I=10
      H1=1./(4.*FLOAT(I))
      H2=1./(2.*FLOAT(I))
      A1=(1.0+H1)*E1+(1.0-H1)*E8
      A2=(1.0+H2)*(E2+E3)
      A3=(1.0+H1)*E4+(1.0-H1)*E5
      A4=(1.0-H2)*(E6+E7)
      A5=A1+A2+A3+A4
      RES=(OPTAP/A5)*((U(I+1,J)*A2)+(U(I-1,J)*A4)+(U(I,J+1)*A1)+(U(I,J-1
     1)*A3)-(U(I,J)*A5))
      U(I,J)=U(I,J)+RES
   12 SUM=SUM+ABS(RES)
      READ (5,900) E1,E2,E3,E4,E5,E6,E7,E8
      M=0
      I=10
      J=126
      GO TO 14
   15 I=9
      J=131
      GO TO 14
   16 I=8
      J=137
      GO TO 14
   17 I=7
      J=141
   14 H1=1./(4.*FLOAT(I))
      H2=1./(2.*FLOAT(I))
      A1=(1.0+H1)*E1+(1.0-H1)*E8
      A2=(1.0+H2)*(E2+E3)
      A3=(1.0+H1)*E4+(1.0-H1)*E5
      A4=(1.0-H2)*(E6+E7)
      A5=A1+A2+A3+A4
      RES=(OPTAP/A5)*((U(I+1,J)*A2)+(U(I-1,J)*A4)+(U(I,J+1)*A1)+(U(I,J-1
     1)*A3)-(U(I,J)*A5))
      U(I,J)=U(I,J)+RES
      SUM=SUM+ABS(RES)
      M=M+1
      GO TO (15,16,17),M
      READ (5,900) E1,E2,E3,E4,E5,E6,E7,E8
```

```
      I=0
      I=9
      J=127
      GO TO 18
   19 I=8
      J=132
      GO TO 18
   21 I=7
      J=138
   18 H1=1./(4.*FLOAT(I))
      H2=1./(2.*FLOAT(I))
      A1=(1.0+H1)*E1+(1.0-H1)*E8
      A2=(1.0+H2)*(E2+E3)
      A3=(1.0+H1)*E4+(1.0-H1)*E5
      A4=(1.0-H2)*(E6+E7)
      A5=A1+A2+A3+A4
      RES=(OMTAP/A5)*((U(I+1,J)*A2)+(U(I-1,J)*A4)+(U(I,J+1)*A1)+(U(I,J-1
     1)*A3)-(U(I,J)*A5))
      U(I,J)=U(I,J)+RES
      SUM=SUM+ABS(RES)
      I=M+1
      GO TO (19,21),M
      READ (5,900) E1,E2,E3,E4,E5,E6,E7,E8
      I=6
      J=142
      DO 28 N=1,2
      H1=1./(4.*FLOAT(I))
      H2=1./(2.*FLOAT(I))
      A1=(1.0+H1)*E1+(1.0-H1)*E8
      A2=(1.0+H2)*(E2+E3)
      A3=(1.0+H1)*E4+(1.0-H1)*E5
      A4=(1.0-H2)*(E6+E7)
      A5=A1+A2+A3+A4
      RES=(OMTAP/A5)*((U(I+1,J)*A2)+(U(I-1,J)*A4)+(U(I,J+1)*A1)+(U(I,J-1
     1)*A3)-(U(I,J)*A5))
      U(I,J)=U(I,J)+RES
      SUM=SUM+ABS(RES)
      I=I-1
      J=J+1
   28 CONTINUE
      READ (5,900) E1,E2,E3,E4,E5,E6,E7,E8
      I=9
      DO 29 J=128,130
      H1=1./(4.*FLOAT(I))
      H2=1./(2.*FLOAT(I))
      A1=(1.0+H1)*E1+(1.0-H1)*E8
      A2=(1.0+H2)*(E2+E3)
      A3=(1.0+H1)*E4+(1.0-H1)*E5
      A4=(1.0-H2)*(E6+E7)
      A5=A1+A2+A3+A4
      RES=(OMTAP/A5)*((U(I+1,J)*A2)+(U(I-1,J)*A4)+(U(I,J+1)*A1)+(U(I,J-1
     1)*A3)-(U(I,J)*A5))
      U(I,J)=U(I,J)+RES
   29 SUM=SUM+ABS(RES)
      READ (5,900) E1,E2,E3,E4,E5,E6,E7,E8
      I=8
      DO 89 J=133,136
      H1=1./(4.*FLOAT(I))
      H2=1./(2.*FLOAT(I))
```

```
      A1=(1.0+H1)*E1+(1.0-H1)*E8
      A2=(1.0+H2)*(E2+E3)
      A3=(1.0+H1)*E4+(1.0-H1)*E5
      A4=(1.0-H2)*(E6+E7)
      A5=A1+A2+A3+A4
      RES=(OPTAP/A5)*((U(I+1,J)*A2)+(U(I-1,J)*A4)+(U(I,J+1)*A1)+(U(I,J-1
     1)*A3)-(U(I,J)*A5))
      U(I,J)=U(I,J)+RES
   89 SUM=SUM+ABS(RES)
      READ (5,900) E1,E2,E3,E4,E5,E6,E7,E8
      I=7
      DO 31 J=139,140
      H1=1./(4.*FLOAT(I))
      H2=1./(2.*FLOAT(I))
      A1=(1.0+H1)*E1+(1.0-H1)*E8
      A2=(1.0+H2)*(E2+E3)
      A3=(1.0+H1)*E4+(1.0-H1)*E5
      A4=(1.0-H2)*(E6+E7)
      A5=A1+A2+A3+A4
      RES=(OPTAP/A5)*((U(I+1,J)*A2)+(U(I-1,J)*A4)+(U(I,J+1)*A1)+(U(I,J-1
     1)*A3)-(U(I,J)*A5))
      U(I,J)=U(I,J)+RES
   31 SUM=SUM+ABS(RES)
      ITN=ITN+1
C
C     NEUMANN BOUNDARY CONDITIONS
C
      DO 77 I=1,10
   77 U(I,1)=U(I,3)
      DO 88 I=1,21
   88 U(I,165)=U(I,163)
      WRITE(6,72) SUM,ITN
   72 FORMAT(F20.5,5X,I3)
      IF(ITN.GT.MAXIT)GO TO 30
      IF(SUM.LE.ERROR)GO TO 30
      GO TO 70
   30 WRITE(6,23)
   23 FORMAT(1H1,/)
      DO 69 J=1,165
   69 WRITE(6,20)(U(I,J),I=1,21)
   20 FORMAT(1X,21F6.2/)
      WRITE(6,23)
C
C     STORE ARRAY OF POTENTIALS ON DISC
C
      WRITE (3) U
      STOP
      END
```

```
      SUBROUTINE ELECT(I,J,U,M,ZZ,XX,YY,A,MM,E,EE,EEE,SUM,OPTAP,EEEE)
C     FCN IS AN EXTERNAL FUNCTION CONTAINING THE POLYNOMIAL EQUATION OF
C     THE DIRICHLET BOUNDARY.
C
      EXTERNAL FCN
      DIMENSION A(5),S(10),C(1),G(1),H(1),U(21,165)
      INTEGER E,EE,EEE,EEEE
```

```
      REAL K1,K2,K3,K4,K5
      NVR=-1
      NCON=1
      NFIG=5
      NTRIPV=200
      INDEX=2
      KWRT=2
      L=10
      YY= FLOAT(J)
      IF(FFF.EQ.1)GO TO 7
      F=1.0
      GO TO 6
    7 U(F,J-1)=MM
      G(1)=J-1
      H(1)=J
      C(1)=(H(1)+G(1))/2.
C
C     CLIMB DETERMINES THE DISTANCE FROM THE NODE  POINT TO THE BOUNDARY.
C
      CALL CLIMB(NVR,C,NCON,V,NFIG,S,L,KWRT,G,H,INDEX,NTRIPV,FCN,YY,A)
      XX=C(1)
    3 T= FLOAT(J)-XX
    6 XX= FLOAT(J)-1.0
      IF(F.EQ.1)GO TO 8
      R=1.0
      GO TO 9
    8 XX= FLOAT(J)
      YY=A(1)+A(2)*XX+A(3)*XX**2+A(4)*XX**3+A(5)*XX**4
      R=YY- FLOAT(I)
      U(I+1,J)=MM
    9 YY= FLOAT(I)
      IF(FFF.EQ.1)GO TO 50
      P=1.0
      GO TO 51
   50 U(I,J+1)=MM
      G(1)=J
      H(1)=J+1
      C(1)=(H(1)+G(1))/2.
      CALL CLIMB(NVR,C,NCON,V,NFIG,S,L,KWRT,G,H,INDEX,NTRIPV,FCN,YY,A)
      XX=C(1)
      P= FLOAT(J)+XX
   51 XX= FLOAT(J)+1.0
      IF(FFF.EQ.1)GO TO 56
      W=1.0
      GO TO 57
   56 XX= FLOAT(J)
      YY=A(1)+A(2)*XX+A(3)*XX**2+A(4)*XX**3+A(5)*XX**4
      W= FLOAT(I)-YY
      U(I-1,J)=MM
   57 CONTINUE
      K1=(1.0+((W*1.0)/(2.0*FLOAT(I))))/(R*(W+R))
      K2=1.0/(P*(P+T))
      K3=(1.0-((R*1.0)/(2.0*FLOAT(I))))/(W*(P+W))
      K4=1.0/(T*(T+P))
      K5=(1.0/(W*R))+(1.0/(T*P))+((W-R)/(2.0*W*R*FLOAT(I)))
      RES =OPTAP*((((U(I+1,J)*K1)+(U(I,J+1)*K2)+(U(I-1,J)*K3)+(U(I,J-1)*
     1K4))/K5)-U(I,J))
      U(I,J)=U(I,J)+RES
      SUM=SUM+ABS(RES)
      RETURN
```

```
      END
      SUBROUTINE FCN(NVAR,C,NFCN,U,G,H,YY,A)
      DIMENSION C(1),G(1),H(1),A(5)
      XX=C(1)
      U= ABS(YY-(A(1)+A(2)*XX+A(3)*XX**2+A(4)*XX**3+A(5)*XX**4))
      RETURN
      END


      SUBROUTINECLIMB(NVR,X,NON,U,NFIG,S,LS,KWRT,G,H,INDEX,NTRIPV,FCN,YY
     1,A)
C     NOTE-THIS SUBROUTINE HAS BEEN MODIFIED TO SINGLE PRECISION NUMBERS.
C
C     FUNCTIONAL OPTIMIZATION BY ROSENBROCK'S METHOD OF HILL-CLIMBING
C
C     THE ARRAY S MUST BE DIMENSIONED AT LEAST  NVAR*(NVAR+5)+NCON
C
C     KWRT SET AS FOLLOWS FOR OUTPUTS -      2   OUTPUTS SUPPRESSED
C                                            1   AT START AND END ONLY
C                                            0   AT END OF EACH STAGE
C                                           -N   AFTER EVERY N TRIALS
C
C     INDEX  POSITIVE  FOR SIGNIFICANT FIGURE CONVERGENCE CRITERION
C            1  NO CONSTRAINTS ON INDEPENDENT VARIABLES - SETS G,H LARGE
C            2  FINITE CONSTRAINTS ON INDEP. VARIABLES SUPPLIED ON ENTRY
C            3  FOR RE-ENTRY WITHOUT INITIALIZATION
C            4  AS IN 3 BUT KTRIAL = 0
C     INDEX NEGATIVE  OF ABOVE FOR EXIT ONLY AFTER SPECIFIED TRIALS
C
      DIMENSION C(3),G(NON),H(NON),X(NON),S(LS)
      DIMENSION A(5)
C
C     INITIALIZATION
C  A LINE COUNTER IS SET SO THAT HEADINGS WILL BE PRINTED AT THE HEAD
C  OF EVERY PAGE.
      LINES=60
      NCON=NON-IABS(NVR)
      NVAR=IABS(NVR)
      SGN=NVR/NVAR
      NWRT=IABS(KWRT)
      NTOT=NVAR+NCON
      N2=NVAR*(NVAR+1)
      N3=N2+NTOT
      N4=N3+NVAR
      N5=N4+NVAR
      NTRIAL=NTRIPV*NVAR
      NCONS=NTOT
      NT=NVAR*(NVAR+5)+NCON
      NEND=0
      CONV=0.5*0.1**NFIG
      IND=IABS(INDEX)
C     THE  COMPROMISE VALUES OF THE 3 HILL-CLIMBING PARAMETERS FOLLOW
C      ALPHA AND BETA ARE FORWARD AND BACKWARD STEPPING PARAMETERS
      ALPHA=3.
      BETA=.5
      FAIL=1.
      CLIFF=.0001
```

```
      IND1=0
      GOTO(1,3,150,5),IND
5     KTRIAL=0
      IND1=1
      MWRT=NWRT
      GOTO39
1     DO2I=1,NVAR
      NCONS=NCONS-1
      G(I)=-1.0*10**75
2     H(I)=-G(I)
3     DO4I=1,NT
4     S(I)=0.
      IF(KWRT.GT.1)GOTO11
      IF(SSN)10,7,7
7     WRITE(6,101)NVAR,NCONS
      GOTO11
10    WRITE(6,102)NVAR,NCONS
101   FORMAT(////5X,'MAXIMUM OF FUNCTION OF ',I3,' VARIABLES WITH ',I3,'
     * CONSTRAINTS')
102   FORMAT(////5X,'MINIMUM OF FUNCTION OF ',I3,' VARIABLES WITH ',I3,'
     * CONSTRAINTS')
11    B(2)=0.
      B(3)=0.
      KTRIAL=0
      MWRT=NWRT
      DO15I=1,NVAR
      IF(G(I)-H(I))13,14,13
13    S(I)=.1
14    NI=(NVAR+1)*I
15    S(NI)=1.
      BIG= ABS(X(1))
      IF(NVAR.EQ.1)GOTO185
16    DO18I=2,NVAR
      ABX= ABS(X(I))
      IF(ABX.GT.BIG)BIG=ABX
18    CONTINUE
185   BIG=10.   *(ALPHA-1.   )*BIG+1.
      KCONV=0
      XO=1.
19    IF(XO.GT.BIG)GOTO21
20    KCONV=KCONV+1
      XO=ALPHA*XO
      GOTO19
C
C     CHECK INITIAL VALUES WRT. CONSTRAINTS
21    IF(NCON.LT.1)GOTO225
215   NV1=NVAR+1
      NC1=NVAR+NCON
      DO22I=NV1,NC1
22    X(I)=.5  *(G(I)+H(I))
225   NG=0
      DO39I=1,NTOT
      IF(H(I)-G(I))35,25,25
25    IF(X(I)-G(I))27,26,26
26    IF(H(I)-X(I))28,38,38
27    IF( ABS(G(I))-1.   )24,24,23
23    X(I)=G(I)+CLIFF*-ABS(G(I))
      GOTO30
24    X(I)=CLIFF
      GOTO30
```

```
28      IF( ABS(H(I)-1.  ))37,37,36
36      X(I)=H(I)-CLIFF* ABS(H(I))
        GOTO38
37      X(I)=CLIFF
38      IF(NG.NE.0)GOTO32
31      WRITE(6,105)
105     FORMAT(/5X,'INITIAL VALUES MUST NOT LIE OUTSIDE OR ON CONSTRAINTS'
       *//)
        NG=1
32      IF(G(I)-H(I))33,34,33
33      WRITE(6,106)I,X(I)
106     FORMAT(10X,'VARIABLE',I4,'  TAKEN AS ',G16.7)
        GOTO38
34      X(I)=G(I)
        WRITE(6,107)I,X(I)
107     FORMAT(10X,'VARIABLE',I4,'  CONSTRAINED TO BE ',G16.7)
        GOTO38
35      WRITE(6,108)I,G(I),H(I)
108     FORMAT(/5X,'FOR VARIABLE',I4,'  LOWER LIMIT',E15.8,'  AND UPPER','
       * LIMIT',E15.8,'  HAD TO BE INTERCHANGED'/)
        G1=G(I)
        G(I)=H(I)
        H(I)=G1
        GOTO25
38      CONTINUE
        U1=0.
        IF(NTRIAL.EQ.0)GOTO86
39      CONTINUE
        CALLFCN(NVAR,X,NCON,U1,G,H,YY,A)
        U1=SGN*U1
        DO40I=1,NTOT
        N2I=N2+I
40      S(N2I)=U1
        IF(KWRT.EQ.2)GOTO90
        GOTO82
C
C       BEGINNING OF HILL-CLIMBING
C
C       STAGE OUTPUTS OR END OF CALCULATION
   80   IF(KWRT-1)82,81,83
81      IF(KTRIAL.EQ.0)GOTO82
        IF(NEND.NE.1)GOTO90
82      CALLFCN(NVAR,X,NCON,B(1),G,H,YY,A)
        IF(LINES.LT.60)GOTO999
        PRINT99
99      FORMAT('1'//T06,'NO. OF  CURRENT TRIAL  LAST SUCCESSFUL  TOTAL DIS
       *TANCE  CHANGE IN DIRECTN'/T6,'TRIALS    VALUE OF    FUNCTIONAL VAL
       *UE        MOVED          OF MOTION'/T14,'IND VARIABLES',T47,'DURING
       * STAGE    FROM LAST STAGE'/)
        LINES=6
999     WRITE(6,110)KTRIAL,B,(X(I),I=1,NVAR)
110     FORMAT(I11,16X,3G16.7/(11X,G16.7))
        LINES=LINES+NVAR+1
        IF(KWRT.EQ.1)GOTO88
83      IF(KTRIAL.LT.NTRIAL)GOTO88
86      CALLFCN(NVAR,X,NCON,B(1),G,H,YY,A)
        U=B(1)
        RETURN
88      IF(NEND.LT.1)GOTO90
89      IF(KWRT.GE.2)GOTO86
```

```
91      WRITE(6,113)NFIG
113     FORMAT(//5X,'CONVERGENCE TO',I4,'  SIGNIFICANT FIGURES REACHED IN
     *ALL  INDEPENDENT VARIABLES.'/)
87      GOTO96
C
C       BEGINNING OF  STAGE
C
C       EXPANDED STEP OF VARIABLES
90      IF(IND1.EQ.1)GOTO93
97      DO92J=1,NVAR
        N3J=N3+J
        N5J=N5+J
        S(N3J)=0.
92      S(N5J)=0.
93      JS=1
        IND1=0
        NEND=0
94      DO96I=1,NVAR
        IF(G(I)-H(I))95,96,95
95      NI=NVAR*I+JS
        X(I)=S(NI)*S(JS)+X(I)
96      CONTINUE
C
C       FUNCTION EVALUATION
        KTRIAL=KTRIAL+1
        CALL FCN(NVAR,X,NCON,U2,G,H,YY,A)
        U2=SGN*U2
C
C       CHECK CONSTRAINTS
        DO123I=1,NTOT
        N2I=N2+I
        IF(G(I)-H(I))125,120,125
125     IF(U1-U2)126,126,145
126     IF(X(I)-G(I))145,145,127
127     IF(H(I)-X(I))145,145,128
128     CONTINUE
        DO135I=1,NTOT
        N2I=N2+I
        IF(G(I)-H(I))120,134,120
120     IF( ABS(G(I))-1.  )121,121,122
121     SN1=CLIFF
        GOTO123
122     SN1=CLIFF* ABS(G(I))
123     IF(X(I)-(G(I)+SN1))129,130,130
129     GO=(G(I)+SN1-X(I))/SN1
        GOTO132
130     IF( ABS(H(I)-1.  ))136,136,137
136     SN1=CLIFF
        GOTO138
137     SN1=CLIFF* ABS(H(I))
138     IF(H(I)-SN1-X(I))131,133,133
131     GO=(X(I)-H(I)+SN1)/SN1
132     HO=U2-S(N2I)
        U2=U2+GO*HO*((4.  -2.  *GO)*GO-3.  )
        IF(U1-U2)135,135,145
133     S(N2I)=U1
        GOTO135
134     S(I)=0.
135     CONTINUE
        IF(G(JS)-H(JS))140,142,140
```

```
 140    N4J=N4+JS
        N5J=N5+JS
        IF(S(N5J)-.5  )141,142,142
 141    S(N4J)=0.
        S(N5J)=1.
 142    N3J=N3+JS
        S(N3J)=S(N3J)+S(JS)
        U1=U2
        S(JS)=ALPHA*S(JS)
        GOTO150
C
C       UNDO UNSUCCESSFUL STEP AND REVERSE DIRECTION WITH REDUCED STEP
  145 DO140I=1,NVAR
        IF(G(I)-H(I))146,148,146
 146    NI=NVAR*I+JS
        X(I)=X(I)-S(NI)*S(JS)
 148    CONTINUE
        S(JS)=-BETA*S(JS)
        N4J=N4+JS
        S(N4J)=S(N4J)+1.
C
C       CHECK FOR STAGE OPTIMUM IN EVERY DIRECTION
 150    IF(KTRIAL.GE.NTRIAL)GOTO80
 151    DO155I=1,NVAR
        IF(G(I)-H(I))152,155,152
 152    N4I=N4+I
        N5I=N5+I
        IF(S(N4I)+.5  -FAIL)160,153,153
 153    IF(S(N5I)-.5  )160,155,155
 155    CONTINUE
        GOTO41
 160    JS=JS+1
        IF(JS.GT.NVAR)GOTO169
 164    IF(KWRT.GE.0)GOTO170
 165    IF(KTRIAL.LT.MWRT)GOTO170
C
C       INTERMEDIATE FORCED OUTPUTS
  166 MWRT=MWRT+NWRT
        UP=SGN*U1
        WRITE(6,115)KTRIAL,UP,(X(I),S(I),I=1,NVAR)
 115    FORMAT(31X,I10,16X,G16.7/(11X,G16.7,16X,G16.7))
 170    IF(JS.LE.NVAR)GOTO94
        GOTO93
 169    IF(KTRIAL.LT.KCONV)GOTO164
 171    IF(INDEX.LE.0)GOTO164
C
C       CONVERGENCE TESTS
  172 DO173I=1,NVAR
        DX=0.
        DO173K=1,NVAR
        NI=NVAR*I+K
 173    DX=DX+S(NI)*S(K)
        IF( ABS(X(I))-1.   )174,174,175
C       IF RELATIVE CONVERGENCE TESTS ARE DESIRED FOR LESS THAN UNITY
C       MAGNITUDES THE PREVIOUS STATEMENT SHOULD BE CHANGED TO SUIT USER'S
C       NEED. FOR EXAMPLE  IF(ABS(X(I))) 175,174,175          MAY BE USED
C       BUT UNDERFLOWS MAY OCCUR IF MAGNITUDES ARE VERY SMALL
 174    CRIT= ABS(DX)
        GOTO176
 175    CRIT= ABS(DX/X(I))
```

```
176   IF(CRIT.GE.CONV)GOTO164
180   CONTINUE
      NEND=1
      GOTO80
C
C
      TRANSFORMATION OF COORDINATES AT END OF STAGE BY GRAM-SCHMIDT ORTH
   41 DO45I=1,NVAR
      NN=NVAR*I+NVAR
      S(NN)=S(N4)*S(NN)
      DO45J=2,NVAR
      NJ=NVAR-J+1
      N3J=N3+NJ
      NI=NVAR*I+NJ
   45 S(NI)=S(N3J)*S(NI)+S(NI+1)
   47 IF(NVAR.EQ.1)S(3)=0.0
      DO50J=2,3
      B(J)=0.
      DO49I=1,NVAR
      NI=NVAR*I+J-1
   49 B(J)=S(NI)**2+B(J)
   50 B(J)= SQRT(B(J))
      B(3)=B(3)/B(2)
   55 J=1
   56 K=1
   57 IF(K.EQ.J)GOTO68
   58 B(1)=0.
      DO60I=1,NVAR
      NI=NVAR*I+J
      NK=NI-K
   60 B(1)=B(1)+S(NI)*S(NK)
      DO65I=1,NVAR
      NI=NVAR*I+J
      NK=NI-K
   65 S(NI)=-S(NK)*B(1)+S(NI)
      K=K+1
      GOTO57
   68 B(1)=0.
      DO70I=1,NVAR
      NI=NVAR*I+J
   70 B(1)=B(1)+S(NI)**2
      B(1)= SQRT(B(1))
      DO75I=1,NVAR
      NI=NVAR*I+J
   75 S(NI)=S(NI)/B(1)
      J=J+1
      IF(NVAR.GE.J)GOTO56
      GOTO80
      END
```

```
C
C     CHANGE FROM COARSE MESH TO FINER MESH IN REGION OF INTEREST.
C     POTENTIALS DESCRIBED BY COARSE MESH BECOME BOUNDARY CONDITIONS
C     IN FINER MESH.  V IS THE NEW ARRAY OF POTENTIALS.
      DIMENSION U(21,165),V(50,201)
      READ (3) U
```

```
      REWIND 3
      ERROR=5.0
      MAXIT=200
      A=50.
      B=201.
      OPTAP=2./(1.+SQRT(1.-((COS(3.142/A)+COS(3.142/B))**2/4.+1))
      DO 1 I=2,49
      DO 1 J=2,200
    1 V(I,J)=70.0
      J=1
      DO 2 I=1,7
    2 V(5*I+15,J)=U(I+3,125)
      J=201
      DO 3 I=1,5
    3 V(5*I+25,J)=U(I+5,165)
      DO 4 J=1,40
    4 V(50,5*J+1)=U(10,J+125)
      J=1
      DO 5 I=20,45,5
      V(I+1,J)=V(I,J)-((V(I,J)-V(I+5,J))*1./5.)
      V(I+2,J)=V(I,J)-((V(I,J)-V(I+5,J))*2./5.)
      V(I+3,J)=V(I,J)-((V(I,J)-V(I+5,J))*3./5.)
      V(I+4,J)=V(I,J)-((V(I,J)-V(I+5,J))*4./5.)
    5 CONTINUE
      J=201
      DO 6 I=30,45,5
      V(I+1,J)=V(I,J)-((V(I,J)-V(I+5,J))*1./5.)
      V(I+2,J)=V(I,J)-((V(I,J)-V(I+5,J))*2./5.)
      V(I+3,J)=V(I,J)-((V(I,J)-V(I+5,J))*3./5.)
      V(I+4,J)=V(I,J)-((V(I,J)-V(I+5,J))*4./5.)
    6 CONTINUE
      I=50
      DO 7 J=1,196,5
      V(I,J+1)=V(I,J) + ((V(I,J+5)-V(I,J))*1./5.)
      V(I,J+2)=V(I,J) + ((V(I,J+5)-V(I,J))*2./5.)
      V(I,J+3)=V(I,J) + ((V(I,J+5)-V(I,J))*3./5.)
      V(I,J+4)=V(I,J) + ((V(I,J+5)-V(I,J))*4./5.)
    7 CONTINUE
      M=20
      DO 8 J=1,201
      IF(J.EQ.92.OR.J.EQ.93.OR.J.EQ.94.OR.J.EQ.95.OR.J.EQ.96)M=M-1
      IF(J.EQ.126)M=M+10
      IF(J.EQ.157.OR.J.EQ.158.OR.J.EQ.159.OR.J.EQ.160.OR.J.EQ.161)M=M-1
     1Q.172.OR.J.EQ.173.OR.J.EQ.174.OR.J.EQ.175.OR.J.EQ.176)M=M+1
      DO 8 I=1,M
    8   V(I,J)=100.0
      ITN=1
   70 SUM=0.0
      M=48
      DO 9 J=2,86
      IF(
     1.J.EQ.22.OR.J.EQ.25.OR.J.EQ.27.OR.J.EQ.10.OR.J.EQ.13.OR.J.EQ.16.OR.J.EQ.19.OR
     2.J.EQ.37.OR.J.EQ.40.OR.J.EQ.43.OR.J.EQ.46.OR.J.EQ.49.OR.J.EQ.52.OR.
     3.J.EQ.55.OR.J.EQ.58.OR.J.EQ.61.OR.J.EQ.64.OR.J.EQ.67.OR.J.EQ.70.OR
     4.J.EQ.73.OR.J.EQ.76.OR.J.EQ.79.OR.J.EQ.82.OR.J.EQ.85)M=M-1
      DO 9 I=21,M
      RES =OPTAP*((V(I,J+1)+V(I,J-1)+V(I+1,J)*(1.+1./(2.*FLOAT(I)))+V(I-
     11,J)*(1.-1./(2.*FLOAT(I))))/4.-V(I,J))
      V(I,J)=V(I,J)+RES
```

```
9       SUM=SUM+ABS(RES)
        READ (5,900) E1,E2,E3,E4,E5,E6,E7,E8
900     FORMAT(8F3.1)
        I=49
        J=19
        DO 10 N=1,6
        H1=1./(4.*FLOAT(I))
        H2=1./(2.*FLOAT(I))
        A1=(1.0+H1)*E1+(1.0-H1)*E8
        A2=(1.0+H2)*(E2+E3)
        A3=(1.0+H1)*E4+(1.0-H1)*E5
        A4=(1.0-H2)*(E6+E7)
        A5=A1+A2+A3+A4
        RES=(OMTAP/A5)*((V(I+1,J)*A2)+(V(I-1,J)*A4)+(V(I,J+1)*A1)+(V(I,J-1
      1)*A3)-(V(I,J)*A5))
        V(I,J)=V(I,J)+RES
        SUM=SUM+ABS(RES)
        I=I-1
        J=J+3
10      CONTINUE
        READ (5,900) E1,E2,E3,E4,E5,E6,E7,E8
        I=42
        J=27
        DO 51 N=1,2
        H1=1./(4.*FLOAT(I))
        H2=1./(2.*FLOAT(I))
        A1=(1.0+H1)*E1+(1.0-H1)*E8
        A2=(1.0+H2)*(E2+E3)
        A3=(1.0+H1)*E4+(1.0-H1)*E5
        A4=(1.0-H2)*(E6+E7)
        A5=A1+A2+A3+A4
        RES=(OMTAP/A5)*((V(I+1,J)*A2)+(V(I-1,J)*A4)+(V(I,J+1)*A1)+(V(I,J-1
      1)*A3)-(V(I,J)*A5))
        V(I,J)=V(I,J)+RES
        SUM=SUM+ABS(RES)
        I=I-1
        J=J+3
51      CONTINUE
        READ (5,900) E1,E2,E3,E4,E5,E6,E7,E8
        I=43
        J=31
        DO 52 N=1,19
        H1=1./(4.*FLOAT(I))
        H2=1./(2.*FLOAT(I))
        A1=(1.0+H1)*E1+(1.0-H1)*E8
        A2=(1.0+H2)*(E2+E3)
        A3=(1.0+H1)*E4+(1.0-H1)*E5
        A4=(1.0-H2)*(E6+E7)
        A5=A1+A2+A3+A4
        RES=(OMTAP/A5)*((V(I+1,J)*A2)+(V(I-1,J)*A4)+(V(I,J+1)*A1)+(V(I,J-1
      1)*A3)-(V(I,J)*A5))
        V(I,J)=V(I,J)+RES
        SUM=SUM+ABS(RES)
        I=I-1
        J=J+3
52      CONTINUE
        READ (5,900) E1,E2,E3,E4,E5,E6,E7,E8
        I=49
        J=9
        DO 11 N=1,6
```

```
      H1=1./(4.*FLOAT(I))
      H2=1./(2.*FLOAT(I))
      A1=(1.0+H1)*E1+(1.0-H1)*E8
      A2=(1.0+H2)*(E2+E3)
      A3=(1.0+H1)*E4+(1.0-H1)*E5
      A4=(1.0-H2)*(E6+E7)
      A5=A1+A2+A3+A4
      RES=(OMTAP/A5)*((V(I+1,J)*A2)+(V(I-1,J)*A4)+(V(I,J+1)*A1)+(V(I,J-1
     1)*A3)-(V(I,J)*A5))
      V(I,J)=V(I,J)+RES
      SUM=SUM+ABS(RES)
      I=I-1
      J=J+3
11    CONTINUE
      READ (5,900) E1,E2,E3,E4,E5,E6,E7,E8
      I=43
      J=26
      DO 53 N=1,2
      H1=1./(4.*FLOAT(I))
      H2=1./(2.*FLOAT(I))
      A1=(1.0+H1)*E1+(1.0-H1)*E8
      A2=(1.0+H2)*(E2+E3)
      A3=(1.0+H1)*E4+(1.0-H1)*E5
      A4=(1.0-H2)*(E6+E7)
      A5=A1+A2+A3+A4
      RES=(OMTAP/A5)*((V(I+1,J)*A2)+(V(I-1,J)*A4)+(V(I,J+1)*A1)+(V(I,J-1
     1)*A3)-(V(I,J)*A5))
      V(I,J)=V(I,J)+RES
      SUM=SUM+ABS(RES)
      I=I-1
      J=J+2
53    CONTINUE
      READ (5,900) E1,E2,E3,E4,E5,E6,E7,E8
      I=41
      J=30
      DO 54 N=1,19
47    H1=1./(4.*FLOAT(I))
      H2=1./(2.*FLOAT(I))
      A1=(1.0+H1)*E1+(1.0-H1)*E8
      A2=(1.0+H2)*(E2+E3)
      A3=(1.0+H1)*E4+(1.0-H1)*E5
      A4=(1.0-H2)*(E6+E7)
      A5=A1+A2+A3+A4
      RES=(OMTAP/A5)*((V(I+1,J)*A2)+(V(I-1,J)*A4)+(V(I,J+1)*A1)+(V(I,J-1
     1)*A3)-(V(I,J)*A5))
      V(I,J)=V(I,J)+RES
      SUM=SUM+ABS(RES)
      I=I-1
      J=J+3
54    CONTINUE
      READ (5,900) E1,E2,E3,E4,E5,E6,E7,E8
      I=48
      J=11
      DO 12 N=1,5
      H1=1./(4.*FLOAT(I))
      H2=1./(2.*FLOAT(I))
      A1=(1.0+H1)*E1+(1.0-H1)*E8
      A2=(1.0+H2)*(E2+E3)
      A3=(1.0+H1)*E4+(1.0-H1)*E5
      A4=(1.0-H2)*(E6+E7)
```

```
      A5=A1+A2+A3+A4
      RES=(OPTAP/A5)*((V(I+1,J)*A2)+(V(I-1,J)*A4)+(V(I,J+1)*A1)+(V(I,J-1
     1)*A3)-(V(I,J)*A5))
      V(I,J)=V(I,J)+RES
      SUM=SUM+ABS(RES)
      I=I-1
      J=J+3
   12 CONTINUE
      READ (5,900) E1,E2,E3,E4,E5,E6,E7,E8
      I=49
      DO 95 J=7,8
      H1=1./(4.*FLOAT(I))
      H2=1./(2.*FLOAT(I))
      A1=(1.0+H1)*E1+(1.0-H1)*E8
      A2=(1.0+H2)*(E2+E3)
      A3=(1.0+H1)*E4+(1.0-H1)*E5
      A4=(1.0-H2)*(E6+E7)
      A5=A1+A2+A3+A4
      RES=(OPTAP/A5)*((V(I+1,J)*A2)+(V(I-1,J)*A4)+(V(I,J+1)*A1)+(V(I,J-1
     1)*A3)-(V(I,J)*A5))
      V(I,J)=V(I,J)+RES
   95 SUM=SUM+ABS(RES)
      READ (5,900) E1,E2,E3,E4,E5,E6,E7,E8
      I=40
      J=82
      DO 14 M=1,18
      H1=1./(4.*FLOAT(I))
      H2=1./(2.*FLOAT(I))
      A1=(1.0+H1)*E1+(1.0-H1)*E8
      A2=(1.0+H2)*(E2+E3)
      A3=(1.0+H1)*E4+(1.0-H1)*E5
      A4=(1.0-H2)*(E6+E7)
      A5=A1+A2+A3+A4
      RES=(OPTAP/A5)*((V(I+1,J)*A2)+(V(I-1,J)*A4)+(V(I,J+1)*A1)+(V(I,J-1
     1)*A3)-(V(I,J)*A5))
      V(I,J)=V(I,J)+RES
      SUM=SUM+ABS(RES)
      I=I-1
      J=J+3
   14 CONTINUE
      READ (5,900) E1,E2,E3,E4,E5,E6,E7,E8
      I=22
      J=86
      H1=1./(4.*FLOAT(I))
      H2=1./(2.*FLOAT(I))
      A1=(1.0+H1)*E1+(1.0-H1)*E8
      A2=(1.0+H2)*(E2+E3)
      A3=(1.0+H1)*E4+(1.0-H1)*E5
      A4=(1.0-H2)*(E6+E7)
      A5=A1+A2+A3+A4
      RES=(OPTAP/A5)*((V(I+1,J)*A2)+(V(I-1,J)*A4)+(V(I,J+1)*A1)+(V(I,J-1
     1)*A3)-(V(I,J)*A5))
      V(I,J)=V(I,J)+RES
      SUM=SUM+ABS(RES)
      READ (5,900) E1,E2,E3,E4,E5,E6,E7,E8
      I=21
      J=87
      H1=1./(4.*FLOAT(I))
      H2=1./(2.*FLOAT(I))
      A1=(1.0+H1)*E1+(1.0-H1)*E8
```

```
      A2=(1.0+H2)*(E2+E3)
      A3=(1.0+H1)*E4+(1.0-H1)*E5
      A4=(1.0-H2)*(E6+E7)
      A5=A1+A2+A3+A4
      RES=(OPTAP/A5)*((V(I+1,J)*A2)+(V(I-1,J)*A4)+(V(I,J+1)*A1)+(V(I,J-1
     1)*A3)-(V(I,J)*A5))
      V(I,J)=V(I,J)+RES
      SUM=SUM+ABS(RES)
      M=49
      DO 15 J=10,200
      IF(J.EQ.13.OR.J.EQ.16)M=M-1
      IF(J.EQ.19.OR.J.EQ.22)M=M-1
      IF(J.EQ.25.OR.J.EQ.27)M=M-1
      IF(J.EQ.29.OR.J.EQ.31)M=M-1
      IF(J.EQ.34.OR.J.EQ.37)M=M-1
      IF(J.EQ.40.OR.J.EQ.43)M=M-1
      IF(J.EQ.46.OR.J.EQ.49)M=M-1
      IF(J.EQ.52.OR.J.EQ.55)M=M-1
      IF(J.EQ.58.OR.J.EQ.61)M=M-1
      IF(J.EQ.64.OR.J.EQ.67)M=M-1
      IF(J.EQ.70.OR.J.EQ.73)M=M-1
      IF(J.EQ.76.OR.J.EQ.79)M=M-1
      IF(J.EQ.82.OR.J.EQ.85)M=M-1
      IF(J.EQ.87.OR.J.EQ.88.OR.J.EQ.92.OR.J.EQ.93.OR.J.EQ.94.OR.J.EQ.95.
     1OR.J.EQ.96)M=M-1
      IF(J.EQ.126)M=M+10
      IF(J.EQ.157.OR.J.EQ.158.OR.J.EQ.159.OR.J.EQ.160.OR.J.EQ.161)M=M-1
      IF(J.EQ.128.OR.J.EQ.130.OR.J.EQ.132.OR.J.EQ.134.OR.J.EQ.136.OR.J.E
     1Q.172.OR.J.EQ.173.OR.J.EQ.174.OR.J.EQ.175.OR.J.EQ.176)M=M+1
      DO 15 I=M,49
      RES=OPTAP*((V(I,J+1)+V(I,J-1)+V(I+1,J)*(1.+1./(2.*FLOAT(I))))+V(I-
     1,J)*(1.-1./(2.*FLOAT(I))))/4.-V(I,J))
      V(I,J)=V(I,J)+RES
15    SUM=SUM+ABS(RES)
      ITN=ITN+1
      WRITE(6,71) SUM,ITN
71    FORMAT(F20.5,5X,I3)
      IF(ITN.GT.MAXIT)GO TO 30
      IF(SUM.LE.ERROR)GO TO 30
      GO TO 70
30    WRITE(6,23)
23    FORMAT(1H1,/)
      DO 19 J=1,201
19    WRITE(6,20)(V(I,J),I=1,25)
20    FORMAT(1X,25F5.1/)
      WRITE(6,23)
      DO 99 J=1,201
99    WRITE(6,20)(V(I,J),I=26,50)
      WRITE (3) V
      STOP
      END
//GO.FT03F001 DD DSNAME=FENG.MALEWICZ.DATA,DISP=(OLD,KEEP),
//   UNIT=2314,VOL=SER=DSUSE3,SPACE=(TRK,(20,5)),
//   DCB=(RECFM=VS,LRECL=804,BLKSIZE=808)
//GO.SYSIN  DD  *
//GO.ANYNAME DD DSN=*.STEP2.LKED.SYSLMOD,DISP=(OLD,DELETE)
//STEP3 EXEC FORTGCLG
//FORT.SYSIN  DD  *
C
C     CALCULATION OF SPACE ANGLES.
```

```
C
      REAL V(50,201),EZ(50,200),A(50,201)
      READ (3) V
      REWIND 3
      Z=3.1415926
      DO 91 J=1,200
      DO 91 I=1,49
   91 EZ(I,J)=V(I,J)-V(I,J+1)
      DO 96 J=1,200
      DO 96 I=1,49
      IF(ABS(EZ(I,J)).EQ.0.)EZ(I,J)=1.0E-8
      A(I,J)=ATAN((V(I,J)-V(I+1,J))/EZ(I,J))
      IF(EZ(I,J).LT.0..AND.(V(I,J)-V(I+1,J)).GT.0.)A(I,J)=Z+A(I,J)
      IF(EZ(I,J).LT.0..AND.(V(I,J)-V(I+1,J)).LT.0.)A(I,J)=Z+A(I,J)
      IF(EZ(I,J).GT.0..AND.(V(I,J)-V(I+1,J)).LT.0.)A(I,J)=2.*Z+A(I,J)
   96 CONTINUE
      IF(EZ(I,J).EQ.1.0E-8)EZ(I,J)=0.
      DO 97 J=1,200
   97 WRITE(6,82)(A(I,J),I=1,25)
   82 FORMAT(25F5.2/)
      WRITE(6,13)
   13 FORMAT(1H1,/)
      DO 98 J=1,200
   98 WRITE(6,82)(A(I,J),I=25,49)
      WRITE (3) V,A
      STOP
      END
```

```
C
CC    DETERMINATION AND PLOTTING OF EQUIPOTENTIAL AND FLUX LINES.
CC    PROGRAM TO PLOT EQUIPOTENTIAL LINES WAS DEVELOPED BY MR. R. HAZEL
C
      REAL V(50,201),A(50,201),X(500),Y(500),IIS(9),JJS(9),PP(9)
      DIMENSION IBUF(1000)
      READ (3) V,A
      REWIND 3
      II=50
      JJ=201
C
CC    READ EQUIPOTENTIAL LINES REQUIRED.
C
      DO 31 I=1,9
      READ(5,11) PP(I)
   11 FORMAT(F6.2)
   31 CONTINUE
      CALL PLOTIC('R.MALLEWICZ        ',&R1260D0238')
      CALL PLOT(0.0,3.5,-3)
      CALL AXIS(0.0,0.0,34HLONGITUDINAL LENGTH (*.0125INCHES),-34,10.,0.
     1,0.,20.0)
      CALL AXIS(0.0,0.0,28HRADIAL LENGTH (*.0125INCHES),28,6.5,90.0,0.0,
     17.7)
      DO 78 K=1,9
      J=1
      DO 111 I=1,II
      IF(V(I,J).GE.PP(K).AND.V(I+1,J).LT.PP(K)) GO TO 77
  111 CONTINUE
```

```
 77    IIS(K)=I
 78    JJS(K)=J
C
CC     EQUIPOTENTIAL LINES.
C
       DO 21 L=1,9
       N1=0
       N2=0
       N3=0
       N4=0
       P=PP(L)
       I=IIS(L)
       IS=IIS(L)
       J=JJS(L)
       JS=JJS(L)
       XO=1.
       YO=1.
       K=0
    9  K=K+1
 62    IF(I.EQ.II.AND.K.NE.1) GO TO 14
       IF(J.EQ.1.AND.K.GT.5) GO TO 14
       IF(J.EQ.JJ.AND.K.NE.1) GO TO 14
    5  IF(N1.EQ.1)GOTO6
       IF(V(I+1,J+1).GE.P.AND.V(I,J+1).LE.P)GOTO2
       IF(V(I+1,J+1).LE.P.AND.V(I,J+1).GE.P)GOTO2
    6  IF(N4.EQ.1)GOTO7
       IF(V(I,J+1).GE.P.AND.V(I,J).LE.P)GOTO3
       IF(V(I,J+1).LE.P.AND.V(I,J).GE.P)GOTO3
    7  IF(N3.EQ.1)GOTO8
       IF(V(I+1,J+1).GE.P.AND.V(I+1,J).LE.P)GOTO4
       IF(V(I+1,J+1).LE.P.AND.V(I+1,J).GE.P)GOTO4
    8  IF(N2.EQ.1)GOTO14
       IF(V(I+1,J).GE.P.AND.V(I,J).LE.P)GOTO1
       IF(V(I+1,J).LE.P.AND.V(I,J).GE.P)GOTO1
       GOTO14
    1  Y(K)=I-YO+(P-V(I,J))/(V(I+1,J)-V(I,J))
       X(K)=J-XO
       N1=1
       N2=0
       N3=0
       N4=0
       J=J-1
       GOTO9
    2  Y(K)=I-YO+(P-V(I,J+1))/(V(I+1,J+1)-V(I,J+1))
       X(K)=J+1-XO
       N1=0
       N2=1
       N3=0
       N4=0
       J=J+1
       GOTO9
    3  Y(K)=I-YO
       X(K)=J-XO+(P-V(I,J))/(V(I,J+1)-V(I,J))
       N1=0
       N2=0
       N3=1
       N4=0
       I=I-1
       GOTO9
    4  Y(K)=I+1-YO
```

```
      X(K)=J-XO+(P-V(I+1,J))/(V(I+1,J+1)-V(I+1,J))
      N1=0
      N2=0
      N3=0
      N4=1
      I=I+1
      GOTO 9
   14 K=K-1
      KK=K
      X(K+1)=0.0
      Y(K+1)=0.0
      X(K+2)=20.0
      Y(K+2)=7.7
      CALL LINE (X,Y,K,1,0,0)
   21 CONTINUE
      K=0
      DO 555 J=1,201
      DO 555 I=1,49
      IF(V(I,J).EQ.100.0.AND.V(I+1,J).LT.100.0)GO TO 444
      GO TO 555
  444 K=K+1
      X(K)=J
      Y(K)=I
  555 CONTINUE
      X(K+1)=0.0
      Y(K+1)=0.0
      X(K+2)=20.0
      Y(K+2)=7.7
      CALL LINE(X,Y,K,1,0,0)
      Z=3.1415926
C
C     FLUX LINES.
C
      DO 66 KK=1,9
      READ(5,119) X(1),Y(1)
  119 FORMAT(2F5.1)
      I=IFIX(Y(1))
      J=IFIX(X(1))
      K=1
   90 K=K+1
      IF(I.EQ.II)GO TO 49
      IF(J.EQ.JJ)GO TO 49
      IF(A(I,J).LT.Z/2.)GO TO 39
      IF(A(I,J).GT.Z/2..AND.A(I,J).LT.Z)GO TO 48
      IF(A(I,J).GT.Z.AND.A(I,J).LT.1.5*Z)GO TO 58
      IF(A(I,J).GT.1.5*Z.AND.A(I,J).LT.2.0*Z)GO TO 68
   48 Y(K)=Y(K-1)+0.5*SIN(Z-A(I,J))
      X(K)=X(K-1)-0.5*COS(Z-A(I,J))
      CALL FIX(I,J,X,Y,K)
      GO TO 90
   39 Y(K)=Y(K-1)+0.5*SIN(A(I,J))
      X(K)=X(K-1)+0.5*COS(A(I,J))
      CALL FIX(I,J,X,Y,K)
      GO TO 90
   58 Y(K)=Y(K-1)-0.5*SIN(A(I,J)-Z)
      X(K)=X(K-1)-0.5*COS(A(I,J)-Z)
      CALL FIX(I,J,X,Y,K)
      GO TO 90
   68 Y(K)=Y(K-1)-0.5*SIN(2*Z-A(I,J))
      X(K)=X(K-1)+0.5*COS(2*Z-A(I,J))
```

```
      CALL FIX(I,J,X,Y,K)
      GO TO 90
   49 K=K-1
      X(K+1)=0.0
      Y(K+1)=0.0
      X(K+2)=20.0
      Y(K+2)=7.7
      PRINT 707,(X(I),Y(I),I=1,K)
  707 FORMAT('0',75(22F6.1,/,' '))
      CALL LINE(X,Y,K,1,0,0)
   66 CONTINUE
      CALL PLTEND(15.0)
      WRITE (3) V
      STOP
      END



      SUBROUTINE FIX(I,J,X,Y,K)
      DIMENSION X(500),Y(500)
      A=Y(K)-IFIX(Y(K))
      IF(A.GE.0.5)I=IFIX(Y(K))+1
      IF(A.LT.0.5)I=IFIX(Y(K))
      B=X(K)-IFIX(X(K))
      IF(B.GE.0.5)J=IFIX(X(K))+1
      IF(B.LT.0.5)J=IFIX(X(K))
      RETURN
      END



C
CC    DETERMINATION AND PLOTTING OF EQUIGRADIENT LINES.
C
      REAL V(50,201),E(50,200),X(500),Y(500),IIS(9),JJS(9),PP(9)
      DIMENSION IBUF(1000)
      READ (3) V
      REWIND 3
C
CC    FIELD INTENSITY (OR GRADIENT) VECTOR E.
C
      DO 41 J=1,200
      DO 41 I=1,49
   41 E(I,J)=SQRT((V(I,J)-V(I+1,J))**2 + (V(I,J)-V(I,J+1))**2)
      DO 44 J=1,200
   44 WRITE(6,98)(E(I,J),I=1,25)
   98 FORMAT(25F5.1/)
      WRITE(6,23)
   23 FORMAT(1H1,/)
      DO 45 J=1,200
      WRITE(6,98)(E(I,J),I=25,49)
   45 CONTINUE
      CALL PLOTID('R.MALEWICZ       ','R126000238')
      CALL PLOT(0.0,0.5,-3)
      CALL AXIS(0.0,0.0,34HLONGITUDINAL LENGTH (*.062 INCHES),-34,10.,0.
     10,1.0,20.0)
```

```
      CALL AXIS(0.0,0.0,28HRADIAL LENGTH (*.062 INCHES),28,6.5,90.0,0.0,
     17.7)
      J=1
      LL=0
   88 LL=LL+1
      II=42
      JJ=200
C
C     EQUIGRADIENT LINES
C
      DO 31 I=1,8
      READ(5,11) PP(I)
   11 FORMAT(F6.2)
   31 CONTINUE
      DO 78 K=1,8
      DO 111 I=1,II
      IF(E(I,J).GE.PP(K).AND.E(I+1,J).LT.PP(K)) GO TO 77
  111 CONTINUE
   77 IIS(K)=I
   78 JJS(K)=J
      DO 21 L=1,8
      N1=0
      N2=0
      N3=0
      N4=0
      P=PP(L)
      I=IIS(L)
      IS=IIS(L)
      J=JJS(L)
      JS=JJS(L)
      XO=1.
      YO=1.
      K=0
    9 K=K+1
   62 IF(I.EQ.II.AND.K.NE.1) GO TO 14
      IF(J.EQ.1.AND.K.GT.5) GO TO 14
      IF(J.EQ.JJ.AND.K.NE.1) GO TO 14
      IF(V(I+1,J).EQ.100.0) GO TO 14
    5 IF(N1.EQ.1)GOTO6
      IF(E(I+1,J+1).GE.P.AND.E(I,J+1).LE.P)GOTO2
      IF(E(I+1,J+1).LE.P.AND.E(I,J+1).GE.P)GOTO2
    6 IF(N4.EQ.1)GOTO7
      IF(E(I,J+1).GE.P.AND.E(I,J).LE.P)GOTO3
      IF(E(I,J+1).LE.P.AND.E(I,J).GE.P)GOTO3
    7 IF(N3.EQ.1)GOTO8
      IF(E(I+1,J+1).GE.P.AND.E(I+1,J).LE.P)GOTO4
      IF(E(I+1,J+1).LE.P.AND.E(I+1,J).GE.P)GOTO4
    8 IF(N2.EQ.1)GOTO14
      IF(E(I+1,J).GE.P.AND.E(I,J).LE.P)GOTO1
      IF(E(I+1,J).LE.P.AND.E(I,J).GE.P)GOTO1
      GOTO14
    1 Y(K)=I-YO+(P-E(I,J))/(E(I+1,J)-E(I,J))
      X(K)=J-XO
      N1=1
      N2=0
      N3=0
      N4=0
      J=J-1
      GOTO9
    2 Y(K)=I-YO+(P-E(I,J+1))/(E(I+1,J+1)-E(I,J+1))
```

```
      X(K)=J+1-XO
      N1=0
      N2=1
      N3=0
      N4=0
      J=J+1
      GOTO9
    3 Y(K)=I-YO
      X(K)=J-XO+(P-E(I,J))/(E(I,J+1)-E(I,J))
      N1=0
      N2=0
      N3=1
      N4=0
      I=I-1
      GOTO9
    4 Y(K)=I+1-YO
      X(K)=J-XO+(P-E(I+1,J))/(E(I+1,J+1)-E(I+1,J))
      N1=0
      N2=0
      N3=0
      N4=1
      I=I+1
      GOTO9
   14 K=K-1
      X(K+1)=0.0
      Y(K+1)=0.0
      X(K+2)=20.0
      Y(K+2)=7.7
      CALL LINE(X,Y,K,1,0,0)
   21 CONTINUE
      K=0
      DO 555 J=1,201
      DO 555 I=1,49
      IF(V(I,J).EQ.100.Q.AND.V(I+1,J).LT.100.0)GO TO 444
      GO TO 555
  444 K=K+1
      X(K)=J
      Y(K)=I
  555 CONTINUE
      X(K+1)=0.0
      Y(K+1)=0.0
      X(K+2)=20.0
      Y(K+2)=7.7
      CALL LINE(X,Y,K,1,0,0)
      IF(LL.EQ.1)GO TO 105
      IF(LL.EQ.2)GO TO 106
      IF(LL.EQ.3)GO TO 108
      GO TO 107
  105 J=174
      GO TO 88
  106 J=124
      GO TO 88
  108 J=120
      GO TO 88
  107 CONTINUE
      CALL PLOT(20.0,0.0,-3)
      CALL AXIS(0.0,0.0,57HDISTANCE FROM CENTER OF CONDUCTOR (0.0125INCH
     1ES PER UNIT),-57,10.0,0.0,15.0,3.5)
      CALL AXIS(0.0,0.0,24HGRADIENT (2 KV PER UNIT),24,6.5,90.0,0.0,0.4)
      K=0
```

```
      DO 100 I=15,49
      J=24
      K=K+1
      Y(K)=I(I,J)
      X(K)=I
100   CONTINUE
      X(36)=15.0
      Y(36)=0.0
      X(37)=3.5
      Y(37)=0.4
      CALL LINE (X,Y,K,1,0,0)
      CALL PLTEND(15.0)
      STOP
      END
//
```

VITA AUCTORIS

1948 Born on April 8, Henley, England.

1967 Completed Secondary Education at Kennedy Collegiate Institute, Windsor, Ontario.

1971 Graduate with B.A.Sc (Electrical) from Windsor University.

1973 Candidate for the degree of M.A.Sc in Electrical Engineering at the University of Windsor, Windsor, Ontario.